การประยุกต์ใช้ตัวเร่งปฏิกิริยา V-Mg-O/TiO_2 ในปฏิกิริยาออกซิเดชันแบบเลือกเกิดของแอลกอฮอล์

นางสาวภูริดา พิมานมาศ

วิทยานิพนธ์นี้เป็นส่วนหนึ่งของการศึกษาตามหลักสูตรปริญญาวิศวกรรมศาสตรมหาบัณฑิต

สาขาวิชาวิศวกรรมเคมี ภาควิชาวิศวกรรมเคมี

คณะวิศวกรรมศาสตร์ จุฬาลงกรณ์มหาวิทยาลัย

ปีการศึกษา 2542

ISBN 974-333-788-1

APPLICATION OF THE V-Mg-O/TiO_2 CATALYST ON THE SELECTIVE OXIDATION OF ALCOHOLS

Miss Purida Pimanmas

A Thesis Submitted in Partial Fulfillment of the Requirements
for the Degree of Master of Engineering in Chemical Engineering
Department of Chemical Engineering
Faculty of Engineering
Chulalongkorn University
Academic year 1999

ISBN 974-333-788-1

Thesis Title	Application of the V-Mg-O/TiO_2 catalyst on the selective oxidation of alcohols
By	Miss Purida Pimanmas
Department	Chemical Engineering
Thesis Advisor	Assistant Professor Tharathon Mongkhonsi, Ph.D.
Thesis Co-advisor	Professor Piyasan Praserthdam, Dr.Ing.

Accepted by the faculty of Engineering, Chulalongkorn University in Partial Fulfillment of the Requirements for the Master's Degree

.....Dean of Faculty of Engineering

(Professor Somsak Panyakeow, Dr.Eng.)

Thesis Committee

.....Chairman

(Professor Wiwut Tanthapanichakoon, Ph.D.)

.....Thesis Advisor

(Assistant Professor Tharathon Mongkhonsi, Ph.D.)

.....Thesis Co-advisor

(Professor Piyasan Praserthdam, Dr.Ing.)

.....Member

(Seeroong Prichanont, Ph.D.)

ภูริดา พิมานมาศ : การประยุกต์ใช้ตัวเร่งปฏิกิริยา V-Mg-O/TiO_2 ในปฏิกิริยาออกซิเดชันแบบเลือกเกิดของแอลกอฮอล์ (APPLICATION OF THE V-Mg-O/TiO_2 CATALYST ON THE SELECTIVE OXIDATION OF ALCOHOLS) อาจารย์ที่ปรึกษาวิทยานิพนธ์ ผศ.ดร.ธราธร มงคลศรี, อาจารย์ที่ปรึกษาวิทยานิพนธ์ร่วม ศ.ดร. ปิยะสาร ประเสริฐธรรม, 104 หน้า. ISBN 974-333-788-1

การประยุกต์ใช้ตัวเร่งปฏิกิริยาวาเนเดียม-แมกนีเซียมออกไซด์บนตัวรองรับไทเทเนียมออกไซด์ โดยใช้ปฏิกิริยาออกซิเดชันแบบเลือกเกิดของเมทานอล, เอทานอล, 1-โพรพานอล และ 2-โพรพานอล ในงานวิจัยนี้ ได้ทำการศึกษาสภาวะต่างๆ เพื่อหาสภาวะที่เหมาสมสำหรับแต่ละปฏิกิริยา โดยทำการเปลี่ยนปริมาณออกซิเจนและแอลกอฮอล์ในช่วง 5-20% โดยปริมาตร และ 4-12% โดยปริมาตร ตามลำดับ ผลิตภัณฑ์หลักที่ได้จากปฏิกิริยาออกซิเดชันของเอทานอลและ1-โพรพานอล คือ อะเซทาลดีไฮด์และโพรพิโอนาลดีไฮด์ ตามลำดับ และคาร์บอนไดออกไซด์ จากการศึกษาผลของปริมาณออกซิเจนและแอลกอฮอล์ พบว่าค่าการเลือกเกิดคาร์บอนไดออกไซด์มีค่าต่ำที่สุดที่ 5% โดยปริมาตรของออกซิเจน และค่ายีลด์ของอัลดีไฮด์มีค่าสูงที่สุดที่ 8% โดยปริมาตรแอลกอฮอล์ ดังนั้นจึงสรุปได้ว่าที่อัตราส่วนของแอลกอฮอล์ต่อออกซิเจนเท่ากับ 8/5 จะให้ผลดีที่สุด จากนั้นจึงศึกษาผลของความเร็วเชิงสเปซ โดยเปลี่ยนค่าจาก 60,000 เป็น 20,000 มิลลิลิตร/ซม. กรัมของตัวเร่งปฏิกิริยา หรือ เพิ่มปริมาณของตัวเร่งปฏิกิริยาจาก 0.1 เป็น 0.3 กรัม ผลที่ได้แสดงให้เห็นว่าค่ายีล์ดของอัลดีไฮด์สูงขึ้น ปฏิกิริยาที่ศึกษาต่อมา คือ ปฏิกิริยาออกซิเดชันของเมทานอล โดยใช้อัตราส่วนของเมทานอลต่อออกซิเจนเท่ากับ 8/5 ผลิตภัณฑ์หลักที่พบคือ คาร์บอนไดออกไซด์ และคาร์บอนมอนออกไซด์ที่อุณหภูมิสูง เนื่องจากมีคาร์บอนมอนออกไซด์เกิดขึ้น จึงทำการทดลองเพิ่มเติมโดยเพิ่มปริมาณของออกซิเจนเป็น 20% โดยปริมาตร จากผลที่ได้พบว่าไม่มีคาร์บอนมอนออกไซด์เกิดขึ้น แสดงว่าเกิดการเผาไหม้อย่างสมบูรณ์ ดังนั้นจึงสามารถสรุปได้ว่าในกรณีที่ใช้ออกซิเจน 5% โดยปริมาตร เป็นการเผาไหม้ที่ไม่สมบูรณ์ สำหรับปฏิกิริยาออกซิเดชันของ 2-โพรพานอล พบว่าผลิตภัณฑ์หลักคือโพรพีน ซึ่งจะแตกต่างจากกรณีของ 1-โพรพานอล

ภาควิชา.....วิศวกรรมเคมี.....	**ลายมือชื่อนิสิต**.....ภูริดา พิมานมาศ.....
สาขาวิชา วิศวกรรมเคมี.....	**ลายมือชื่ออาจารย์ที่ปรึกษา**.....
ปีการศึกษา...2542.....	**ลายมือชื่ออาจารย์ที่ปรึกษาร่วม**.....

417 04579 21 : MAJOR CHEMICAL ENGINEERING
KEY WORD: SELECTIVE OXIDATON / METHANOL / ETHANOL / 1-PROPANOL / 2-PROPANOL / V-Mg-O/TiO_2 CATALYST
PURIDA PIMANMAS : APPLICATION OF THE V-Mg-O/TiO_2 CATALYST ON THE SELECTIVE OXIDATION OF ALCOHOLS. THESIS ADVISOR : ASSIST. PROF. THARATHON MONGKHONSI, Ph.D. THESIS CO-ADVISOR : PROF. PIYASAN PRASERTHDAM, Dr.Ing. 104 pp. ISBN 974-333-788-1

The application of V-Mg-O/TiO_2 catalyst on the selective oxidation of methanol, ethanol, 1-propanol and 2-propanol was investigated. In this research, the various conditions have been performed to determine the suitable condition for each reaction. The amounts of oxygen and alcohol are varied in the range of 5-20 vol% and 4-12 vol%, respectively. The main products from ethanol and 1-propanol oxidation are acetaldehyde and propionaldehyde, respectively, and CO_2. From investigating the effect of amounts of oxygen and alcohols, it is found that the CO_2 selectivity has the lowest value at 5 vol% oxygen and the highest aldehyde yield obtained at 8 vol% alcohols. Thus, it can be concluded that one of the best alcohol/oxygen ratio is 8/5 which gives the best results. Then, the effect of GHSV is studied by changing from 60,000 to 20,000 ml/hr. g of catalyst or increasing the catalyst content from 0.1 to 0.3 g. The results show that an increase in the amount of catalyst or a decrease in the GHSV values gives the higher aldehydes yield. After that, the methanol oxidation is examined by using the methanol/oxygen ratio equals to 8/5. CO_2 is the main product while CO is detected at high temperature. Due to CO formed, a further experiment is carried out by increasing the oxygen content to 20 vol%, the result shows that no CO is obtained. Therefore, it can be concluded that at 5 vol% oxygen used, the reaction is not complete combustion. For the oxidation of 2-propanol, propene and CO_2 are the major product, which is different from the case of 1-propanol.

ภาควิชา.....วิศวกรรมเคมี..... ลายมือชื่อนิสิต.....

สาขาวิชา วิศวกรรมเคมี..... ลายมือชื่ออาจารย์ที่ปรึกษา.....

ปีการศึกษา...2542..... ลายมือชื่ออาจารย์ที่ปรึกษาร่วม.....

ACKNOWLEDGEMENTS

I would like to express my greatest gratitude to Assistant Professor Tharathon Mongkhonsi, my advisor for his invaluable guidance and supervision during my study. I am grateful to Professor Dr. Piyasan Praserthdam for his guidance and encouragement.

Furthermore, I am also grateful to Professor Dr. Wiwut Tanthapanichakoon and Dr. Seeroong Prichanont for serving as chairman and member of the thesis evaluating committee, respectively, whose comments have been especially helpful.

The determination of BET surface area of catalyst using a delicate instrument could not have been carried out without the help and experience of Mr. K. Piboon.

I also would like to thank Miss Sudarat Matawan and Mr. Sakchai Kittikerdkulchai for their valuable suggestions and useful help and many best friends in the Petrochemical Research Laboratory at the Department of Chemical Engineering who have provided encouragement and cooperation throughout this study.

Thanks for the financial support are to Thailand Research Fund (TRF).

Finally, I would like to express my highest gratitude to my parents for their inspiration and valuable support throughout this study.

CONTENTS

PAGE

ABSTRACT (IN THAI) iv

ABSTRACT (IN ENGLISH) v

ACKNOWLEDGEMENTS vi

LIST OF TABLES ix

LIST OF FIGURES x

CHAPTER

I INTRODUCTION 1

II LITERATURE REVIEW 4

2.1 Reviewed literature 4

2.2 Comment on previous works 13

III THEORY 14

3.1 Monolayer surface coverage 16

3.2 Stability of the surface vanadia monolayer 17

3.3 Oxidation state of calcined surface vanadia monolayer 17

3.4 Molecular structures of surface vanadia species 18

3.5 Influence of metal oxide additives 19

3.6 Acidity of surface vanadia species 20

3.7 Mechanism of action of V_2O_5/TiO_2 catalyst in oxidation of hydrocarbon 21

IV EXPERIMENT 22

4.1 Preparation of catalyst 23

4.2 Catalyst characterization 24

4.3 Catalytic reaction 25

V RESULTS AND DISCUSSION 29

5.1 Catalyst characterization 29

5.2 Catalytic reaction 35

VI CONCLUSIONS AND RECOMMENDAATIONS 67

6.1 Conclusions 67

6.2 Recommendations for future studies 68

REFEERENCES 69

PAGE

APPENDICES..... 72
APPENDIX A. CACULATION OF CATALYST PREPARATION..... 73
APPENDIX B. CALCULATION OF DIFFUSIONAL LIMITATION EFFECT..... 74
APPENDIX C. GAS CHROMATOGRAPH..... 90
APPENDIX D. DATA OF EXPERIMENT..... 98
VITA..... 104

LIST OF TABLES

TABLE PAGE

4.1 The chemicals used in this research..... 24

5.1 The compositions of catalyst and BET surface area..... 29

LIST OF FIGURES

FIGURE PAGE

2.1 The model of aqueous solution on the surface of the oxide support..... 9

2.2 The vanadium oxide species on supported vanadium oxide surface..... 10

3.1 Different $[VO_x]_n$ species on TiO_2 anatase support..... 16

4.1 Flow diagram of the oxidation reaction system..... 27

5.1 The X-ray diffraction pattern of TiO_2 catalyst..... 31

5.2 The X-ray diffraction pattern of V_2O_5 catalyst..... 31

5.3 The X-ray diffraction pattern of 10V2MgTi catalyst..... 32

5.4 IR spectrum of TiO_2 catalyst..... 34

5.5 IR spectrum of 10V2MgTi catalyst 34

5.6 The result of 1-propanol oxidation over 0.1 g of 10V2MgTi catalyst ($1\text{-propanol}/O_2 = 4/20$)..... 38

5.7 The result of 1-propanol oxidation over 0.1 g of 10V2MgTi catalyst ($1\text{-propanol}/O_2 = 4/10$)..... 39

5.8 The result of 1-propanol oxidation over 0.1 g of 10V2MgTi catalyst ($1\text{-propanol}/O_2 = 4/5$)..... 40

5.9 The result of 1-propanol oxidation over 0.1 g of 10V2MgTi catalyst ($1\text{-propanol}/O_2 = 8/5$)..... 41

5.10 The result of 1-propanol oxidation over 0.1 g of 10V2MgTi catalyst ($1\text{-propanol}/O_2 = 12/5$)..... 42

5.11 The result of 1-propanol oxidation over 0.3 g of 10V2MgTi catalyst ($1\text{-propanol}/O_2 = 8/5$)..... 43

5.12 Space time yield of propionaldehyde for all conditions..... 44

5.13 The result of ethanol oxidation over 0.1 g of 10V2MgTi catalyst ($\text{ethanol}/O_2 = 4/20$)..... 48

5.14 The result of ethanol oxidation over 0.1 g of 10V2MgTi catalyst ($\text{ethanlo}/O_2 = 4/10$)..... 49

5.15 The result of ethanol oxidation over 0.1 g of 10V2MgTi catalyst ($\text{ethanol}/O_2 = 4/5$)..... 50

5.16 The result of ethanol oxidation over 0.1 g of 10V2MgTi catalyst ($\text{ethanol}/O_2 = 8/5$)..... 51

FIGURE PAGE

5.17 The result of ethanol oxidation over 0.1 g of 10V2MgTi catalyst (ethanol/O_2 = 12/5)..... 52
5.18 The result of ethanol oxidation over 0.3 g of 10V2MgTi catalyst (ethanol/O_2 = 8/5)..... 53
5.19 Space time yield of ethanal for all conditions..... 54
5.20 The result of methanol oxidation over 0.1 g of 10V2MgTi catalyst (methanol/O_2 = 8/5)..... 57
5.21 The result of methanol oxidation over 0.1 g of 10V2MgTi catalyst (methanol/O_2 = 8/20)..... 58
5.22 The result of 2-propanol oxidation over 0.1 g of 10V2MgTi catalyst (2-propanol/O_2 = 8/5)..... 60
5.23 The mechanism of the oxidation of 1-propanol to propionaldehyde..... 62
5.24 The mechanism of the oxidation of 2-propanol to propene..... 63
5.25 The result of 2-propanol oxidation over 0.1 g of 10V2MgTi catalyst (2-propanol/O_2 = 8/0)..... 66

CHAPTER I

INTRODUCTION

Selective catalytic oxidation and ammoxidation processes of hydrocarbons comprise approximately one quarter of the value produced by all catalytic processes worldwide. Selective oxidation plays an important role both in the production of material required and in the destruction of undesired products. Supported vanadium oxide which form a group of industrially important catalysts are extensively employed for many selective oxidations of hydrocarbons. It has been found that, in many cases, supported vanadium oxide catalysts are doped with promoters to improve their activity and/or selectivity, and supports are used to improve mechanical strength, thermal stability and lifetime. In recent years, such supported vanadia catalysts have found wide commercial application as oxidation catalysts such as selective oxidation of *o*-xylene to phathalic anhydride, selective oxidation of methanol to formaldehyde, oxidation of butane to maleic anhydride, selective catalytic reduction of NO_x with NH_3 and controlling the oxidation of SO_2 to SO_3 during SCR.

The acidic and basic nature is the one important property of metal oxide catalysis. Transition metal oxide catalysts for oxidation processes also exhibit acid-base properties, being capable of sorbing acids and/or bases, as well as catalyzing reactions such as the dehydration of alcohols and isomerization of hydrocarbons. Supported vanadium oxide catalysts may exhibit different catalytic properties depending on the nature of the oxide carrier. When vanadium oxide is deposited on TiO_2 (anatase), monolayer of vanadium oxide, represented as VO_x, is formed on the surface of TiO_2 (anatase). It has been found that VO_x monolayer was particularly stable on TiO_2 (anatase), where aggregation to V_2O_5 was occurred on the other support such as SiO_2. Species in the monolayer are believed to be the effective catalysts for oxidation of *o*-xylene to phathalic anhydride, for ammoxidation of aromatics and for selective reduction of nitric oxide by ammonia.

On the contrary, the magnesia supported vanadia system, vanadium oxide does not form the monolayer structure like the above titania supported vanadia system because of the acid-base reaction between the acidic vanadium oxide and basic magnesia. The strong interaction between vanadia and magnesia results in the formation of a mixed metal oxide compound, V-Mg-O, rather than a stable surface vanadia overlayer on the magnesia support. Vanadium-magnesium oxides are well known catalysts for the oxidative dehydrogenation of hydrocarbons, as in the transformation of propane to propene, butane to butene and butadiene, and ethylbenzene to styrene.

Supported vanadium oxides can exhibit interesting properties depending on the composition of the catalyst and on the nature of the support. Generally, bulk V_2O_5 cannot be used because of its poor thermal stability and mechanical strength. However its stability may be greatly enhanced when vanadia is incorporated on a support of high surface area such as Al_2O_3, SiO_2, TiO_2, MgO etc. It has been found that the V_2O_5/TiO_2 and V-Mg-O systems are the effective catalysts for many selective oxidations. Anyway, there is no information about the catalytic performance of V-Mg-O/TiO_2 systems. For this research, thus, the combination of V-Mg-O and V_2O_5/TiO_2 system was established to apply this new catalysts system, V-Mg-O/TiO_2, on the selective oxidation of alcohols i.e. methanol, ethanol, 1-propanol, 2-propanol. Hence, this work was set up to investigate:

1. The effect of the content of O_2 in the feed stream
2. The effect of the content of alcohol used in the feed stream
3. The effect of GHSV
4. The oxidation property of V-Mg-O/TiO_2 catalyst in each condition on the selective oxidation of methanol, ethanol, 1-propanol and 2-propanol.

The present work is arranged as follows:

Chapter II presents literature reviews of investigation related supported vanadia systems on the selective oxidation.

The theory of this work, studies about the structure and reactivity of vanadium oxide species on oxide support especially TiO_2 and MgO, are described in chapter III.

The experimental systems and the operational procedure are presented in chapter IV.

The experimental results of the characterization of catalyst and the methanol, ethanol, 1-propanol and 2-propanol oxidation reactions over V-Mg-O/TiO_2 are shown in chapter V.

In the last chapter, the overall conclusion emerged from this work is presented.

Finally, the sample of calculation of catalyst preparation, diffusional limitation effect, the details of gas chromatograph including the operating conditions, the calibration curves and data of experiments which has emerged from this study are included in appendices at the end of this thesis.

CHARPTER II

LITERATURE REVIEW

Selective oxidation is at present the main method of synthesis of a series of important chemical products such as aldehydes, acids, nitriles, etc. A large body of patent literature is concerned with the development of catalysis for this reaction. Supported vanadium oxide catalysts have been reported to be effective in many selective oxidations of hydrocarbons. They can exhibit interesting catalytic properties depending on the composition of the catalyst and on the nature of support. Many recent studies have shown that supported V_2O_5/TiO_2 is a superior catalyst to unsupported crystalline V_2O_5 for the selective oxidation of hydrocarbon, especially for the partial oxidation of *o*-xylene to phathalic anhydride. A number of observations on V-Mg-O system have also been made. It has been proposed that the V-Mg-O system was efficient for the oxidative dehydrogenation of butane and propane.

In addition to the V_2O_5/TiO_2 and the V-Mg-O system, the other V-containing systems have been investigated too. However, many significant fundamental questions still remain unanswered about these oxidation catalysts: (1) monolayer coverage of the surface vanadia species, (2) the stability of the surface vanadia monolayer, (3) the molecular structures of the surface vanadia species, (4) influence of the oxide support and metal oxide additives on the molecular structures and reactivity. Thus, a large number of investigations have been made in order to understand clearly about these catalyst systems in the selective oxidation reaction.

2.1 Reviewed literature

Charr *et al.* (1987) reported that the V-Mg-O catalysts are quite selective for the oxidative dehydrogenation of butane to butenes and butadiene. The active and selective component of V-Mg-O catalyst was the compound magnesium orthovanadate, $Mg_3 (VO_4)_2$. No oxygenated product was formed over V-Mg-O

catalyst. They could not observe characteristic V=O stretching in the V-Mg-O. Thus they suggested that the vanadium oxide in V-Mg-O did not form a layer structure of V_2O_5 on the MgO surface. They also reported that the selectivity for the oxidative dehydrogenation increased with decreasing oxygen-to-butane ratio, decreasing conversion and decreasing temperature. A selectivity of up to 60% was obtained. The high selectivity for the oxidative dehydrogenation instead of oxygenate production was attributed to two factors: the basic surface which facilitated desorption of basic butenes and butadiene, and the absence of V=O which lowered the oxidation activity of the surface.

Charr *et al.* (1988) studied the oxidative dehydrogenation of propane to propene. They reported that vanadium-magnesium oxide catalysts were active and selective for this reaction. A selectivity of up to 65% was obtained at 10% conversion, but decreased with increasing conversion. The major products were propene, CO and CO_2. No oxygenates were formed. The reaction rate was 0.6±0.15 order in propane and zeroth order in oxygen. For comparison, the rate for butane oxidative dehydrogenation was 0.85±0.15 in butane and zeroth order in oxygen. Both reactions probably proceeded by first breaking a methylene C-H bond to from an adsorbed alkyl radical species.

Nieto *et al.* (1990) investigated the selective oxidation of propene with oxygen in the presence of steam on Al_2O_3-, SiO_2- and TiO_2 (anatase)-supported vanadium oxide. They found that V_2O_5/TiO_2 preparations were more highly active catalysts than the V_2O_5/Al_2O_3 or V_2O_5/SiO_2 preparations. While the V_2O_5/TiO_2 catalysts were highly active and selective toward acetic acid, the V_2O_5/Al_2O_3 and V_2O_5/SiO_2 catalysts were much less active and selective toward acetone. They indicated that the structure of surface vanadia defined by the active phase-support interaction played an important role in the selective oxidation reaction.

Bhattacharyya *et al.* (1992) have investigated the effects of different promoters (Cr_2O_3, MoO_3 and TiO_2) added to V-Mg-O catalyst for the selective oxidation of n-butane to butadiene. The detailed experimental investigation of these

catalysts with respect to variables: the reaction temperature, contact time and n-butane feed concentration indicated the order of activity as follows: 24V-Mg-O+ Cr_2O_3 > 24V-Mg-O+ MoO_3 > 24V-Mg-O > 24V-Mg-O+ TiO_2 and the order of selectivity was 24V-Mg-O+ TiO_2 > 24V-Mg-O+ Cr_2O_3 > 24V-Mg-O > 24V-Mg-O+ MoO_3. It was likely that butenes and butadiene, being basic in nature, interacted more strongly with acidic catalysts than with relatively basic catalysts. Besides, they proposed that the catalyst 24V-Mg-O incorporating both Cr_2O_3 and TiO_2 provided not only higher activity but also better selectivity. A maximum yield of 35.6 mol% was obtained with this catalyst. They suggested a very low chance of the operation of $V^{4+} \leftrightarrow V^{3+}$ redox cycle for this oxidation reaction.

Centi *et al* (1993) reviewed the works on the selective heterogeneous oxidation of light alkanes, especially on V-P-O catalysts. The paper reported that the deep oxidation products (i.e. oxygenates and carbon oxides) starting from an alkane and its respective alkene could be different. This phenomenon was due to the difference between the strength of adsorption of alkane, alkene and oxygen. In the direct oxidation of alkane, both alkane and oxygen could adsorb on the catalyst surface, hence, the surface concentration of alkene was limited. In the direct oxidation of alkene, on the contary, almost all the active sites were covered by alkene and therefore inhibited the adsorption of oxygen.

Burch and Crabb (1993) studied the oxidative dehydrogenation of ethane to ethene in a quartz reactor in the absence and in the presence of range of MgO-based catalysts and/or inert packing. Their experiment on thermal pyrolysis ethane with no oxygen present using an empty reactor showed that the non-oxidative pyrolysis of ethane was not really significant until reaction temperatures were of at least 700°C. When air was added, they could observe that the oxidative route became important at temperatures at least 100°C lower than for the thermal pyrolysis reaction. Using ethane/air ratio of 1/2 at a temperature of 600°C, a conversion of 45% was achieved at a selectivity of 73.7%. However, when the reactor filled with quartz wool was used, the gas-phase radical reactions were greatly inhibited. They suggested that the

packing material inhibited the gas-phase radical reaction by reducing the residence time in the hot zone and possibly by trapping radicals.

Corma *et al.* (1993) interested in preparing of V-Mg-O catalysts by using MgO or magnesium oxalate and aqueous solutions of vanadyl oxalate or ammonium metavanadate as vanadium sources. After calcination, large differences in the V/Mg surface atomic ratios were observed on the different catalysts, indicating differences in the V-Mg interaction, which were related to the preparation method of catalysts. By X-ray diffraction, IR, UV-VIS and X-ray photoelectron spectroscopic characterization of samples before and after the calcination step, different Mg- and V-compounds have been observed. Before the calcination step, $Mg(OH)_2$ and/or magnesium-oxalate, as well as V^{5+} and/or V^{4+} species, depending on vanadium sources and vanadium content, were observed. After the calcination step, the formation of magnesium vanadates depended only on the vanadium content of the catalysts. $Mg_3V_2O_8$ formed at low vanadium content of the catalysts and $Mg_3V_2O_8$ + α-$Mg_2V_2O_7$ at high vanadium content.

Michalakos *et al.* (1993) have studied the catalytic oxidation of ethane, propane, 2-methylpropane, butane, pentane and cyclohexane over three vanadate catalysts ($Mg_3V_2O_8$-MgO, $Mg_2V_2O_7$ and $(VO)_2P_2O_7$). These reactions produced a wide range of products ranging from alkenes, dienes, anhydrides, acids and oxides. They classified the sets of products into two groups by using the average oxygen stoichiometry (AOS). First group in which dehydrogenation products were dominant and for which the initial AOS values were about two, and the second group in which oxygen-containing products are dominant and for which the initial AOS values were about four. In addition, they explained the selectivity patterns in terms of the formation of dehydrogenation products versus oxygen-containing products including carbon oxides by assuming that there existed a selectivity – determining step, which could be the reaction of the surface alkyl species or the adsorbed alkene before its desorption. The formation of oxygen-containing products would be facilitated if the surface alkyl or adsorbed alkene could interact with the vanadium ions in two

adjacent VO_x units such that it could be easily react with the reactive oxygen in the V-O-V bridge.

Okuhara *et al.* (1993) studied the structures and dehydrogenation activities of vanadium oxide overlayers on supports (MgO, Al_2O_3, and SiO_2). On MgO, the vanadium was not in the form of V_2O_5. They reported that vanadium oxides reacted readily with the surface of MgO to form new phases such as $Mg_3V_2O_8$ and $Mg_2V_2O_7$, $Mg_3V_2O_8$ consisted of V ions in tetrahedral sites (V-O) and Mg ions in octahedral sites, and $Mg_2V_2O_7$ had V_2O_7 groups (V=O, V-O). EXAFS spectra revealed that the structure of V_2O_5 was very sensitive to the supports and the preparation method (impregnation or chemical vapor deposition, CVD). They indicated that the preparation by CVD let to be thin films, which had high thermal stability and catalytic activities for dehydrogenation.

Nakamura *et al.* (1993) have investigated heterogeneous liquid phase oxidation of alcohols over V_2O_5 on several supports such as ZrO_2, SiO_2, Al_2O_3, TiO_2 and Fe_2O_3. They found that vanadium oxide supported on zirconia is a good reagent for this reaction at moderate temperature. The liquid-phase oxidation of cyclohexanol to cyclohexanone was performed at reflux temperature of toluene, and the reactivity was found to be highly dependent on metal oxides used as support. ZrO_2 is the most effective support, yield of cycloxanone is up to 89% after 36 h. V_2O_5/TiO_2 also showed high activity, but particle of this material became too fine to remove from the reaction mixture by filtration. In addition, they have also examined the effect of concentration of vanadium oxide to ZrO_2. The best activity was observed with 10wt% of V_2O_5. Moreover, when V_2O_5/TiO_2 oxidant was removed by filtration and then calcined at 500°C in air for 3 h. and then used for the same reaction, the yield of cyclohexanone in second run with recycled oxidation was 80% compared with 60% for the first reaction. Thus the oxidation activity was remained or increased with repeated operation.

Deo *et al.* (1994) investigated the molecular structural and reactivity properties of supported vanadium oxide catalysts (MgO, γ-Al_2O_3, TiO_2, ZnO_2, Nb_2O_5 and SiO_2) by using various characterization techniques (e.g. XPS, Raman, IR, X-ray absorption). They suggested that in all the supported vanadium oxide samples (exception of V_2O_5/MgO), the vanadium ion presented as an aqueous solution on the surface of the oxide support under ambient condition. Under dehydrated condition, the surface vanadium oxide species bonded directly with the oxide support surface. In the case of V_2O_5/MgO, no drastic change occurred in Raman spectra between under ambient and dehydrated conditions. This result could be explained that vanadium oxide predominantly forms compounds with MgO on MgO surface. Moreover, they found that the net surface pH at point of zero charge (pzc) of the surface moisture depended on the specific oxide support and the vanadium oxide loading. This pH value controlled the structure of the hydrated surface vanadium oxide species. Hence, more vanadium oxide loading and lower pH value, the surface vanadium oxide structures became more polymer. The model of aqueous solution and the samples of vanadium oxide species are shown in Figures 2.1 and 2.2 respectively.

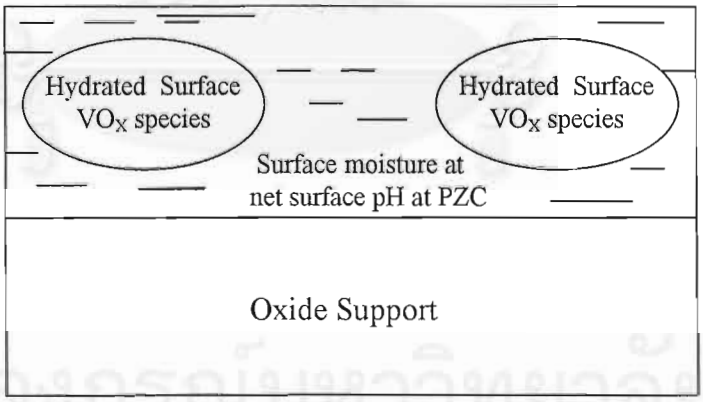

Figure 2.1 The model of aqueous solution on the surface of the oxide support.

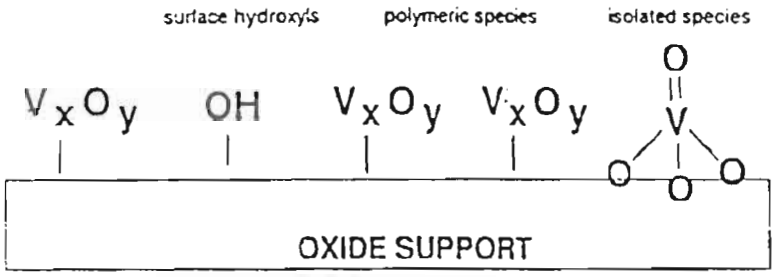

Figure 2.2 The vanadium oxide species on supported vanadium oxide surface

Finocchio *et al.* (1996) studied the interaction of n-butane, 1-butene, 1,3-butadiene and of C_4 oxygenates on the surface of oxidized magnesium chromite and magnesium vanadate catalysts by FTIR. They found that the interaction of magnesium vanadates with butane did not give detectable adsorbed species. Because above 350°C, the resulting partially oxidized surface species desorbed or further transformed very fast whereas the interaction of 1-butane and of 1,3-butadiene over this surface were extremely weak. Thus, it did not give rise to any detectable reaction. They noted that the polar molecules like alcohol reacted with the surface of magnesium vanadates, giving rise to dissociated adsorption. The behavior observed upon 2-butanol adsorption suggested that the main way of its transformation was its dehydration to n-butene. The key step determining selectivity was suggested to be the evolution of the alkoxides that over the vanadates could be in part decomposing to the olefin.

Guerrero-Ruiz *et al.* (1997) have studied surface and lattice oxygen atoms over vanadium pentoxide, magnesium oxide and magnesium vanadate phases (α-$Mg_2V_2O_7$, $Mg_3V_2O_8$ and β-MgV_2O_6) by isotopic exchange with a $C^{18}O_2$. They found that on MgO an important surface exchange process occurred with $C^{18}O_2$ of the gas phase, while this exchange was very low on V_2O_5 and pure V-Mg-O phases. A comparison of the different magnesium vanadate phases in the same experimental conditions indicated that the α-$Mg_2V_2O_7$ (which exhibited the highest selectivity for

oxidative dehydrogenation of propane to propene) showed the lowest lattice oxygen exchange with $C^{18}O_2$ of the gas phase.

Ponzi *et al.* (1998) have studied a series of V_2O_5-based catalyst and the influence of surface acidity on the partial oxidation of toluene to benzaldehyde. In this work, they have prepared three series of catalysts i.e. pure V_2O_5, V_2O_5-K and V-K-SiO_2. Then, the partial oxidation of toluene to benzaldehyde was used for measuring the catalytic activity. From the results, they found that both toluene conversion and selectivity to benzaldehyde are related to the presence of acidic site in the catalyst. The catalyst activity of this reaction decreases in the following order: V_2O_5 > V_2O_5-K > V-K-SiO_2, whereas the selectivity to total oxidation products keeps constant. The addition of K_2SO_4 to the V_2O_5 catalyst decreases the number of acid site, which lower the conversion to other partial oxidation products without modifying the selectivity to total oxidation products. Therefore, the selectivity to benzaldehyde becomes increased.

Wilddberger *et al.* (1998) have prepared vanadia-silica mixed oxides (aerogels and xerogens) derived from the sol-gel preparation route. These catalysts were 5LT, 10LT, 20LT, 10HT and 10X, the first numeral displays the designed of V_2O_5 in wt%, based on the theoretical system V_2O_5-SiO_2. The capital letters represent the drying method used (LT : Low temperature supercritical drying, HT : High temperature supercritical drying and X : Conventional drying in vacuo). These catalysts were tested in the partial oxidation of n-butane and 1,3-butadiene to furan. The dependence of the furan selectivity on morphological properties and vanadium dispersion in the silica matrix has been studied. The catalysts were characterized by N_2 and Ar physisorption, AAS, XPS and FTIR spectroscopy. Surface acidic centers of the materials were assessed by means of DRIFT-measurements of adsorbed NH_3 probe molecules. The structural properties mainly influenced by the drying procedure of the sol-gel materials. Aerogels were the most selective catalyst, converting butane to furan with only 3% selectivity. The maximum furan selectivity in butadiene transformation was about 25%, but considerable coke formation was also observed. Microporosity, found in conventionally dried sol-gel materials seems to be

unfavorable for furan selectivity. The presence of Brønsted acidic sites was proved to be necessary for furan formation. Studies involving V_2O_5, SiO_2 and vanadia-silica low-temperature aerogels with 5-20% vanadia contents revealed that selectivity to furan was diminished by silica due to its intrinsic high activity for total oxidation and cracking. A comparison to literature data indicated that vanadia-silica mixed oxides and vanadia grafted on silica are markedly less selective towards furan than VPO catalysts.

Benjaram *et al.* (1999) have designed stable and reactive vanadium oxide catalysts supported on binary oxides. V_2O_5/TiO_2 is used in practice as one of the best catalysts for the medium temperature range SCR of NO_x with NH_3 and for selective oxidation of various hydrocarbons. In both cases, TiO_2 in the form of anatase is used as the support. However, TiO_2 has a lot of disadvantages such as limited surface area, lack of abrasion resistance, poor mechanical strength, and high price. In addition, the anatase phase of titania has poor thermal stability at high temperatures. Because of these reasons, they have attempted to obtain a titania based support, combined with a highly stable support in order to improve the thermal stability, mechanical strength and high surface area. In this study, the objective is to explore the effect of thermal treatments on the dispersion and stability of vanadia on TiO_2-SiO_2, TiO_2-Al_2O_3, TiO_2-ZrO_2 and TiO_2-Ga_2O_3 mixed oxide supports. They found that these mixed oxides exhibit reasonably high specific surface area and good thermal stability. High-dispersed vanadium oxide monolayer catalysts with vanadia loadings nearly equivalent to the theoretical monolayer capacity of the supports can be obtained. The vanadia-impregnated catalysts when calcined at 500°C were found to be highly dispersed state on the carrier. When these catalysts were subject to thermal treatment from 200 to 800°C a gradual transformation of anatase into rutile was noted. These mixed oxide based V_2O_5 catalysts were also found to be vary active and selective for the synthesis of isobutyraldehyde from methanol and ethanol and for the selective oxidation of 4-methylanisole to anisaldehyde.

2.2 Comment on previous works

From the above reviewed literature, several supported vanadium oxide or V-containing systems have been studied in the selective oxidation reactions such as V-Mg-O [Charr et al. (1987,1988), Corma et al. (1993), Guerrero-Ruiz et al. (1997)], V_2O_5-K and V-K-SiO_2 [Ponzi et al. (1998)], V-P-O [Centi et al. (1993)], V_2O_5/TiO_2 [Benjaram et al. (1999)]. It can be seen that supported vanadium oxide catalysts have a good performance in many hydrocarbon oxidation reactions. Bulk V_2O_5 indeed has a poor thermal stability and mechanical strength, these properties can be enhanced when vanadium oxide impregnated on a suitable support especially TiO_2 and MgO.

Although many studies have focused on the vanadia-titania and vanadium-magnesium oxide system, there are no informations about the combination of these two systems. In this research, therefore, the system consists of oxides of vanadium, titanium and magnesium is investigated to study the catalytic property in the oxidation reactions.

CHAPTER III

THEORY

Heterogeneous catalytic oxidation on oxide catalysts is one of the most important fields of catalysis which have been actively developed in recent years. Catalytic oxidation can be categorized as selective and non-selective oxidation. Non-selective oxidation or complete oxidation is the combustion of hydrocarbon (HC) and oxygen to the combustion products, CO_2 and H_2O. Selective oxidation is the reaction between HC and oxygen to produce oxygenates (such as alcohols, aldehydes, carboxylic acids which are produced from partial oxidation processes) or unsaturated hydrocarbons (such as ethene and propene which can be produced from oxidative dehydrogenation processes).

In studies on oxidative catalysis, commonly great attention is attached to the state of oxygen on the catalyst surface. A relatively inert oxygen molecule is activated by interacting with the surface of oxide catalyst. The activation process falls into the following steps (all or some of them): coordination, electron transfer, dissociation, and incorporation into the oxide lattice. Depending upon the rate ratio of these steps, a certain amount of various activated states will exist on the catalyst surface. The main parameter determining oxygen reactivity on the catalyst is considered to be the energy of oxygen with the catalyst. Correlations between rates of catalytic oxidation and oxygen binding energy on oxide catalysts have been established: The weaker the oxygen binding with catalyst surface, the more efficient is complete oxidation with this catalyst.

In partial oxidation reactions, it usually necessitates H atom(s) abstraction, and O atom(s) insertion from the surface into the hydrocarbon molecule and several electron transfers. In the well accepted Mars and van Krevelen mechanism, lattice oxygen anions are assumed to be inserted in the substrate molecule or to facilitate its dehydrogenation by forming H_2O while the metallic cations inserted the redox

mechanism to occur by changing their oxidation state. This was postulated that the catalytic reaction comprises two steps by the followings:

1). Reaction between catalyst in an oxidized form, Cat-O, and the hydrocarbon R, in which the oxide becomes reduced.

$$Cat - O + R \rightarrow R - O + Cat$$

2). The reduced catalyst, Cat, becomes oxidized again by oxygen from the gas phase.

$$2\ Cat + O_2 \rightarrow Cat - O$$

Supported vanadium oxide catalysts find a variety of applications in a number of heterogeneous catalytic oxidation reactions. In these catalysts, the vanadium oxide phase on an oxide support (e.g. TiO_2) is the active phase and is usually more active than bulk crystalline vanadium pentoxide (V_2O_5).

Knowledge of the structure of the surface vanadium oxide species in supported vanadium oxide catalysts is critical to the fundamental understanding of the surface vanadium oxide phase-support and surface vanadium oxide phase-reactant gas interactions. The structure of the surface vanadium oxide phase in supported vanadium oxide catalysts depends on both the particular gas and solid environment. Recent developments in the characterization of surface vanadium oxide phases with the use of one or more of the characterization techniques have had a major impact on determining the molecular structure of the surface vanadium oxide species. The structure of the surface vanadium oxide species in supported vanadium oxide catalysts is discussed here with respect to the different environments experienced.

3.1 Monolayer surface coverage

Monolayer surface coverage is defined as the maximum amount of amorphous or two-dimensional vanadia in contact with the oxide support. Monalayer surface coverage of the surface vanadia overlayer on oxide supports has been estimated from structural calculations [Bond (1991), Bond *et al.* (1994)] and experimental determinations [Deo *et al.* (1994), Wachs (1996)]. Species in the monolayer are found to be effective catalysts for many hydrocarbon oxidation reactions such as oxidation of *o*-xylene to phathalic anhydride, ammoxidation of aromatics and selective oxidation of nitric oxide by ammonia.

At very low loading, corresponding to about 10% of the monolayer, only monomeric isolated forms have been observed. With increase in loading their amount increases and a new type of vanadyls is formed. Beginning from about 20% of the monolayer the appearance of polymeric forms has been observed. Their amount and the size (number of vanadium atoms in species) increase with the loading. At loading exceeding 1 monolayer amorphous and crystalline V_2O_5 are also observed [Machej *et al.* (1991)]. Figure 3.1 shows the different $[VO_x]_n$ species on the surface of TiO_2 (anatase) support

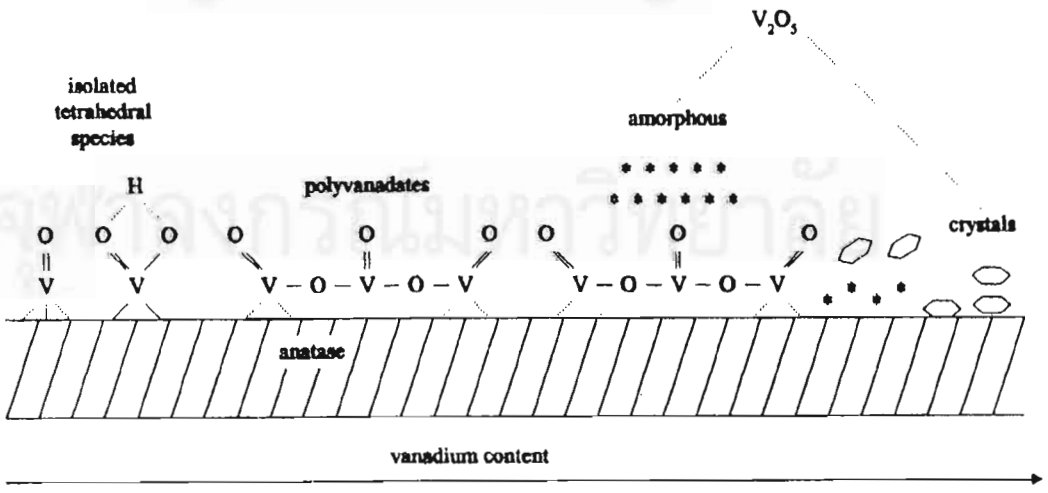

Figure 3.1 Different $[VO_x]_n$ species on TiO_2 anatase support [Wachs *et al.* (1997)].

3.2 Stability of the surface vanadia monolayer

The surface vanadia monlayer is stable after its initial formation on many typical oxide supports (Al_2O_3, TiO_2, ZrO_2, Nb_2O_5 and CeO_2). The surface vanadia monolayer on oxide supports is also stable under reducing and reaction environments. The surface vanadia monolayer can be converted to crystalline V_2O_5 or vanadia species dissolved in the oxide support only after high temperature treatments that cause the collapse of the oxide surface area, which reduces the number of available adsorption sites for the surface vanadia species [Wachs *et al.* (1997)]. In the case of V_2O_5/TiO_2 (anatase) phase to the TiO_2 (rutile) phase that can accommodate dissolved V(4+) species in the rutile lattice [Bond (1991)]. The stability of the surface vanadia monolayers is reflected in the long life of such industrial oxidation catalysts [Wachs (1997)].

3.3 Oxidation state of calcined surface vanadia monolayer

There has been some discussion over the years about the oxidation state of the surface vanadia species in calcined supported vanadia catalysts [Bond *et at.* (1994)]. Only V(5+) is observed in calcined supported vanadia catalysts by XPS, when the sample is not artificially reduced by the measuring conditions, and only traces of V (4+) are detected in EPR and UV-VIS DRS measurements. Furthermore, calcined supported vanadia catalysts give rise to solid state ^{51}V NMR signals which cannot be obtained for V(4+) species would also broaden the ^{51}V NMR signals of V(5+) species. However, chemical titration of extracted vanadia by H_2SO_4 has suggested that the surface vanadia species in the monolayer are present as V(4+) [Centi *et al.* (1991)]. Characterization of a standard supported vanadia catalyst, EUROCAT OXIDE vanadia-titania catalyst, has demonstrated that this chemical titration method may actually result in the reduction of the V(5+) species by sulfuric acid and that extreme care must be taken when employing this method since it may not lead to reproducible results [Bond *et al.* (1994)]. Thus, calcined supported vanadia catalysts possess V (5+) species with only trace amounts of V(4+) species.

3.4 Molecular structures of surface vanadia species

The molecular structures of the surface vanadia species have been extensively investigated in the past few years with many different spectroscopies: Raman [Wachs (1997)], IR [Wachs (1997)], XANES/EXAFS [Tanaka *et al.* (1992)]. These studies have revealed that the surface structures and oxidation states of the surface vanadia species are dynamic and are strongly dependent on the environment (oxidizing and reducing gases, moisture and temperature).

3.4.1 Dehydrated conditions

Dehydrated conditions are created by heating the supported vanadia catalysts to elevated temperature, 300-700°C, in a flowing oxygen-containing stream that does not contain any reducing gases. Such a treatment desorbs adsorbed moisture from the catalyst surface and maintains the surface vanadia species in the V(5+) oxidation state.

- V_2O_5/(Al_2O_3, TiO_2, ZrO_2, Nb_2O_5 and CeO_2)

The dehydrated surface vanadia species on these oxide supports are primarily present as isolated and polymerized on VO_4 unit. The relative concentrations of isolated and polymerized surface vanadia species have not been quantified by the above Raman studies. Oxygen-18 isotopic labeling experiments demonstrated that these surface vanadia species only possess one terminal V=O bond. The molecular structures of these surface vnnadia species are tentatively thought to consist of a terminal V=O bond and three bridging V-O support bonds for the isolated species, and a terminal V=O bond with one bridging V-O support and two bridging V-O-V bonds for the polymerized species. There may also be a minor amount of surface VO_6 units (octahedral coordination) present at monolayer coverages.

- V_2O_5/MgO

Unlike the above supported vanadia catalysts, the magnesia supported vanadia catalyst system cannot form a complete close packed surface vanadia monolayer because of acid-base reaction between acidic vanadia and basic magnesia. The strong interaction between vanadia and magnesia results in the formation of a mixed metal oxide compound rater than a stable surface vanadia overlayer on the magnesia support [Deo *et al.* (1992)]. The vanadia coordination in bulk V-Mg-O mixed metal oxide catalysts consists of VO_4, VO_5 and VO_6 units. Thus, the magnesia supported vanadia catalyst system possesses both surface and bulk vanadia species.

3.5 Influence of metal oxide additives

3.5.1 Noninteracting additives

Noninteracting additives are defined as surface metal oxides that preferentially coordinate with the oxide support rather than the surface vanadia species under dehydrated conditions. Typical noninteracting additives are surface oxides of W, Nb, S, Si, Mo, Ni, Co and Fe. Consequently, the noninteracting additives can only indirectly affect the molecular structure of the surface vanndia species via lateral interactions. Such lateral interactions have been found to influence the ratio of polymerized to isolated surface vanadia species in supported metal oxide catalysts: Fe>Ni~Co>S>Mo>Nb>Si.

3.5.2 Interacting additives

Interacting additives are defined as surface metal oxides that preferentially coordinate with the surface vanadia species rather that the oxide support under dehydrated conditions. Typical interacting additives are P and alkali/alkaline earth oxides (K, Na, Ca, etc.) that tend to complex with the acidic surface vanadia species [Ramis *et al.* (1993)]. The basic alkali/alkaline earth additives do not change the trigonal-pyramidal coordination of the dehydrated surface vanadia species, but do

affect the V-O bond lengths by significantly increasing the terminal V=O bond length and, consequently, decreasing the bridging V-O bond lengths [Ramis *et al.* (1993)]. Thus, the basic surface additives do not form three-dimensional mixed vanadate compounds, but just alter the V-O bond lengths of the surface vanadia species. However, the interaction between P and the surface vanadia species can result in the formation of crystalline $VOPO_4$ phases, at the expense of the surface vanadia phase, after calcination due to the strong interaction between these two oxides. The formation of crystalline $VOPO_4$ can only be avoided if the surface phosphorous oxide species is first anchored to the oxide support surface before the introduction of the vanadia precursor. Thus, interacting additives can both modify the local structure of the surface vanadia species, affecting the V-O bond lengths, as well as form crystalline mixed metal oxide phases because of their chemical affinity for vanadia.

3.6 Acidity of surface vanadia species

The oxide supports only possess surface Lewis acid sites and the relative strength of these sites is $Al_2O_3>Nb_2O_5>TiO_2>ZrO_2$, and no surface Lewis acid sites are detected for SiO_2. In contrast to the oxide supports, unsupported V_2O_5 crystalline powders possess both surface Brønsted and surface Lewis acid sites [Busca *et al.* (1989)]. The formation of the surface vanadia species on the oxide supportes is accompanied by a decrease in the number of surface Lewis acid sites and an increase in the number of surface Brønsted acid sites. Only a very small fraction of the surface vanadia species are also surface Brønsted acid sites since the concentration of surface Brønsted acid sites, measured by pyridine adsorption, corresponds to only 5-10% of the surface vanadia at monolayer coverage. Several in situ IR studies have assigned an OH vibration of dehydrated titania supported vanadia catalysts to Brønsted V-OH sites [Topsoe *et al.* (1995)]. The acidic characteristics of the surface vanadia overlayer are influenced by the specific oxide support ligand, but the molecular structural characterization studies reveal that the same dehydrated surface vanadia species are present on all the oxide supports (with the exception of silica). This suggests that the surface Brønsted hydroxyls may be located as bridging V-OH-support sites, but no direct spectroscopic evidence is currently available to support

any assignment for the location of the surface Brønsted acid sites which are only present for the oxidized V(5+) surface vanadia species. Thus, probing surface acidity with reducing probe molecules will alter the surface Brønsted acidity properties of the supported vanadia catalysts.

3.7 Mechanism of action of V_2O_5/TiO_2 catalyst in oxidation of hydrocarbons

It has been generally accepted that selective oxidation of hydrocarbons requires the presence of three essential types of centers on a catalyst surface: (a) the sites for activation of C-H bond in a hydrocarbon molecule which is a rate determining step in most oxidation processes, (b) the sites for insertion of oxygen into an organic molecule species adsorbed on the surface after step (a), (c) centers for reoxidation (or adsorption of molecular oxygen). Most of experimental works as well as quantum chemical calculations indicate that it is an oxygen atom (most probably O^{2-} ion on the catalyst surface) which is an active center for a rupture of a C-H bond. The ability of an oxygen atom (ion) to abstract a hydrogen atom from a C-H bond can be related to its nucleophilicity (basicity). The activity of the oxidation reaction would then increase with the increase in the oxygen basicity. The rate of the insertion of oxygen (step (b)) would depend in the first place on a Metal-O bond energy, and in the second place on a number of oxygen atoms in the vicinity of an organic adsorbed species.

CHAPTER IV

EXPERIMENT

The experimental systems and the experimental procedure used in this work are divided into three parts: (i) The catalyst preparation; (ii) The catalyst characterization; (iii) The catalytic test by oxidation of methanol, ethanol, 1-propanol and 2-propanol. The details of the experiments are described as the following:

The Scope of This Study

The reaction conditions are chosen as follow:

Catalyst	: 10wt%V2wt%Mg/TiO_2
Reactant	: methanol
	: ethanol
	: 1-propanol
	: 2-propanol
	: N_2
	: air (used as O_2 source)
Flow rate of reactant	: 100 ml/min
Reaction temperature	: 200-500°C
Gas hourly space velocity	: 60,000 and 20,000 ml/hr.g of catalyst

*The wt% of V calculated as V_2O_5

The wt% of Mg calculated as Mg

4.1 Preparation of catalyst

4.1.1 Materials

The detail of chemicals used in this experiment are shown in Table 4.1

Table 4.1 The chemicals used in this research

Chemical	Grade	Manufacturer
Titanium oxide [TiO_2]	Analytical	BDH Laboratory Suppliers
Ammonium metavanadate [NH_4VO_3]	Analytical	Carlo Ebra, Italy
Magnesium nitrate [$Mg(NO_3)_2$]	Analytical	Fluka, Switzerland

4.1.2 Preparation of V-Mg-O/TiO_2 Catalyst

V-Mg-O/TiO_2 catalyst was prepared by wet impregnation method. First step of the preparation, TiO_2 powder was added to an aqueous solution of ammonium metavanadate (NH_4VO_3) at 70°C. The suspension was dried at 80°C and calcined in air at 550°C for 6 hours. The sample obtained was V_2O_5/TiO_2. Then Mg was introduced into the V_2O_5/TiO_2 by impregnation from magnesium nitrate [$Mg(NO_3)_2$] solution and the suspension was dried and calcined in the same above condition. The catalyst was denoted as xVyMgTi where x was wt% of V calculated as V_2O_5 and y is wt% of Mg. For 10V2MgTi, the vanadium oxide and magnesium content were 10 and 2 wt%, respectively.

Moreover, due to the previous work [Leklertsunthorn (1997)], there was an investigation about the vanadium and magnesium contents in the range of 3-10 wt% and 1-2 wt%, respectively, including the sequence of impregnating on TiO_2 surface. It was found that 10V2MgTi catalyst gives the best results. Therefore, for this research, only 10V2MgTi is chosen as catalyst for the catalytic test.

4.2 Catalyst characterization

4.2.1 Determination of composition content of catalyst

The actual composition contents of catalyst were determined by atomic absorption spectroscopy (AAS) at the center service of science. The sample of calculation is shown in Appendix A.

4.2.2 Surface Area Measurement

The BET surface area of the sample was determined by nitrogen absorption in an automatic apparatus ASAP 2000 constructed by Micromeritics U.S.A. The data obtained were recorded by a microcomputer.

4.2.3 X-ray Diffraction Experiments

The crystal structure of the catalyst was identified by X-ray diffraction (XRD) analysis carried out on a Siemens D500 diffractometer with CuKα radiation in the 2θ range of 10-80°

4.2.4 Fourier Transform Infrared Spectroscopy

The sample was mixed with KBr with ratio of sample:KBr equal to 1:100. Then the mixture was ground into a fine powder and pressed into a thin wafer. Infrared spectra were recorded between 2000 and 400 cm^{-1} with FT-IR spectroscopy, Nicolet Impact 400, Nicolet Instrument Corporation, U.S.A. The spectra were used to study the functional group of surface vanadium oxide species of V-Mg-O/TiO_2 catalyst.

4.3 Catalytic Reaction

4.3.1 Apparatus

Flow diagram of the reaction system is shown in Figure 4.1. The methanol, ethanol, 1-propanol and 2-propanol oxidation system consist of a reactor, an automatic temperature controller, an electrical furnace, a gas controlling system and a saturator for evaporating these reactants before entering the reactor.

The microreactor is made from a stainless steel tube. Two sampling points are provided above and below the catalyst bed. Catalyst is placed between quartz glass wool layer.

An automatic controller consists of a magnetic contactor, a variable voltage transformer, RKC series RE-96 temperature controller and Eurotherm digital temperature indicator model Telex 87114. Temperature was measured at the bottom of the catalyst bed in the reactor. The temperature control setpoint is adjustable within the range of 0-800°C.

Electrical furnace supplies heat to the reactor for methanol, ethanol, 1-propanol and 2-propanol oxidation. The reactor can be operated from room temperature up to 800°C at the maximum voltage of 220 volt.

The gas supplying system consists of cylinders of:

1. A cylinder of air, equipped with a pressure regulator (0-120 psig), an on-off valve and a fine-metering valve used for adjusting the flow rate of air that passes through the saturator.

2. A cylinder of N_2, equipped with a pressure regulator (0-120 psig), an on-off valve and a fine-metering valve used for adjusting the flow rate of air that passes through the saturator.

The compositions of hydrocarbons in the feed and product streams were analyzed by flame ionization detector gas chromatograph Shimadzu 14B and 14A. The amount of CO_2 formed in the reaction was measured using a gas chromatograph Shimadzu GC-8A equipped with thermal conductivity detector. The operating conditions of GC are described in appendix C.

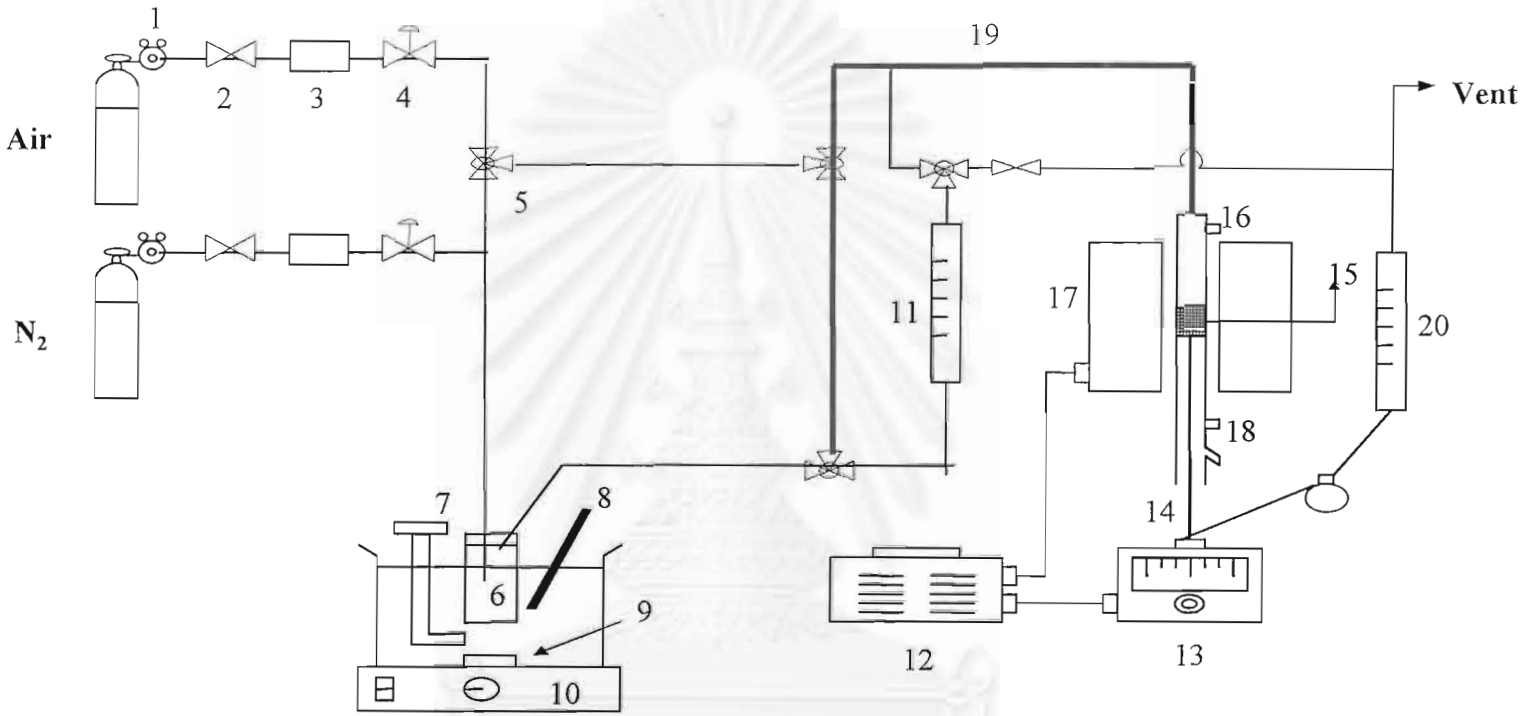

1. Pressure Regulator
2. On-Off Valve
3. Gas Filter
4. Metering valve
5. 3-way Valve
6. Saturator
7. Heater
8. Thermometer
9. Magnetic bar
10. Stirring controller
11. Flow meter
12. Variable Voltage Transformer
13. Temperature Controller
14. Thermocouple
15. Catalyst bed
16. Reactor
17. Furnace
18. Sampling point
19. Heating Line
20. Bubble Flow Meter

Figure 4.1 Flow diagram of methanol, ethanol, 1-propanol, 2-propanol, and 1-butanol oxidation system

4.3.2 Procedure

1. The certain amount of catalyst was packed in the middle of the stainless steel microreactor. Then, the reactor was placed in the electrical furnace.

2. Flow rates of reactants were adjusted to the required values and fed into the reactor. The feed compositions were

- 4 vol% 1-propanol, 20 vol% O_2 and balanced N_2
- 4 vol% 1-propanol, 10 vol% O_2 and balanced N_2
- 4 vol% 1-propanol, 5 vol% O_2 and balanced N_2
- 8 vol% 1-propanol, 5 vol% O_2 and balanced N_2
- 12 vol% 1-propanol, 5 vol% O_2 and balanced N_2
- 4 vol% ethanol, 20 vol% O_2 and balanced N_2
- 4 vol% ethanol, 10 vol% O_2 and balanced N_2
- 4 vol% ethanol, 5 vol% O_2 and balanced N_2
- 8 vol% ethanol, 5 vol% O_2 and balanced N_2
- 12 vol% ethanol, 5 vol% O_2 and balanced N_2
- 8 vol% methanol, 5 vol% O_2 and balanced N_2
- 8 vol% 2-propanol, 5 vol% O_2 and balanced N_2

3. The reaction temperature was between 200-500°C. The reactor was heated up with the heating rate of 10°C/min. Effluent gas was analyzed by the gas chromatograph.

4. The result of catalytic test was calculated in the term of:

$$\%\text{A conversion} = \frac{\text{mole of A reacted}}{\text{mole of A in feed}} \times 100\%$$

$$\%\text{Selectivity to B} = \frac{\text{mole of A converted to B}}{\text{mole of A reacted}} \times 100\%$$

where A is reactant

B is reaction product

CHAPTER V

RESULTS AND DISCUSSION

In this chapter, the results and discussion are categorized into two main parts : (1) The catalyst characterization, (2) The catalytic test by the selective oxidation of methanol, ethanol, 1-propanol and 2-propanol.

5.1 Catalyst Characterization

5.1.1 Determination of composition content of catalyst and surface area

The composition and the BET surface area of 10V2MgTi catalyst, which was determined by AAS and BET surface area measurement, are listed in Table 5.1.

Table 5.1 The composition of catalyst and BET surface area.

Catalyst	%V[a]	%Mg[b]	Surface area (m^2/g)	Average pore diameter (Å)
10*V2MgTi	9.1	2	9.27	93.7982

*The number in the catalyst symbol denotes the approximate weight percentage of V calculated as V_2O_5
[a] The content of vanadium is calculated in terms of %by weight of V_2O_5
[b] The content of magnesium is calculated in terms of %by weight

5.1.2 X-ray Diffraction

The crystal structure of all samples is characterized by XRD. Figure 5.1 and 5.2 illustrate XRD spectra of TiO_2 and V_2O_5, respectively. XRD spectrum of V_2O_5 shows three dominant peaks at the 2θ values of 20.5°, 26.5° and 31°.

From figure 5.3, spectrum of 10V2MgTi shows peaks at the same 2θ values as TiO_2 (figure 5.1). It can be seen that crystalline V_2O_5 peaks can not be detected in this sample. That means the amount of vanadium oxides on 10V2MgTi surface may be not enough to be determined by XRD or the vanadium oxide did not form a V_2O_5

crystal structure on the TiO_2 support. From the preparation method of 10V2MgTi, V_2O_5 which first deposited on TiO_2, forms a dispersed vanadia species on TiO_2 surface after calcination at 550°C. Although, the melting point of pure V_2O_5 is 700°C, when vanadia is dispersed on TiO_2 surface it can be melted at a lower temperature than bulk V_2O_5 . Therefore, after the impregnation of magnesium, the catalyst is then calcined at 550°C and vanadia species can be melted at this calcination temperature and react with MgO to form a new oxide compound, V-Mg-O, not form vanadium oxide. For this reason, the crystalline V_2O_5 peaks at 20.5° and 26.5° and 31° disappear.

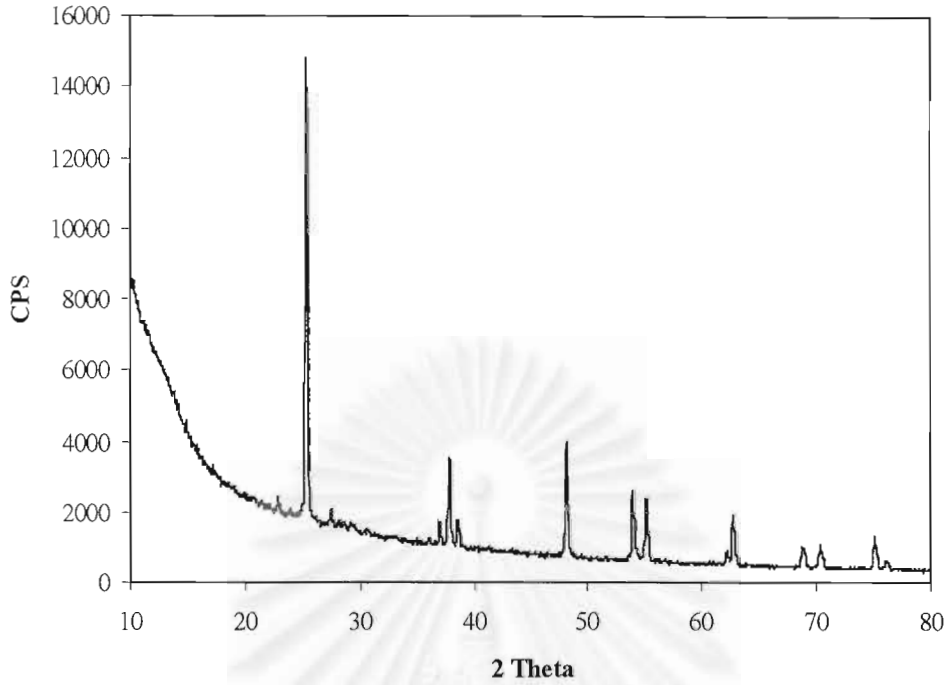

Figure 5.1 X-ray diffraction of TiO_2

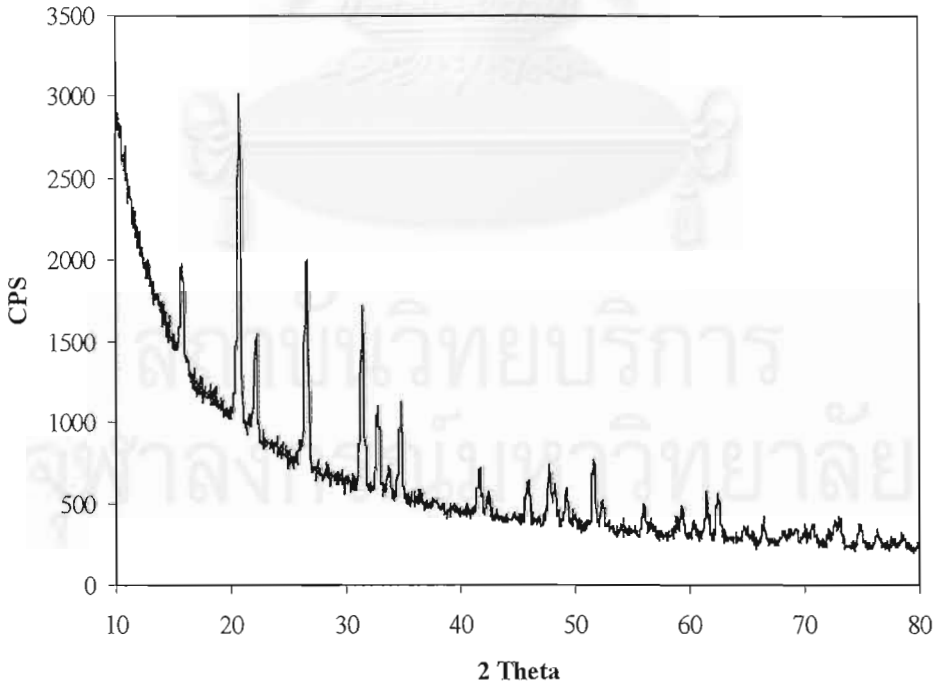

Figure 5.2 X-ray diffraction of V_2O_5

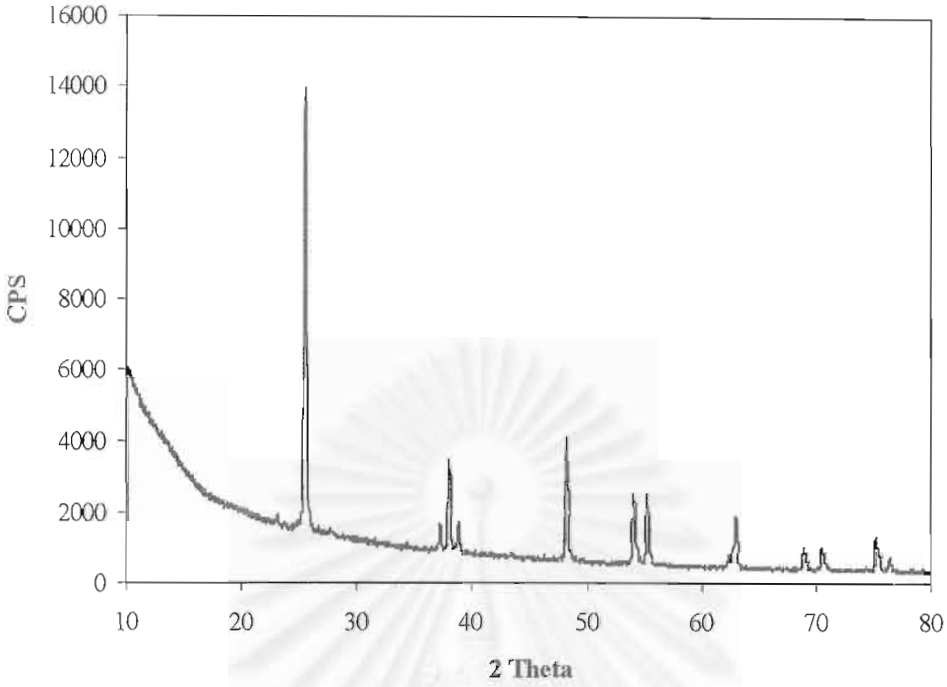

Figure 5.3 X-ray diffraction of 10V2MgTi catalyst

5.1.3 Fourier Transform Infrared Spectrometer (FT-IR)

The functional group on the surface of 10V2MgTi catalyst can be identified by using infrared radiation in the wavelength of 400-2000 cm^{-1}, which is the proper wavelength for determining the solid surface. Figure 5.4 presents IR spectrum of TiO_2. Strong absorption IR bands at 580 and 680 cm^{-1} are observed. As presented in figure 5.5, IR spectrum of 10V2MgTi catalyst exhibits the absorption bands at the same position as TiO_2. This can be indicated that the amounts of vanadium and magnesium on TiO_2 surface are much less to observe the changes in IR bands.

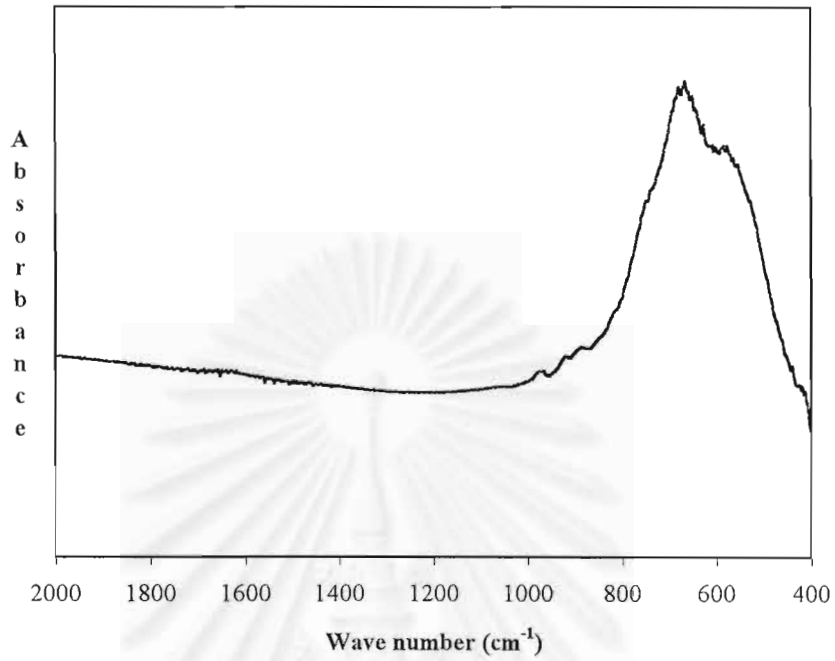

Figure 5.4 IR spectrum of TiO_2 catalyst

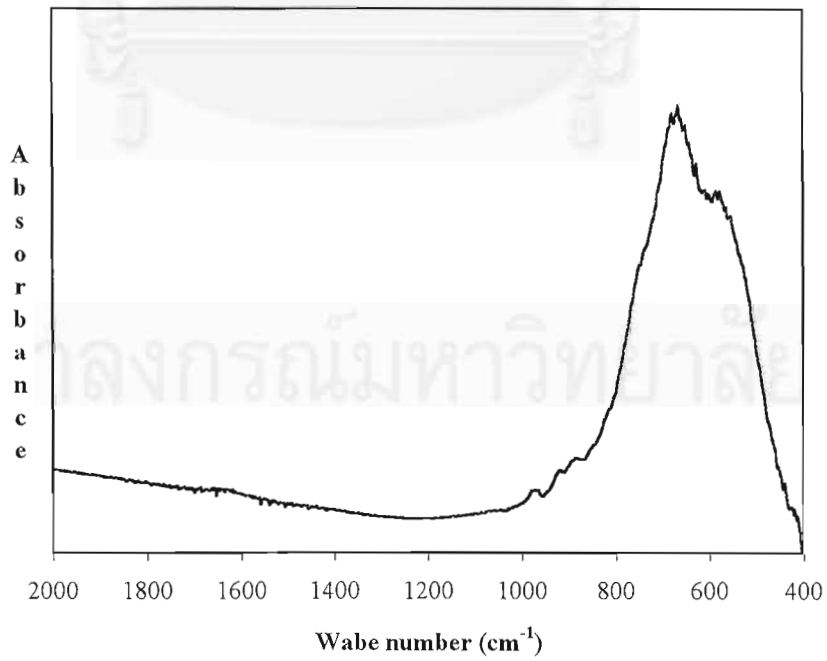

Figure 5.5 IR spectrum of 10V2MgTi catalyst

5.2 Catalytic reaction

For the volumetric flow rate used in this work, 100 ml/min, it has been found by calculation that this value (100 ml/min) do not affect the external and internal mass transfer resistant as presented in Appendix B.

It has been known that alcohols can be oxidized, and the products of oxidation depend on the class of the alcohol and on the nature of the oxidizing agent. In this work, the oxidation of methanol (CH_3OH), ethanol (C_2H_5OH), 1-propanol (1-C_3H_7OH) and 2-propanol (2-C_3H_7OH) were carried out to investigate the catalytic behavior of 10V2MgTi catalyst.

5.2.1 1-Propanol Oxidation

1-Propanol is a primary alcohol. It is expected that the product obtained from 1-propanol oxidation should be propionaldehyde (C_3H_6O). To investigate the catalytic behavior of 10V2MgTi catalyst on this reaction, the first run, 1-propanol/O_2 = 4/20, was chosen to examine the products obtained.

As presented in figure 5.6, the main products observed are propionaldehyde and CO_2. Small amounts of methane, ethene and propene are also produced. An increase of reaction temperature causes conversion to approach 100% but the selectivity to propionaldehyde substantially falls to nearly zero at 450°C while the selectivity to CO_2 rises to reach a maximum value about 95% at 500°C. Trace of formaldehyde (CH_2O) is also detected in the range 250-300°C.

Because CO_2 is considerably produced and it is not useful, the next studies were performed by decrease the amount of O_2 from 20 to 10 and 5 vol%, respectively, in order to decrease the production of CO_2.

The results of the second and third run, 1-propanol/O_2 = 4/10 and 4/5, respectively, are presented in figures 5.7 and 5.8, respectively. For these two

reactions, the main products are still propionaldehyde and CO_2. Formaldehyde and trace of methane, ethene and propene are also produced. In addition, the product distribution has the same trend as the first run (1-propanol/O_2 = 4/20). From figure 5.7, 1-propanol/O_2 = 4/10, the conversion rises continuously to almost 100% at 500°C. The selectivity to propionaldehyde drops gradually to about 26% while the selectivity to CO_2 enhances to a maximum value about 63% at 500°C. It is noted that the selectivity to CO_2 is still high. Formaldehyde is detected in the range 250-300°C and its maximum value is about 8 % at 350°C.

For the third run (figure 5.8), 1-propanol/O_2 = 4/5, the conversion increases with reaction temperature to about 85% at 500°C. The selectivity to propionaldehyde drops slowly and still higher than the previous cases. Its value is about 52% at 500°C. In contrast, the selectivity to CO_2 increases slowly to about 34% at 500°C.

From the above results, it can be seen that the third run (1-propanol/O_2 = 4/5) shows the best result. The selectivity to CO_2 is the lowest and the propionaldehyde yield obtained is the highest (the highest yields for the first, second and third run are 27% at 350°C, 30% at 350°C and 50% at 300°C, respectively and slightly decrease after 350°C for these three cases).

However, to receive the higher yield, there were more studies by varying the amount of 1-propanol from 4 to 8 and 12 vol%, respectively, and the amount of O_2 is fixed at 5 vol%. It can be seen from figure 5.9 (1-propanol/O_2 : 8/5) that the selectivities to propionaldehyde and CO_2 have the same values as the previous one (1-propanol/O_2 = 4/5) almost all reaction temperature. Considering the conversion of this run, at 200-300°C, it has the higher the value. After 300 °C, it is quite the same as the case of 4 vol% 1-propanol and reach the maximum value about 84% at 500°C. Additionally, the propionaldehyde yields are higher almost all reaction temperature. Figure 5.10 shows the result of the fifth run (1-propanol/O_2 = 12/5). It is observed that propionaldehyde and CO_2 selectivities exhibit the similar values as the fourth run (1-propanol/O_2 = 8/5) but the conversion is lower at all reaction temperature. Thus,

the yields of propionaldehyde in this case are lower than the previous one (1-propanol/O_2 = 8/5).

From the above results, it can be concluded that the fourth run, 1-propanol/O_2 = 8/5, give the best results, the propionaldehyde yields obtained have the highest values. Anyway, the catalyst used in the above experiments is only 0.1g or GHSV equals to 60,000 ml/hr. g of catalyst. To investigate the amount of catalyst or GHSV, the 1-propanol/O_2 ratio remains the same as 8/5 and then varies the amount of catalyst to 0.3 g or GHSV change to 20,000 ml/hr g of catalyst.

As described in figure 5.11, when the amount of catalyst enhances to 0.3 g, the height of bed is higher, which means that the feed stream has more contact time. The conversion is higher than the case of 0.1 g of catalyst used and relatively constant about 85% since 300°C. The selectivities to propionaldehyde is higher than all the above cases, the maximum yield is about 66% at 300°C.

Furthermore, the space time yield of propionaldehyde is presented in order to view more clearly about the influence of catalyst content on the yield obtained. As shown from figure 5.12, the condition with the 1-propanol/O_2 ratio = 8/5 and the amount of catalyst is 0.1 g give the highest space time yield of acetaldehyde. When comparing with the case of 0.3 g catalyst, it is found that the space time yield of propionaldehyde is rather low and lower than the case of 4 vol% 1-propanol.

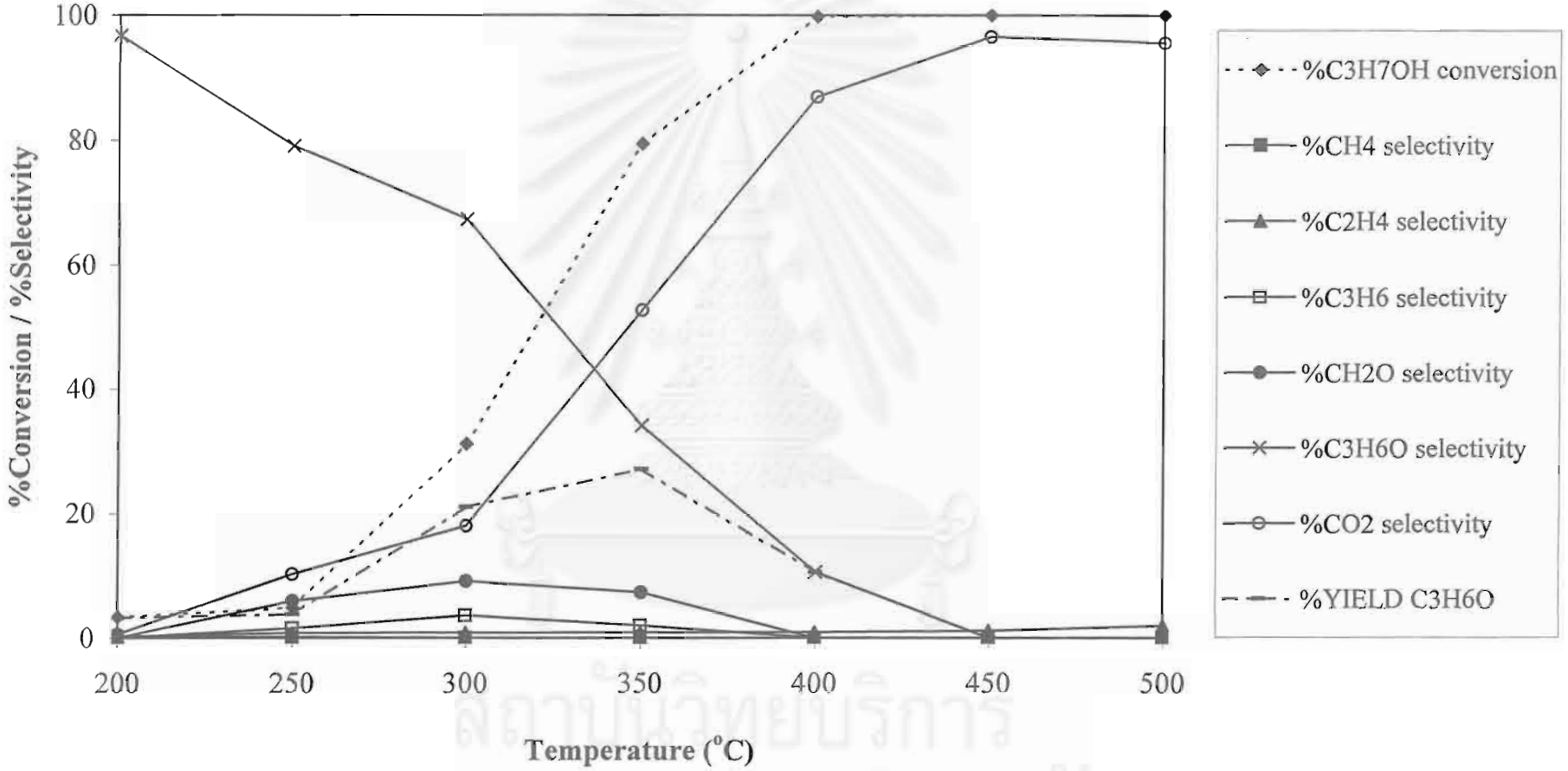

Figure 5.6 The result of 1-propanol oxidation over 0.1 g of 10V2MgTi catalyst (1-propanol/O_2 = 4/20)

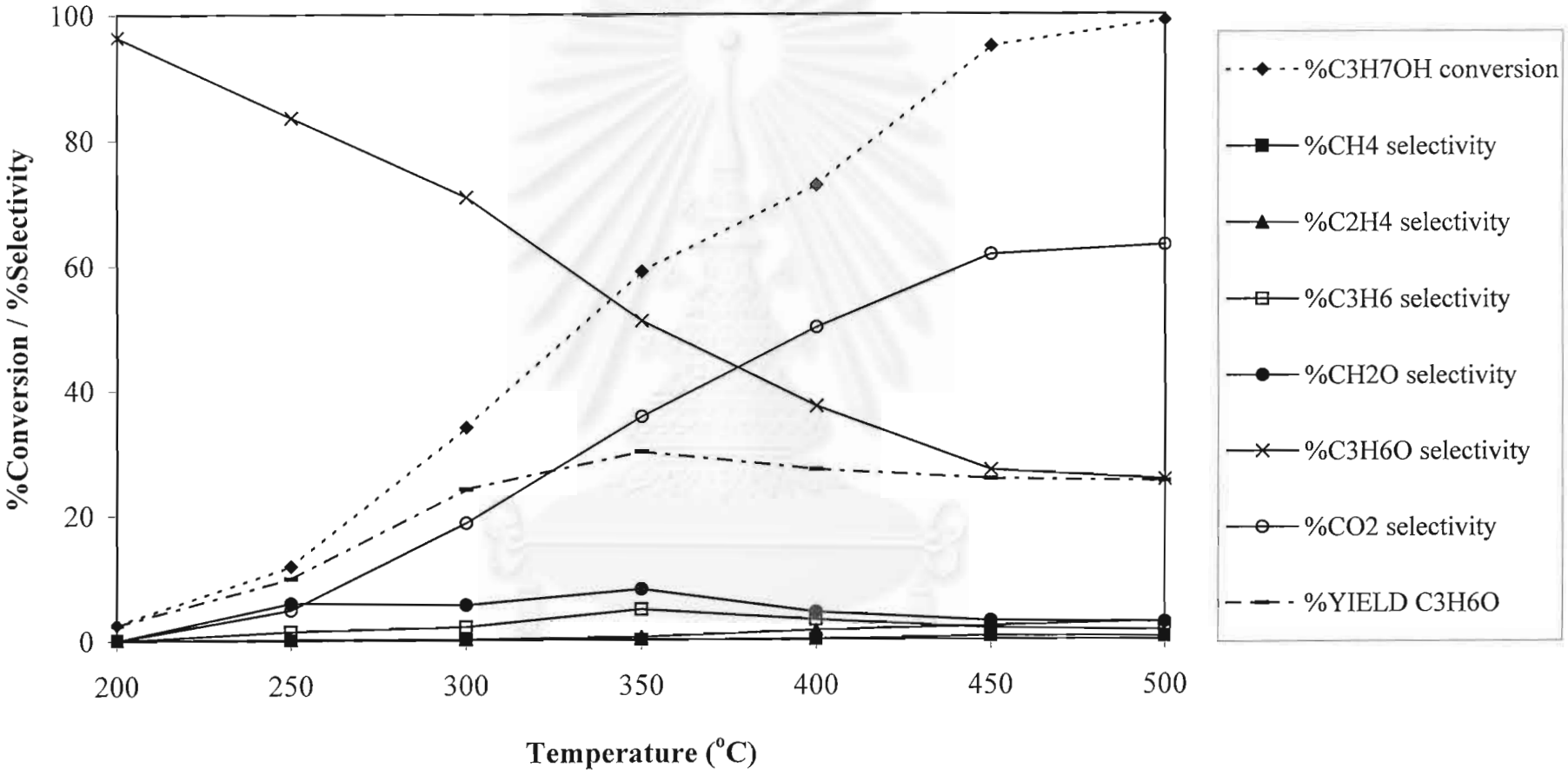

Figure 5.7 The result of 1-propanol oxidation over 0.1 g of 10V2MgTi catalyst (1-propanol/O_2 = 4/10)

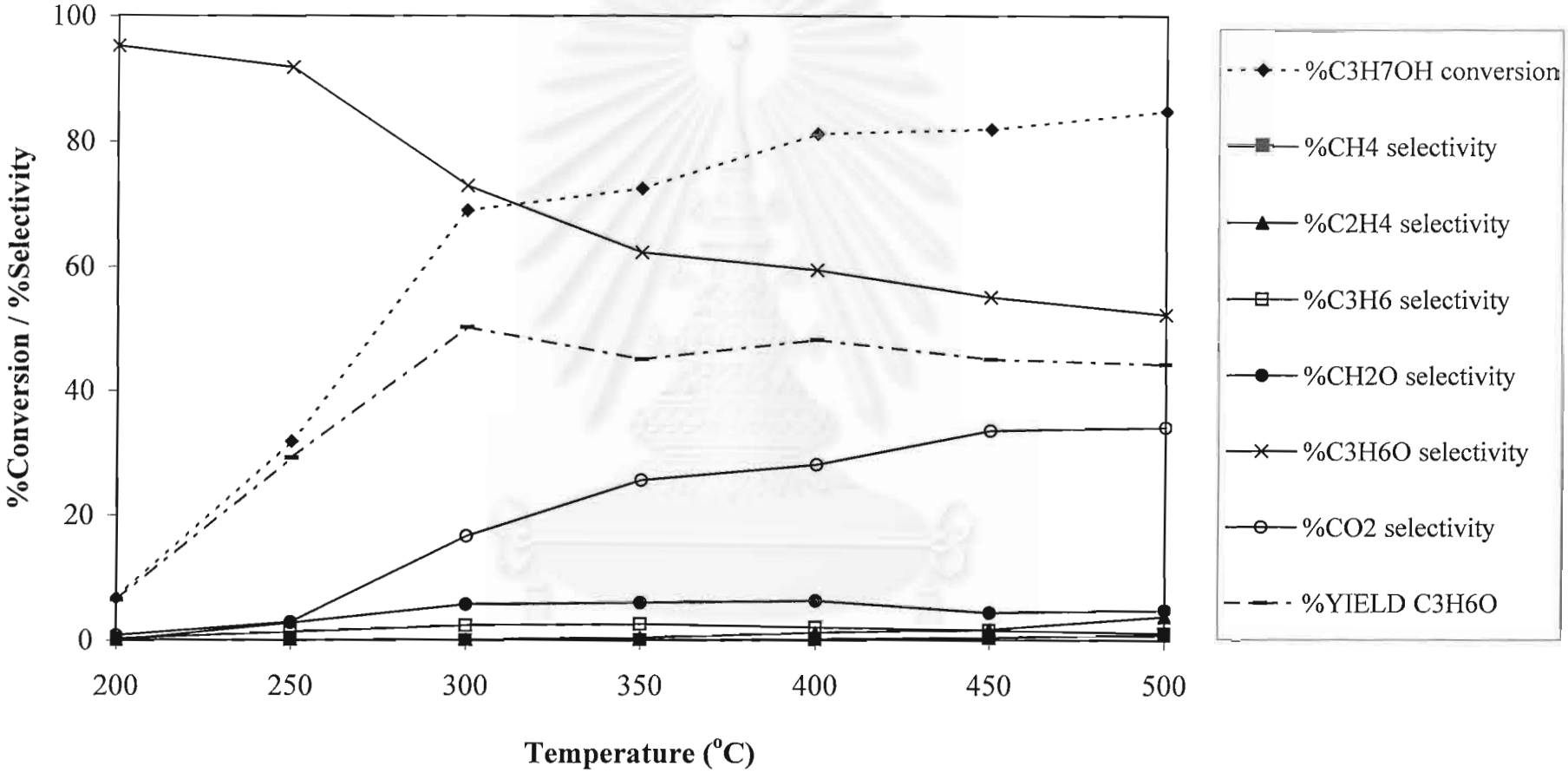

Figure 5.8 The result of 1-propanol oxidation over 0.1 g of 10V2MgTi catalyst (1-propanol/O_2 = 4/5)

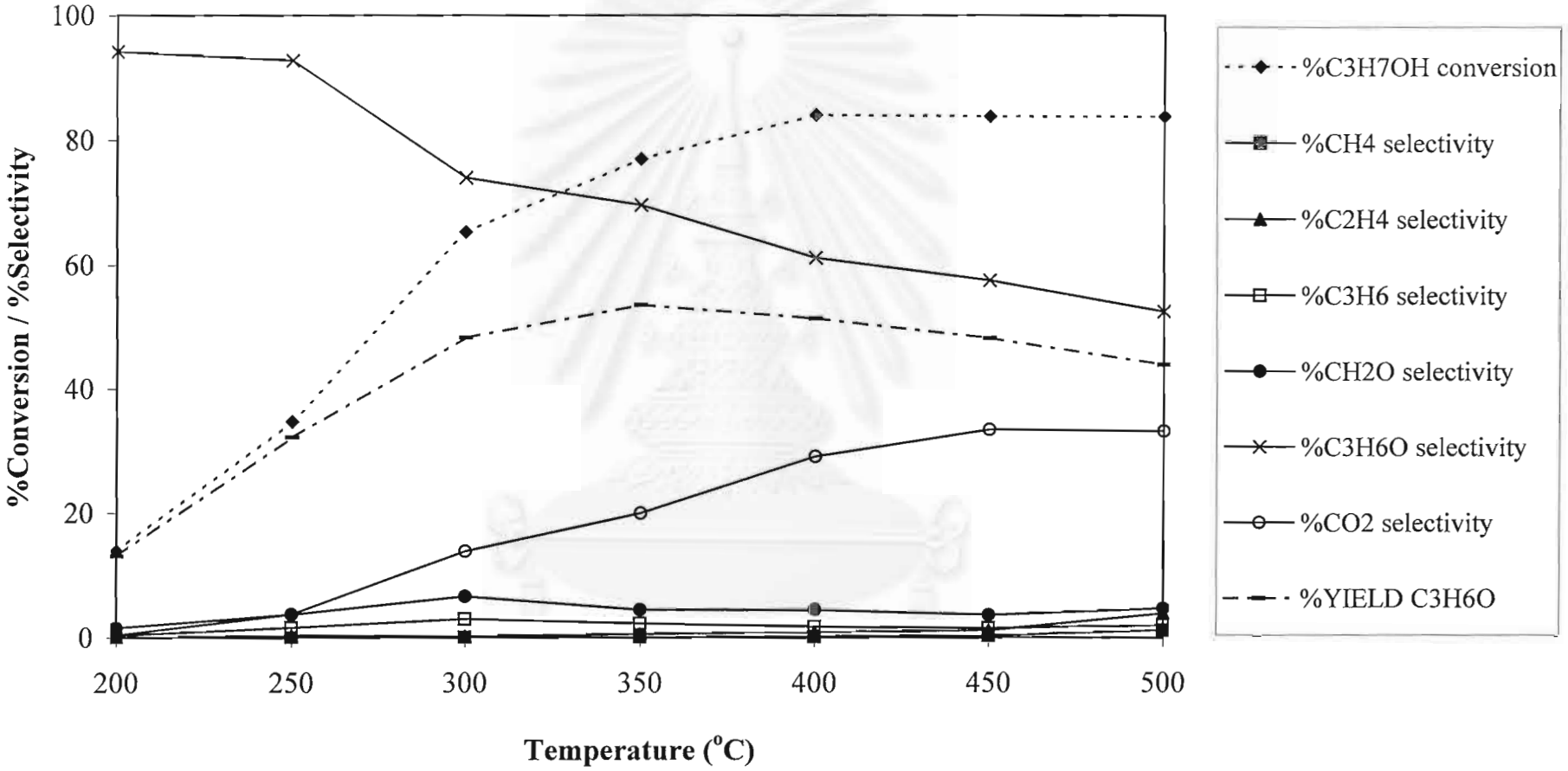

Figure 5.9 The result of 1-propanol oxidation over 0.1 g of 10V2MgTi catalyst (1-propanol/O_2 = 8/5)

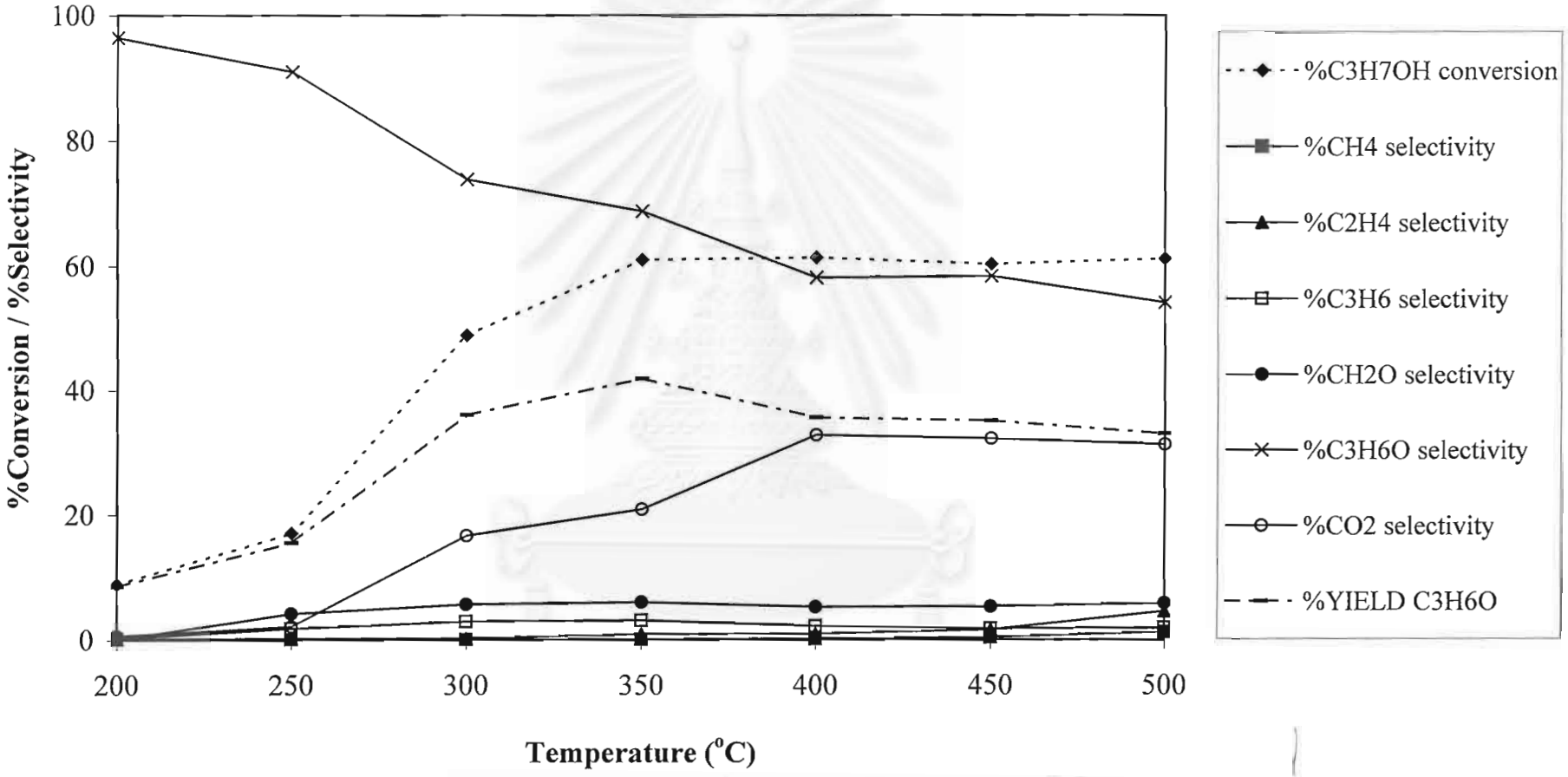

Figure 5.10 The result of 1-propanol oxidation over 0.1 g of 10V2MgTi catalyst (1-propanol/O_2 = 12/5)

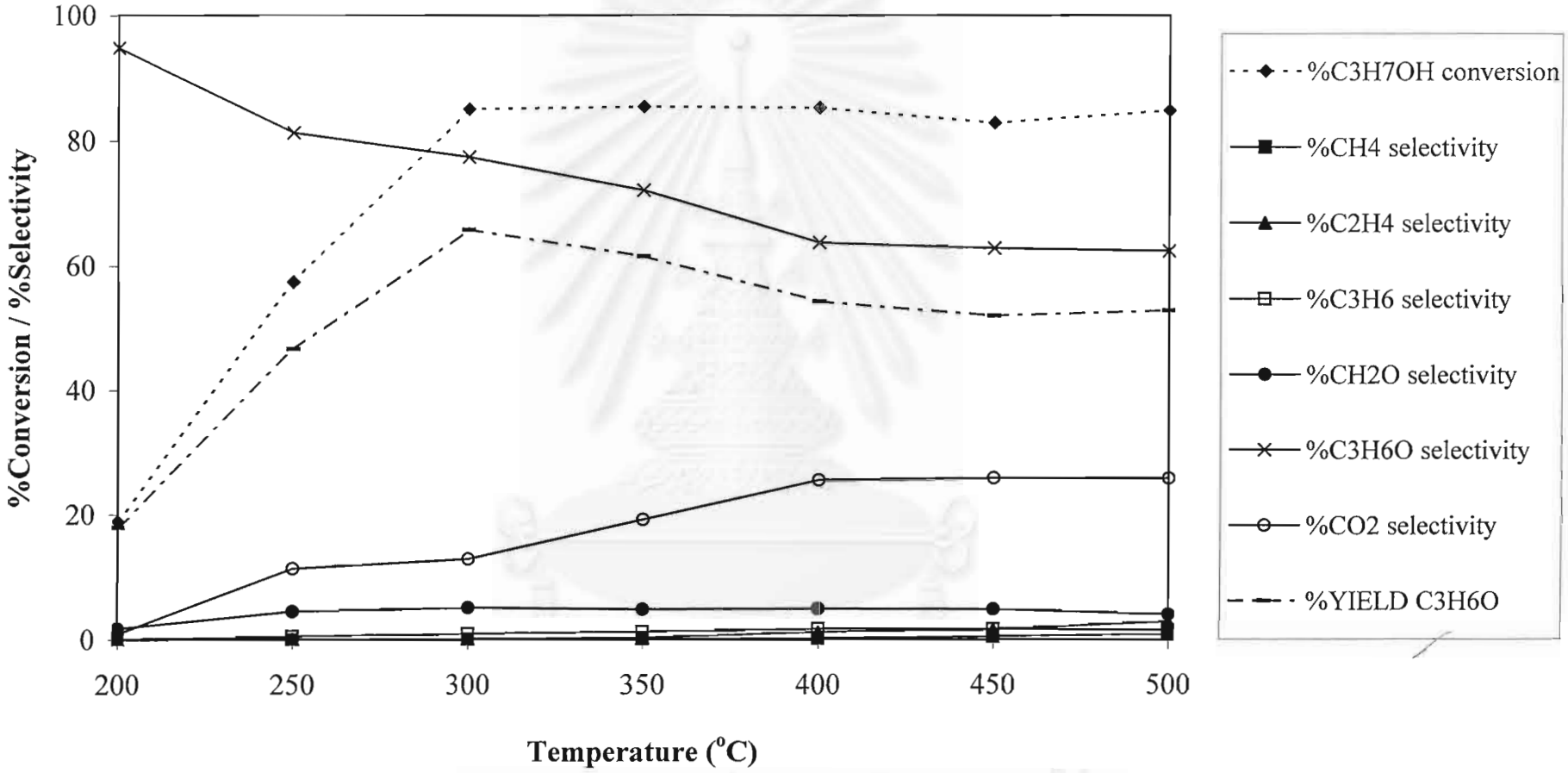

Figure 5.11 The result of 1-propanol oxidation over 0.3 g of 10V2MgTi catalyst (1-propanol/O_2 = 8/5)

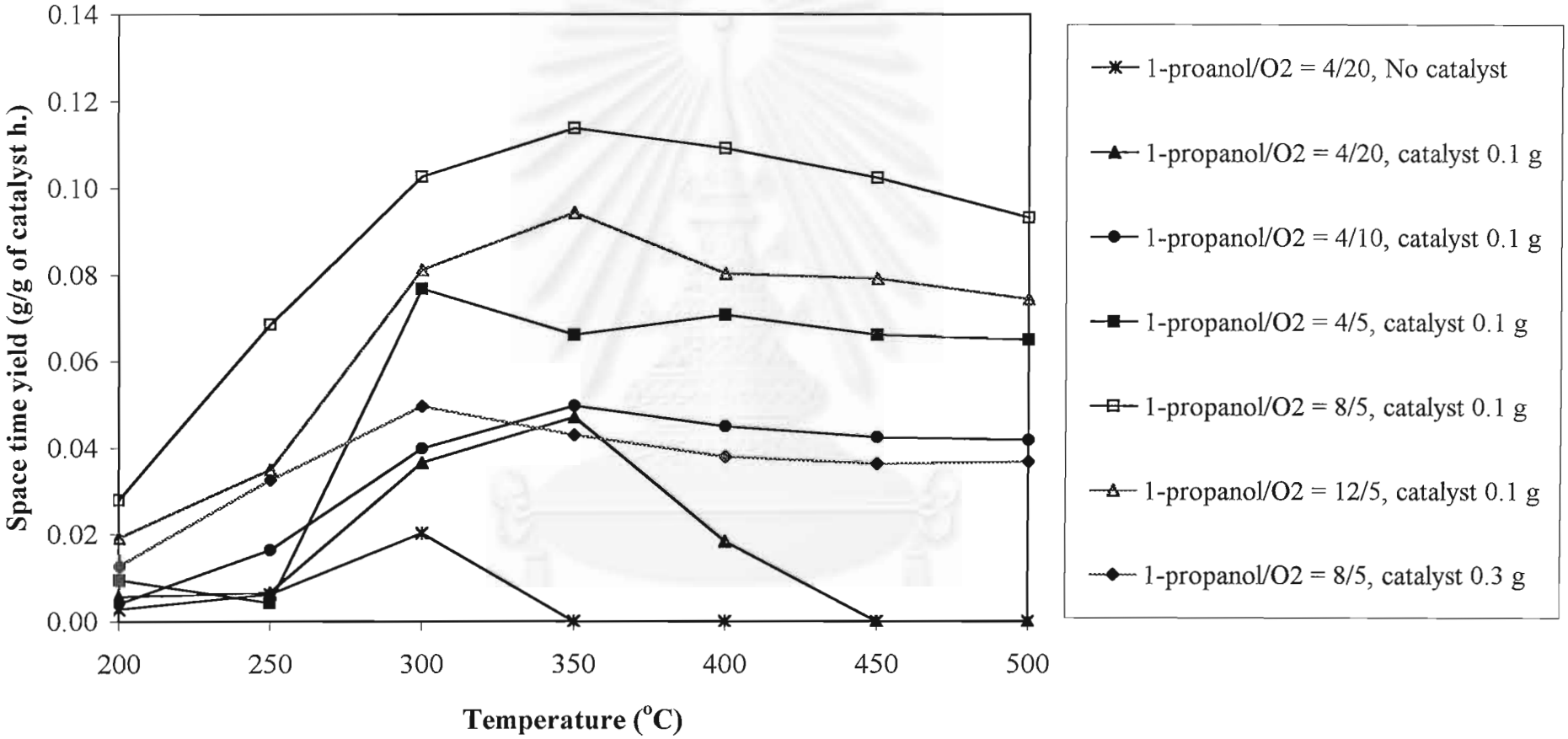

Figure 5.12 Space time yield of propionaldehyde for all conditions

5.2.2 Ethanol Oxidation

Ethanol is in the class of primary alcohol. Thus, the oxidation of ethanol may give acetaldehyde. The performance of 10V2MgTi as catalyst in ethanol oxidation reactions are described in figures 5.13 to 5.19. The ethanol/O_2 ratio used in this reaction are the following: (1) 4/20, (2) 4/10, 3) 4/5, (4) 8/5, (5) 12/5 as in the 1-propanol oxidation.

For all experiments, the major products obtained are acetaldehyde and CO_2. Small amounts of methane, ethene and propene are also detected.

From figures 5.13 to 5.15, the selectivities to acetaldehyde and CO_2 have similar pattern in all cases. This means that the selectivity to acetaldehyde drops continuously with reaction temperature while the selectivity to CO_2 rises continuously to a high value at 500°C. In the first run (ethanol/O_2 = 4/20), as shown in figure 5.13, the conversion of ethanol increases to a maximum value nearly 100% at 400°C. The selectivity to acetaldehyde decreases from 97% at 200°C to 12% at 500°C. In contrast, the selectivity to CO_2 increases from 1% at 200°C to 81% at 500°C. It can be seen that the selectivity to CO_2 is very high. The conversion and product selectivities of the second run (ethanol/O_2 = 4/10), are demonstrated in figure 5.14. It can be observed that the ethanol conversion in this case is identical to the previous one. In addition, a decrease in acetaldehyde selectivity and an increase in CO_2 selectivity are slower, and acetaldehyde yields obtained are higher almost all reaction temperature than the first run (ethanol/O_2 = 4/20). A maximum value of CO_2 selectivity is about 71% at 500°C, which is still high. For the third run (ethanol/O_2 = 4/5), as described in figure 5.15, the conversion and product selectivity trends are rather similar as to the previous cases. But there is the one important point, which should be noted here. It can be obviously seen that the selectivity to CO_2 is much lower than the early two cases, the maximum amount is only 35% at 500°C. Acetaldehyde yield around 50% can be achieved in the reaction temperature range 300-350°C.

From the above results, it can be observed that the conversion and product selectivities are quite the same as 1-propanol oxidation. 5 vol%O_2 content is the best condition, further studies were carried out to get higher acetaldehyde yields. Thus, the amount of ethanol was varied from 4 to 8 and 12 vol%, respectively, and the amount of O_2 was fixed at 5 vol% as in 1-propanol oxidation.

The results of these two later cases (8 and 12 vol% ethanol) are shown in figures 5.16 to 5.17. Considering the conversion of the fourth run (figure 5.16), ethanol/O_2 = 8/5, an increase in reaction temperature causes it to a maximum value about 87% at 500°C. Although, the selectivity to acetaldehyde declines, it is still high. Its value is about 66% at 500°C, the acetaldehyde yields are also higher due to the higher acetaldehyde selectivity. The selectivity to CO_2 enhances slowly, the maximum amount is 25% at 500°C which is lower than the results obtained from figure 5.15 (ethanol/O_2 = 4/5).

Anyway, to get more acetaldehyde yields, the fifth ratio (ethanol/O_2 = 12/5) was used. As presented in figure 5.17, however, the conversion of ethanol is lower than the fourth run (ethanol/O_2 = 8/5), the maximum value is only 70% at 500°C. The selectivities to acetaldehyde and CO_2 have the same trend as the previous case (ethanol/O_2 = 8/5). Acetaldehyde yields obtained are lower for all reaction temperature due to the lower conversions, its maximum value is only 53% at 400°C while the maximum value of 8 vol% ethanol is around 62% at 300°C.

From varying the amounts of O_2 and ethanol, it can be concluded that 5 vol% O_2 and 8 vol% ethanol are suitable for the ethanol oxidation reaction. The selectivity to CO_2 is quite low while acetaldehyde yields are rather high.

Moreover, from all above experiments, only 0.1 g of 10V2MgTi is used. Thus, there was a further study to investigate the influence of catalyst content or GHSV. The ethanol/O_2 ratio remained constant at 8/5 and the amount of 10V2MgTi was varied form 0.1 to 0.3 g or GHSV changes from 60,000 to 20,000 ml/hr. g of catalyst.

As shown in figure 5.18, the conversion rises faster than the case of 0.1 g. The selectivity to acetaldehyde is higher whereas CO_2 selectivity is nearly constant with the previous one (0.1 g of catalyst). The highest acetaldehyde yield obtained is about 73% at 350°C.

From the above results, it can be observed that an increase in the amount of catalyst gives the better acetaldehyde yields. It is known that the reaction is occurred in the catalyst bed when increase the amount of catalyst, the height of bed is higher too. The reactants have more contact time and the reaction should be more occurred.

For the space time yield of acetaldehyde as described in figure 5.19, it is shown that the result obtained has similar pattern as the case of propioanldehyde. At the ethanol/O_2 ratio = 8/5 and 0.1 g of catalyst give the highest acetaldehyde space time yield. Its value is also lower than the case of 4 vol% ethanol as in the case of propanol oxidation.

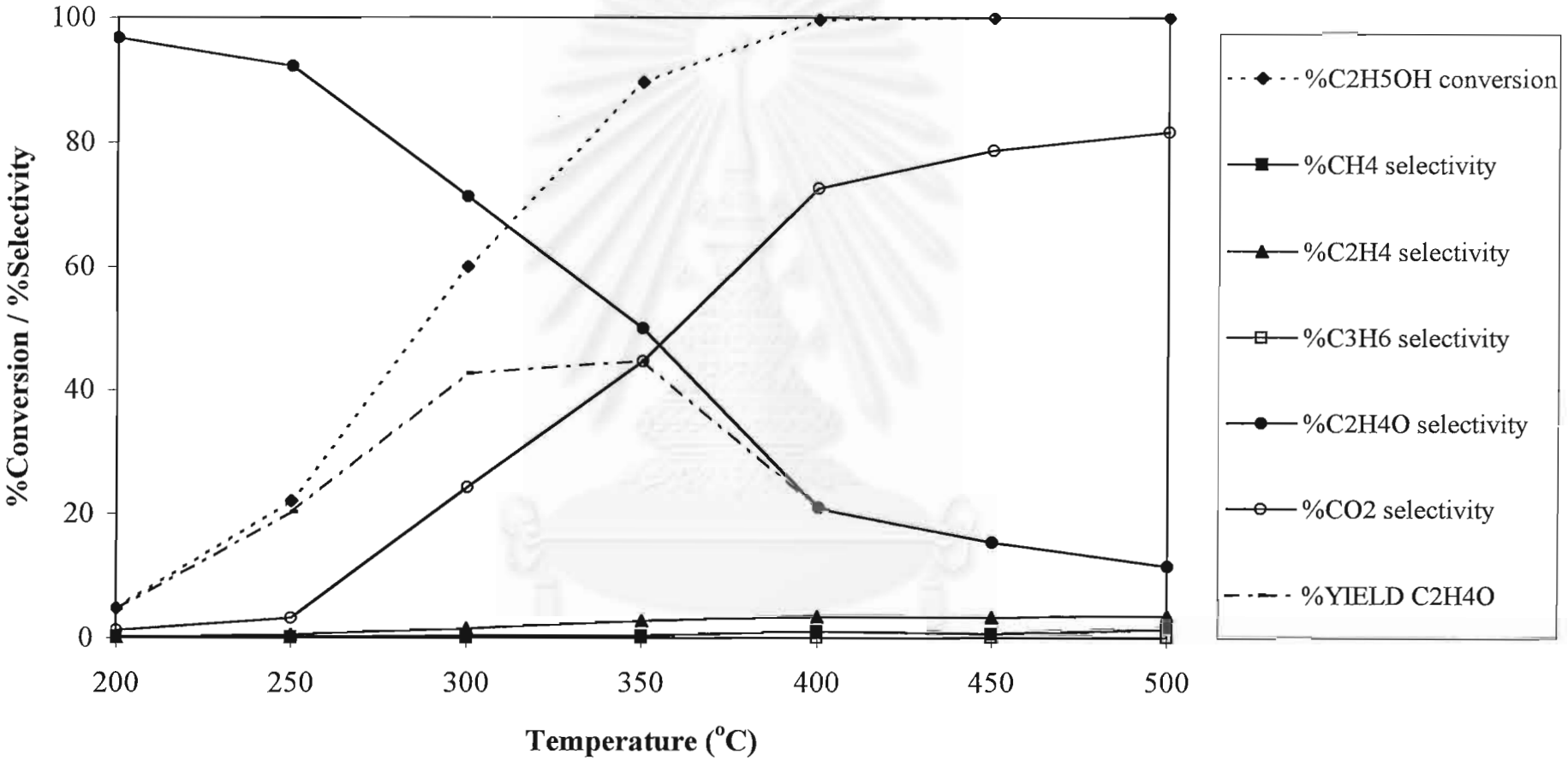

Figure 5.13 The result of ethanol oxidation over 0.1 g of 10V2MgTi catalyst (ethanol/O_2 = 4/20)

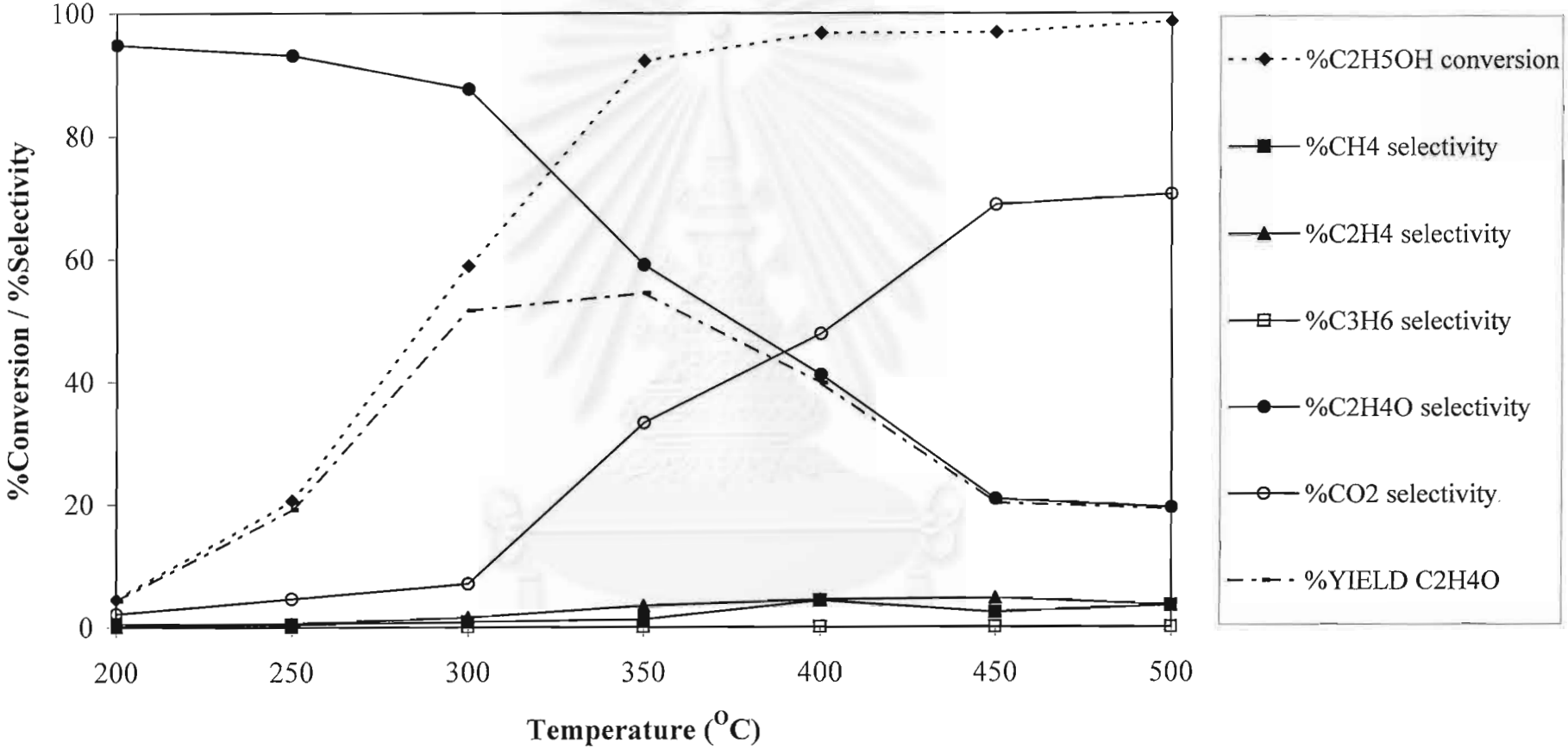

Figure 5.14 The result of ethanol oxidation over 0.1 g of 10V2MgTi catalyst (ethanol/O_2 = 4/10)

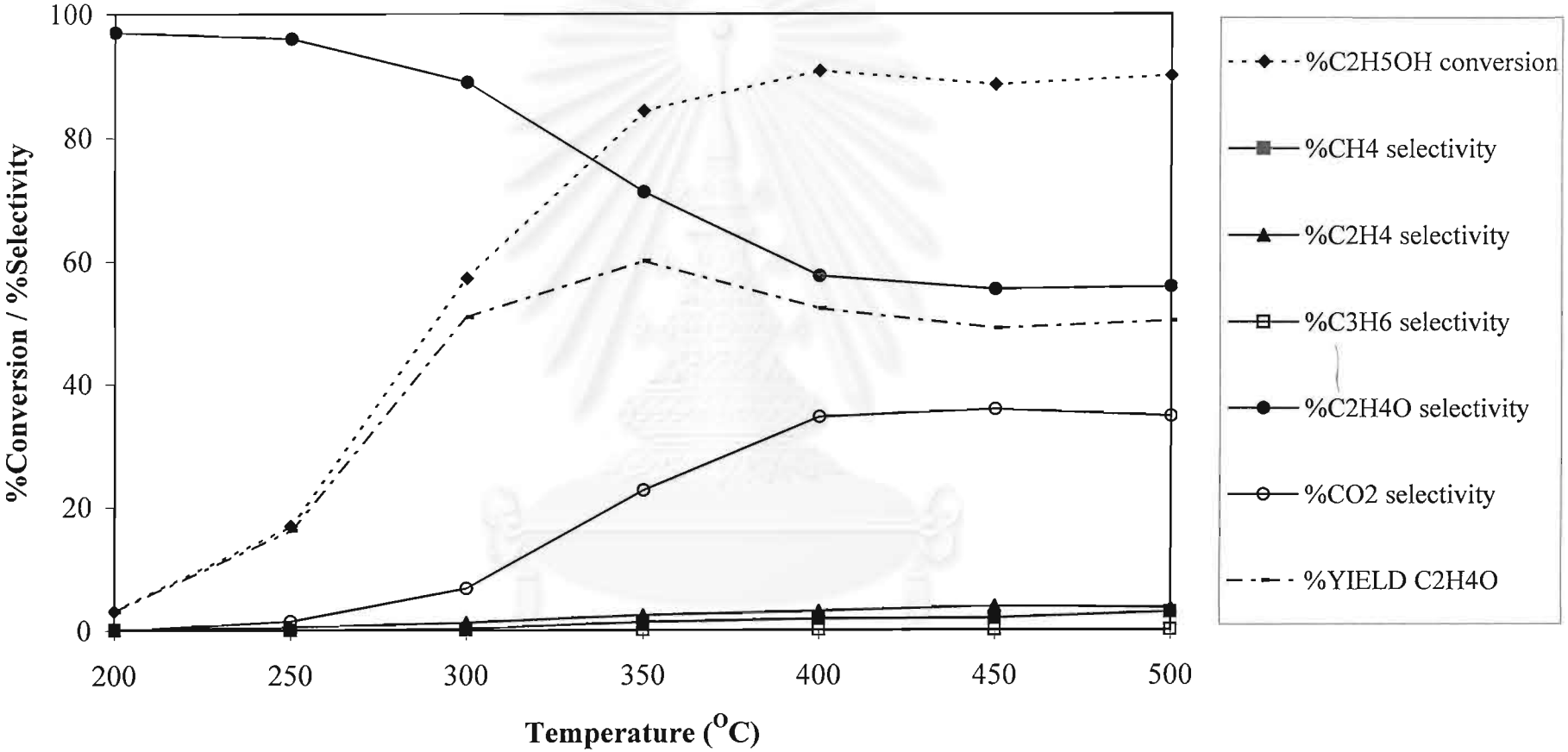

Figure 5.15 The result of ethanol oxidation over 0.1 g 10V2MgTi catalyst (ethanol/O_2 = 4/5)

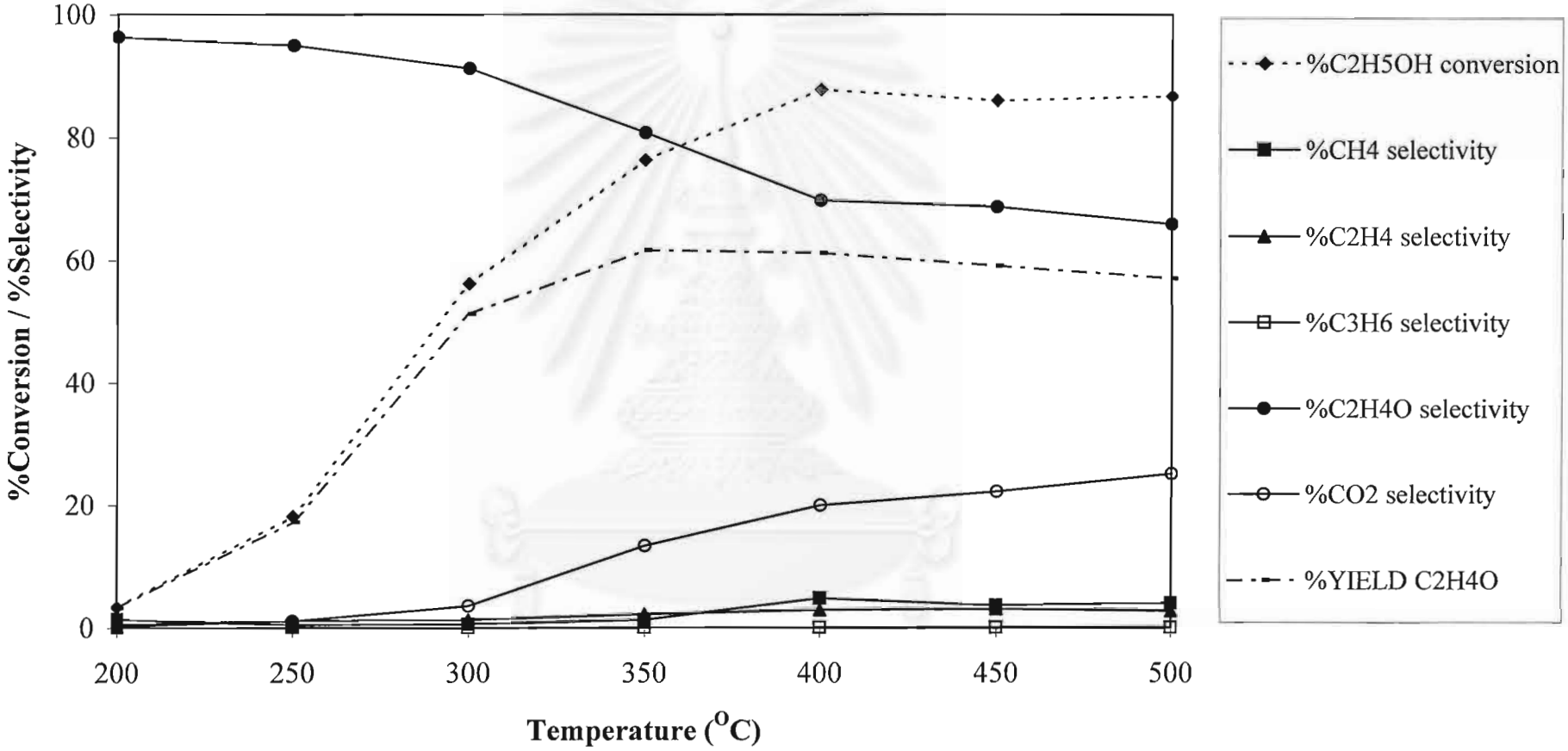

Figure 5.16 The result of ethanol oxidation over 0.1 g of 10V2MgTi catalyst (ethanol/O_2 = 8/5)

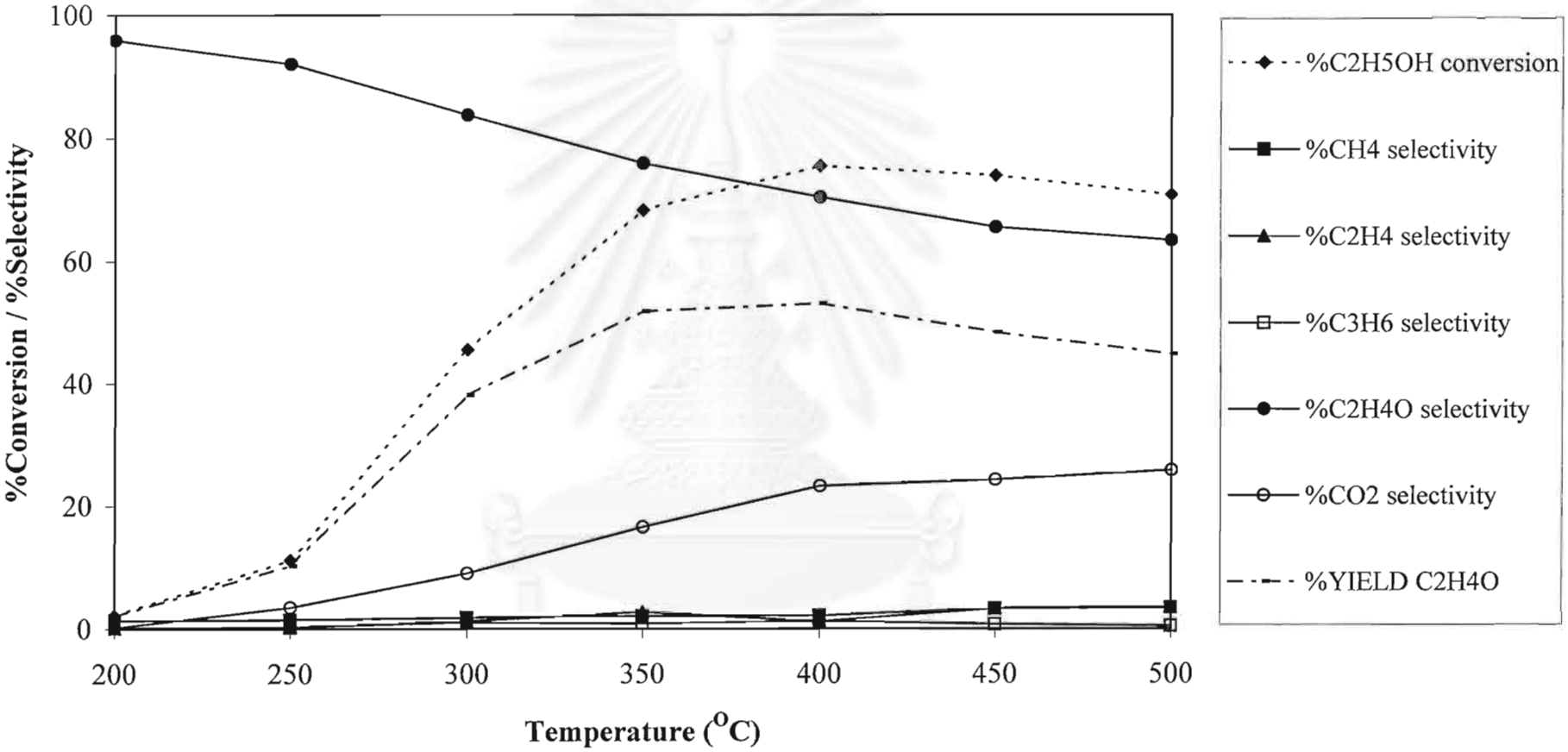

Figure 5.17 The result of ethanol oxidation over 0.1 g of 10V2MgTi catalyst (ethanol/O_2 = 12/5)

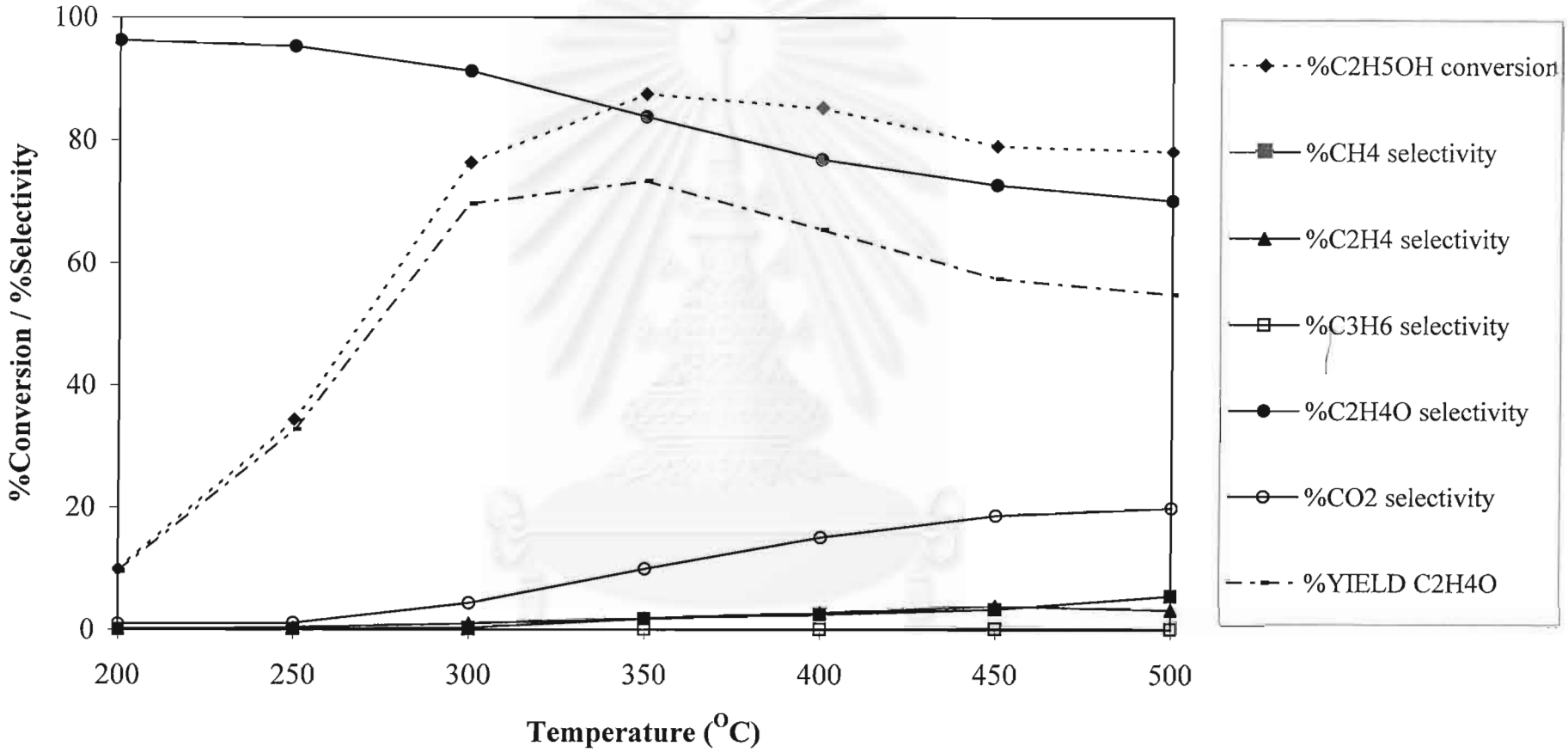

Figure 5.18 The result of ethanol oxidation over 0.3 g of 10V2MgTi catalyst (ethanol/O_2 = 8/5)

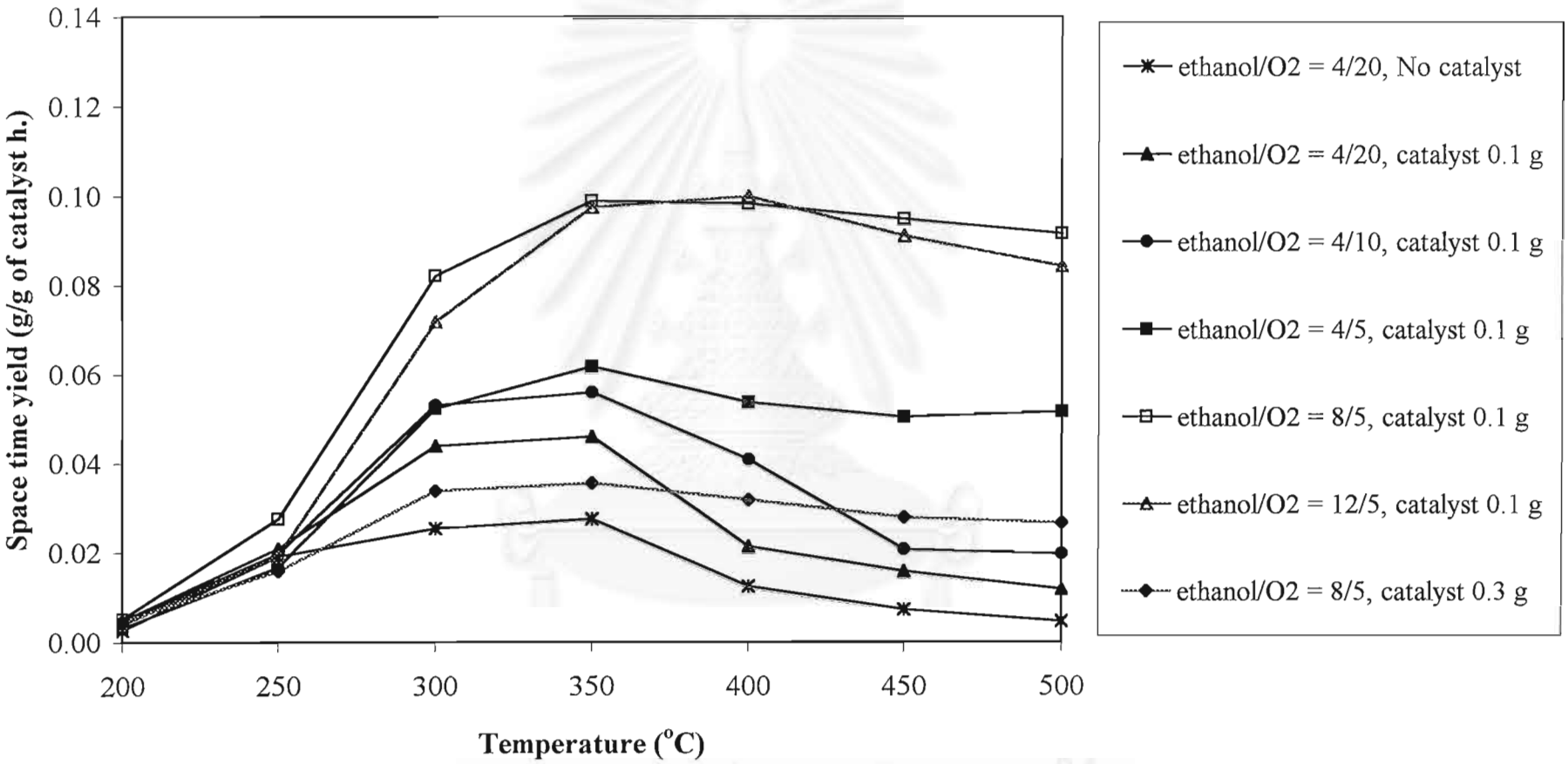

Figure 5.19 Space time yield of acetaldehyde for all conditions

From the results of 1-propanol and ethanol oxidation reactions, as shown in figures 5.6 to 5.19, the main products obtained at low temperature are aldehydes, namely propionaldehyde and acetaldehyde, respectively. Whereas CO_2 comes to be important at high temperature. It can be proposed that propionaldehyde and acetaldehyde are the intermediates in these two reactions by further reacting to the combustion product, CO_2.

In both reactions a decrease in the amount of O_2 in feed stream causes the reduction of CO_2 formed and an increase in the amount of alcohol results in the higher of aldehyde yields produced. However, there is one optimal alcohols/O_2 ratio, which gives the best results, i.e., 8/5. Additionally, an increase in the content of catalyst used from 0.1 to 0.3 g also gives better results. Nevertheless, when considering the space time yields of acetaldehyde and propionaldehyde, at the alcohol/O_2 ratio =8/5 with 0.3 g of catalyst is not the best condition since the space time yields are lower than the case of 0.1 g of catalyst at the same alcohol/O_2 ratio.

5.2.3 Methanol Oxidation

The performances of 10V2MgTi catalyst for methanol oxidation are described in figures 5.20 and 5.21. From figure 5.20 (methanol/O_2 = 8/5), it can be observed that CO_2 and a small amount of methane are the main products in this reaction. CO is observed at high temperature and traces of ethene and propene are also obtained. The conversion rises continuously with the reaction temperature up to nearly 100% at 500°C. The selectivity to methane slightly rises from about 3% at 200°C to 6% at 400°C, and is thereafter approximately constant at 6%. The selectivity to CO_2 declines slowly from 96% at 200°C to 75% at 500°C, while the selectivity to CO increases gradually from 0.85% at 300°C to 18.5% at 500°C.

Because of the production of CO at high temperature, this reaction is proposed to be non-complete combustion. Thus, the amount of O_2 in feed stream is raised from 5 vol% to 20 vol% in order to investigate a type of combustion.

From figure 5.21 (methanol/O_2 = 8/20), CO_2 is the major product observed. Small amount of methane is also formed but not exceed 1%. The conversion increases with reaction temperature from 5% at 200°C nearly to 100% at 350°C. The selectivity of CO_2 is ca. 98% and nearly constant at all reaction temperature.

From the results in figure 5.21(methanol/O_2 = 8/20), since CO_2 is the only main product, it can be concluded that an excess amount of O_2 is necessary to proceed this reaction to the complete combustion. As presented from figure 5.20, it can be seen that CO_2 is the major product for all reaction temperature whereas CO is produced at high temperature. Consequently, it can be concluded that this reaction is not complete combustion.

Furthermore, from the above results, it can be seen that the main products obtained are CO_2 and CO, hence, 10V2MgTi is not a selective catalyst for the methanol oxidation.

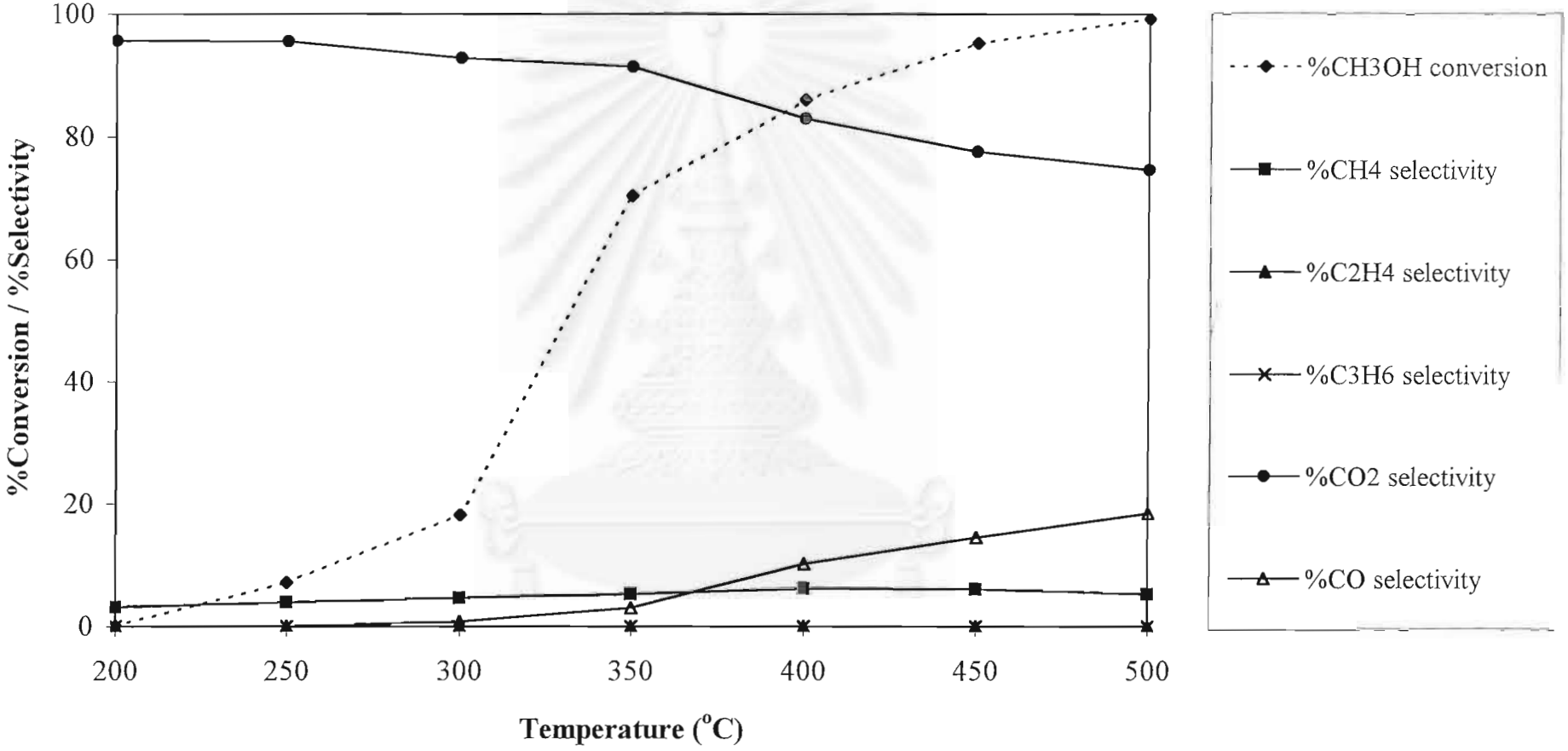

Figure 5.20 The result of methanol oxidation over 0.1 g of 10V2MgTi catalyst (methanol/O_2 = 8/5)

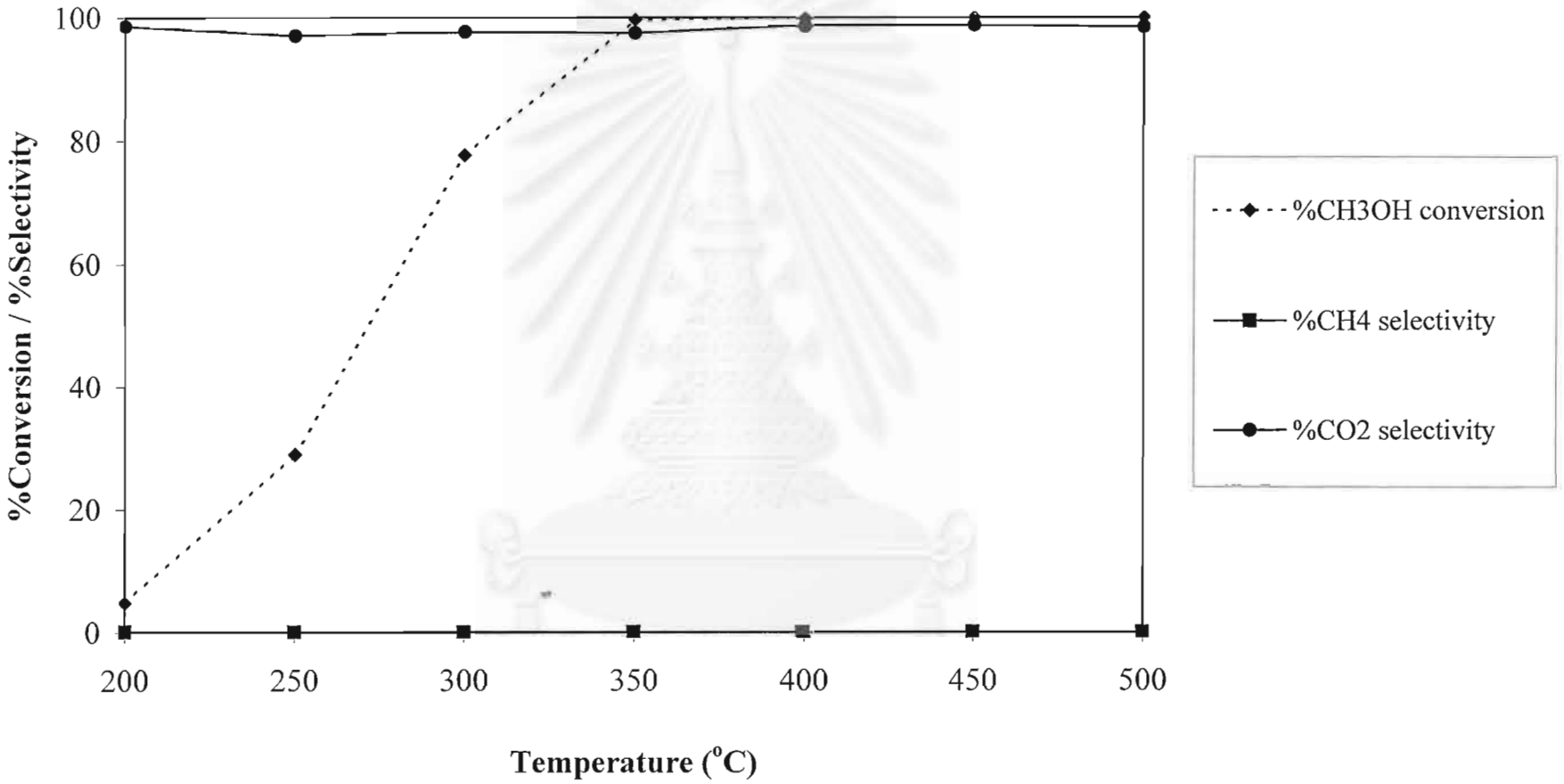

Figure 5.21 The result of methanol oxidation over 0.1 g of 10V2MgTi catalyst (methanol/O_2 = 8/20)

5.2.4 2-Propanol Oxidation

The behavior of 10V2MgTi catalyst for 2-propanol oxidation is presented in figure 5.22. From this figure, propene and CO_2 are the major products. Small amounts of methane, ethene and propane are also formed. The conversion increases continuously from 1% at 200°C to 49% at 450°C. The selectivity to propene is very high at the beginning reaction temperature but drops gradually to 36% at 500°C. In contrast, CO_2 selectivity rises to a maximum value about 56%.

In this reaction, propene produced as the main product, not acetone which contains the carbonyl group, C=O, as in 1-propanol oxidation reaction. It is known that 2-propanol is in the class of secondary alcohol, the reaction mechanism, thus, may be or may be not the same as in 1-propanol oxidation. One reason that can be attributed to the production of propene is the ease of the dehydration which follows by this order: tertiary > secondary > primary. The intrinsic mechanism of this reaction including of 1-propanol oxidation will be discussed in the next topic.

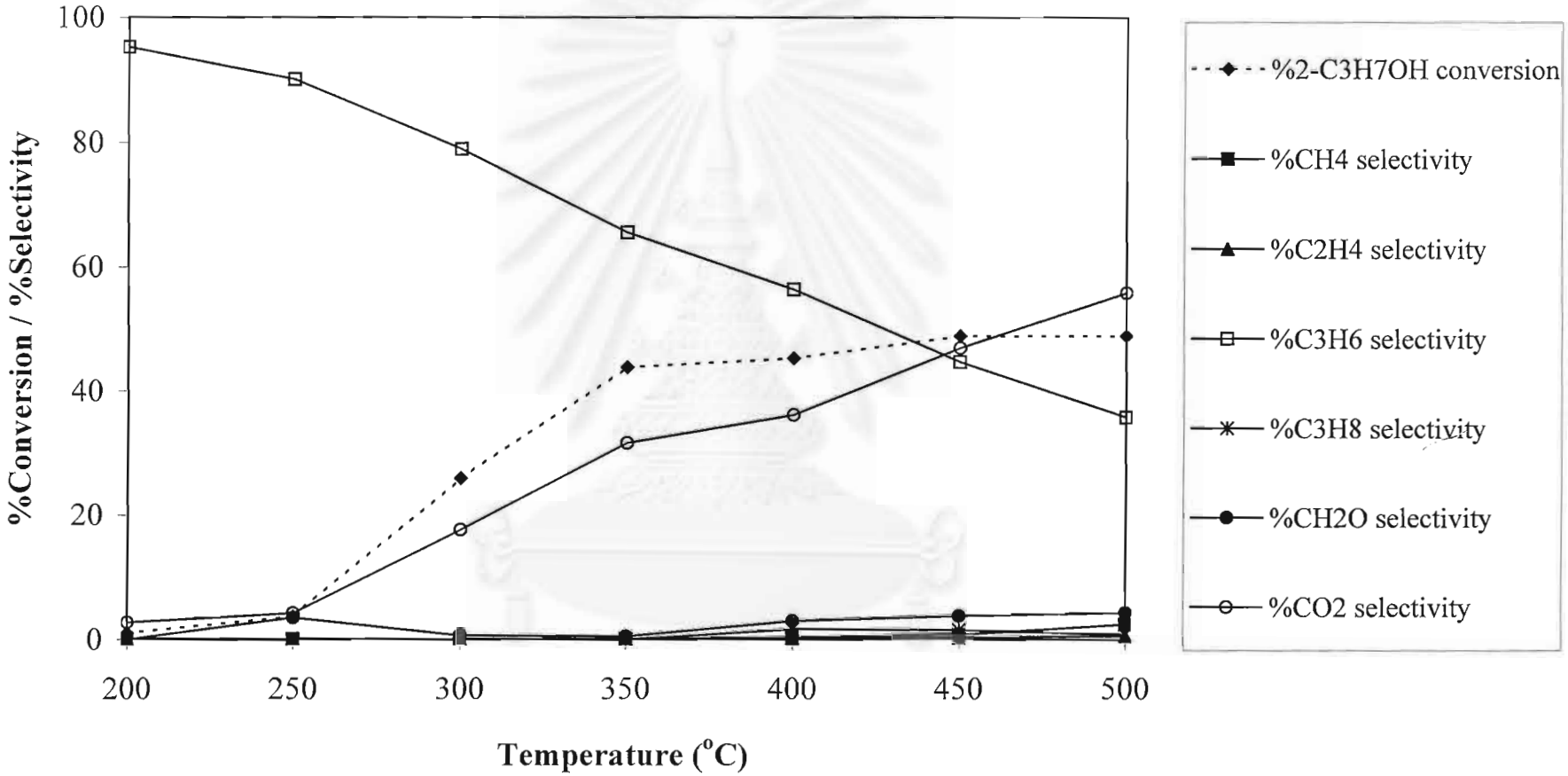

Figure 5.22 The result of 2-propanol oxidation over 0.1g of 10V2MgTi catalyst (2-propanol/O_2 = 8/5)

5.2.5 Reaction mechanism

The products obtained from ethanol and 1-propanol oxidation reactions are acetaldehyde and propionaldehyde, respectively, which are the same kind compounds. Thus, the mechanisms of these two reactions have the same pattern.

For 2-propanol oxidation reaction, the product obtained is propene which is different from the case of 1-propanol oxidation. Hence, the reaction mechanism of 2-propanol oxidation will be different from the mechanism of 1-propanol oxidation.

Due to the difference in the product obtained form 1-propanol and 2-propanol oxidation, namely, propionaldehyde and propene, respectively. Therefore, the reaction mechanisms of 1-propanol and 2-propanol oxidation are proposed in the following pictures to describe this difference.

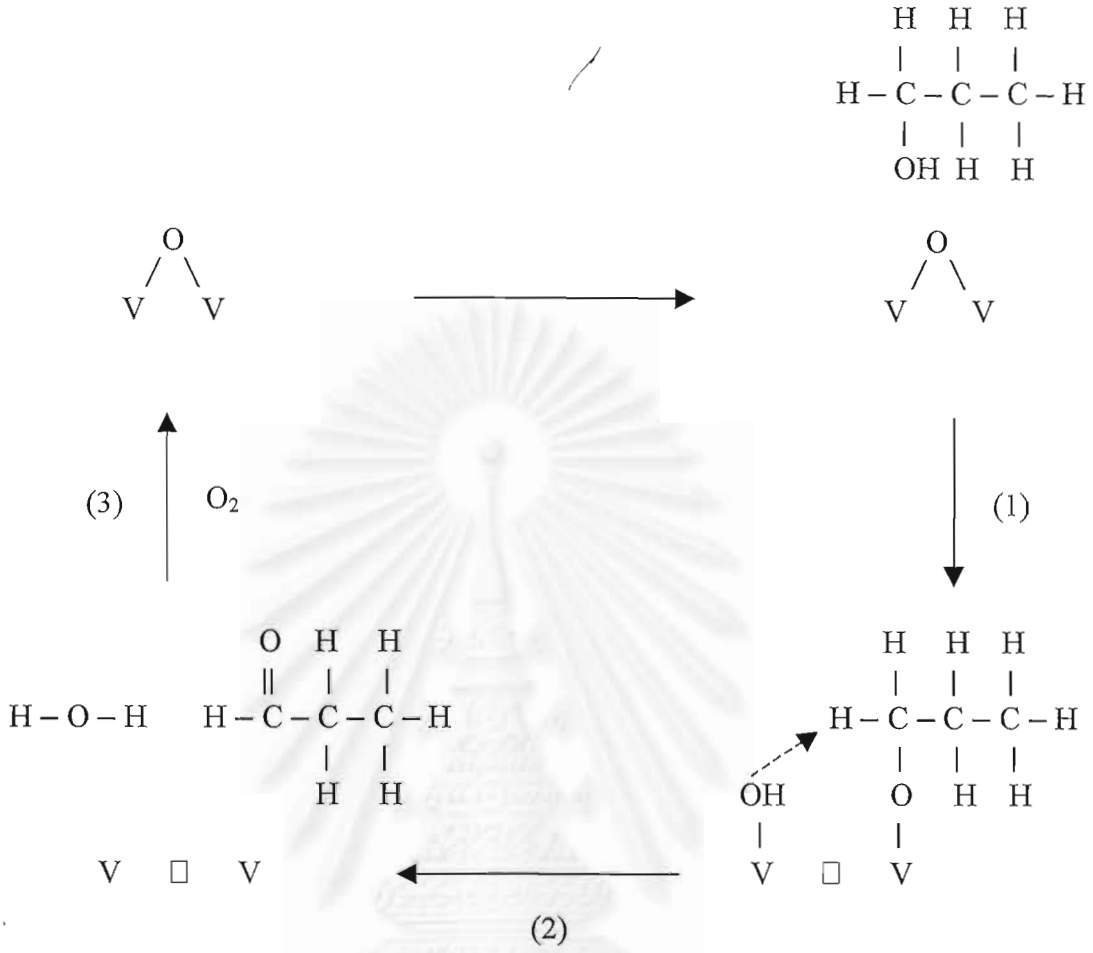

Figure 5.23 The mechanism of the oxidation of 1-propanol to propionaldehyde

The reaction mechanism of 1-propanol as presented in figure 5.21 is comprised of the following steps:

1. Adsorption of 1-propanol on V– O – V site to produce adsorbed alkoxide species and – OH species.

2. Abstraction of H atom from the adsorbed alkoxide species by the – OH species to form water and aldehyde product. The desorption of water causes a vacant oxygen V–□–V site on the catalyst surface.

3. Oxygen from the gas phase reoxidized V–□–V site to produce V–O–V site again.

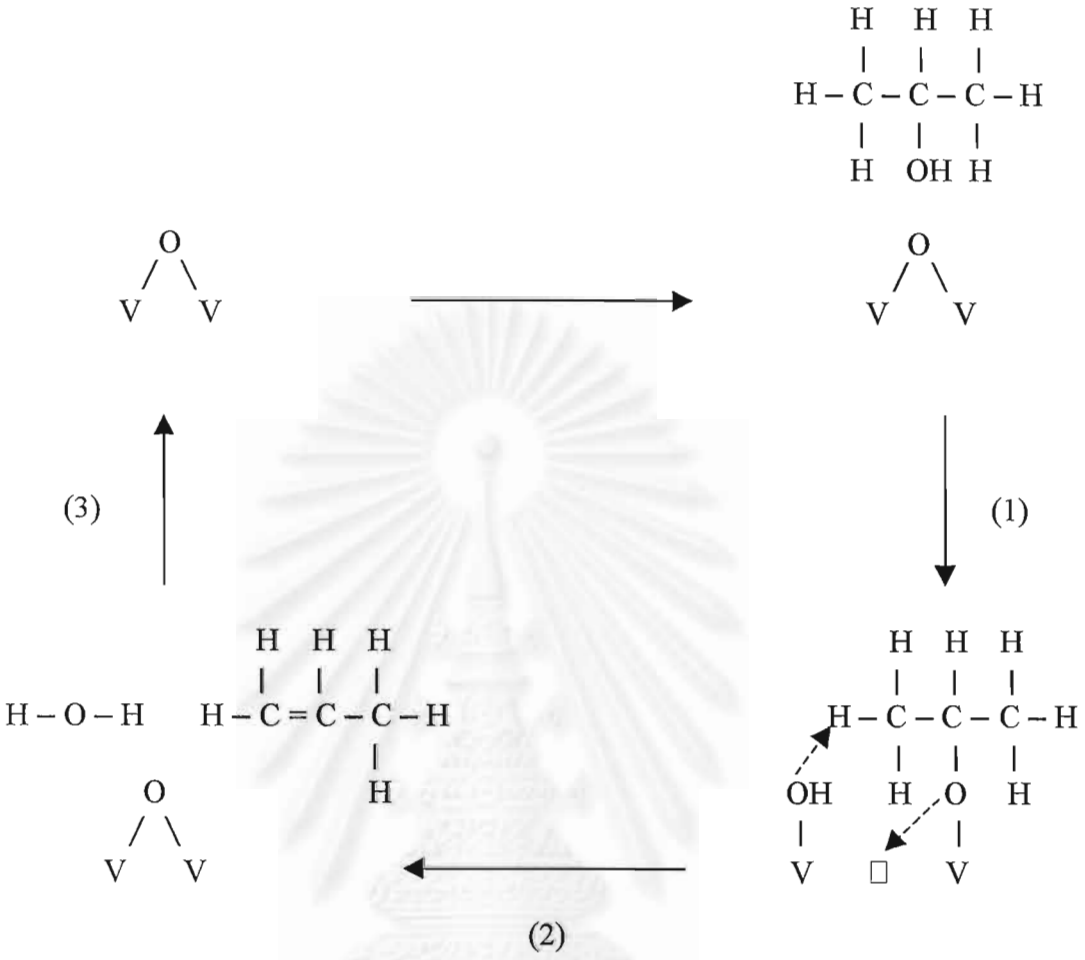

Figure 5.24 The mechanism of the oxidation of 2-propanol to propene

The reaction mechanism of 2-propanol as presented in figure 5.22 is comprised of the following steps:

1. Adsorption of 2-propanol via –OH group on V–O–V site to produce adsorbed alkoxide species and –OH group on catalyst surface.

2. Abstraction of H atom from the adsorbed alkoxide species by the surface –OH group to produce H_2O and propene. The catalyst surface return to V–O–V site.

Moreover, from these mechanisms, as presented in figures 5.23 and 5.24, it should be noted that propionaldehyde formed from the 1-propanol oxidation is the dehydrogenation product which is occurred by breaking the O-H bond. While the dehydration product, propene, from 2-propanol oxidation is occurred by breaking the C-O bond.

Since alkyl groups have a +I effect, there will be an increased electron displacement towards the oxygen atom in going from primary to secondary to tertiary alcohol. This may be represented (qualitatively) as follows:

$$\mathrm{Me \rightarrow CH_2 \rightarrow {}^{\delta-}O \rightarrow H} \qquad \begin{matrix} \mathrm{Me} \\ \downarrow \\ \mathrm{CH} \rightarrow\rightarrow \end{matrix} {}^{2\delta-}\mathrm{O} \rightarrow\rightarrow \mathrm{H} \qquad \begin{matrix} \mathrm{Me} \\ \downarrow \\ \mathrm{Me \rightarrow C} \rightarrow\rightarrow\rightarrow \end{matrix} {}^{3\delta-}\mathrm{O} \rightarrow\rightarrow\rightarrow \mathrm{H}$$

$$\begin{matrix} \uparrow \\ \mathrm{Me} \end{matrix} \qquad\qquad \begin{matrix} \uparrow \\ \mathrm{Me} \end{matrix}$$

The greater the negative charge on the oxygen atom, the closer is the covalent pair in the O-H bond driven to the hydrogen atom and consequently separation of a proton becomes increasingly difficult. Thus the acid strengths of alcohols will be in the order : primary > secondary > tertiary.

From what has been said above, it can be seen that the tendency for the C-O bond to break will be the reverse of that for the O-H bond, i.e., reactions involving the breaking of the C-O bond will follow the order of reactivity : tertiary > secondary > primary.

Consequently, from these mechanisms (figures 5.23 and 5.24) and all the above results, it can be ascribed that why the cleavage of O-H bond of an intermediate in the oxidation of 1-propanol which is in the class of primary alcohol is more preferentially occurred. Whereas the cleavage of C-O bond of an intermediate in the oxidation of 2-propanol which is in the class of secondary alcohol to form propene is more favored happened than in the case of 1-propanol oxidation.

Additionally, from the mechanism of 2-propanol oxidation to propene as presented in figure 5.24, it can be seen that O_2 in gas phase is not incorporated in this mechanism. Consequently, a further study is performed by using the 2-propanol/O_2 ratio equals to 8/0 to investigate the sensitivity of O_2 content in this reaction.

From figure 5.25, it is shown that the reaction can occur without O_2 in the feed stream. Propene is the main product observed in this reaction. The conversion is very high, its value is almost constant about 97%. The selectivity to propene is about 25%. However, it should be noted that the total selectivity of C-balanced is not 100% because there is a carbonaceous compound formed.

Hence, O_2 is necessary in the 2-propanol oxidation for preventing the production of the carbonaceous compound, although, it is not incorporated in the reaction mechanism.

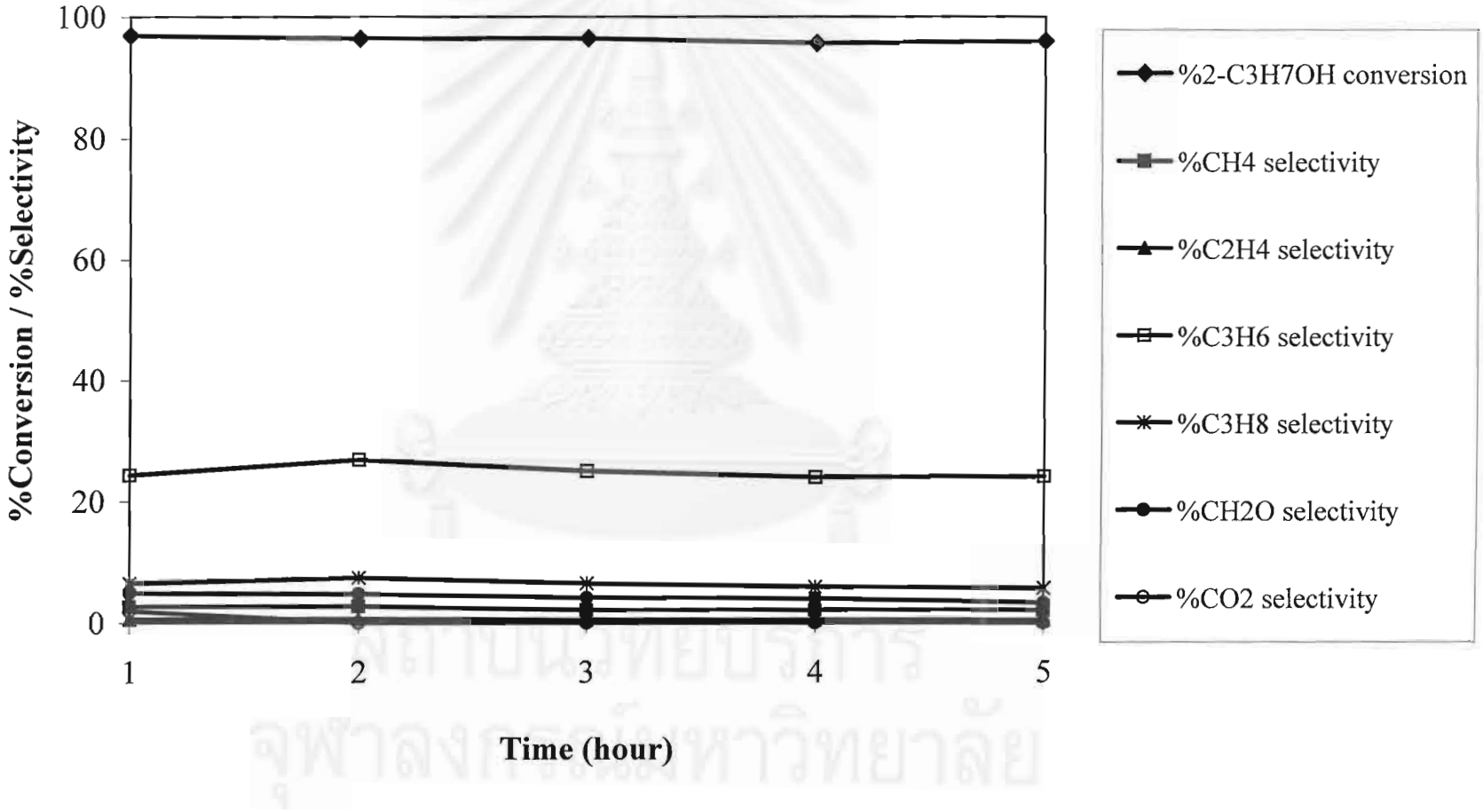

Figure 5.25 The result of 2-propanol oxidation over 0.1 g of 10V2MgTi catalyst (2-propanol/O_2 = 8/0)

CHAPTER VI

CONCLUSIONS AND RECOMMENDATIONS

6.1 Conclusions

The conclusions of this research are summarized as follows:

The selective oxidation of ethanol and 1-propanol

1. The results of these two reactions are rather the same both in the conversion and in the product selectivity trends. The main products obtained at low temperature are aldehydes namely acetaldehyde and propionaldehye, respectively. While CO_2 becomes important at high temperature.

2. A decrease in the amount of O_2 causes the reduction of CO_2 selectivity while an increase in the amount of alcohol and catalyst results in the higher aldehyde yields obtained.

The selective oxidation of methanol

10V2MgTi is not a suitable catalyst for this reaction since the main product observed is CO_2 which is not the valuable product as in ethanol and 1-propanol oxidation.

The selective oxidation of 2-propanol

The product obtained from this reaction is propene which is different from the case of 1-propanol oxidation. Because they are in the different class of alcohol, thus, the mechanisms for these two reactions are dissimilar.

6.2 Recommendation for future studies

1. From the above conclusions, it can be seen that 10V2MgTi is the effective catalyst for the selective oxidation reactions of ethanol and 1-propanol which are in the class of primary alcohol. Hence, it will be interesting to further study the selective oxidation of the higher primary alcohol molecule such as 1-butanol and 2-pentanol. Moreover, due to the difference of the product obtained from 2-propanol and 1-propanol, it will also be interesting to study the selective oxidation of higher secondary alcohol molecule such as 2-butanol and 2-pentanol in order to investigating the product distributions.

2. In this research, only 10V2MgTi catalyst is used, therefore, it will be interesting to study the influence of the amounts of vanadium and magnesium on the conversion and the product distributions of the selective oxidation of alcohol.

REFERENCES

Bettahar, M.M.., Costentin, G., Savary, L. and Lavalley, J.C., "On the partial oxidation of propane and propylene on mixed metal oxide catalysts", Appl. **Catal. A. General. 145** (1996) : 1.

Bhattacharyya, D., Bej, S.K. and Rao, M.S., "Oxidative dehydrogenation of n-butane to butadiene. Effect of different promoters on the performance of vanadium-magnesium oxide catalysts", **Appl. Catal. 87** (1992) : 29.

Bond, B.C. and Tahir, S.F., "Vanadium oxide monolayer catalysts. Preparation, characterization and catalytic activity", **Appl. Catal. 71** (1991) : 1.

Busca, G., "Spectroscopic characterization of the acid properties of metal oxide catalysts", **Catal. Today. 41** (1998) : 191.

Cavani, F. and Trifiro, F., "The oxidative dehydrogenation of ethane and propane as an alternative way for the production of light olefins", **Catal. Today. 24** (1995) : 307.

Chaar, M.A., Patel, D., Kung, M.C. and Kung, H.H., "Selective oxidative dehydrogenation of butane over V-Mg-O catalysts", **J. Catal. 105** (1987) : 483.

Chaar, M.A., Patel, D. and Kung, H.H., "Selective oxidative dehydrogenation of propane over V-Mg-O catalysts", **J. Catal. 109** (1988) : 463.

Corma, A., Nieto, J.M.L. and Paredes, n., 'Preparation of V-Mg-O catalysts: Nature of active species precursors", **Appl. Catal. 104** (1993a) : 161.

Courtine,P., "Mode of arrangement of components in mixed vanadia catalyst and its bearing for oxidation catalysis", **Appl. Catal. A. General. 157** (1997) : 45.

Deo, G., Wachs, I.E. and Haber, J., "Supported vanadium oxide catalysts : Molecular structural characterization and reactivity properties",**Critical Reviews in Surface Chemistry. 4** (1994) : 141.

Deo, G., Turek, A. M., Wachs, I.E., Machej, T., Haber, J., Das, N., Eckert, H. and Hirt, A.M., "Physical and chemical characterization of surface vanadium oxide supported on titania: influence of the titania phase (anatase, rutile, brookite and B)", **Appl. Catal. A. General. 91** (1992) : 27.

Dias, C.R., Portela, M.F., Galan-Fereres, M., Bañares, M.A., Lopez Granados, M., Peña M.A. and Fierro, J.L.G., "Selective oxidation of *o*-xylene to phthalic anhydride on V_2O_5 supported on TiO_2-coated SiO_2", **Catal. Lett. 43** (1997) : 117.

Gao, X., Ruiz, P, Xin, O., Guo, X. and Delmon, B., "Preparation and characterization of three pre magnesium vanadate phases as catalysts for selective oxidation of propane to propene", **Catal. Lett. 23** (1994) : 321.

Grzybowska-Swierkosz, B., "Vanadia-titania catalysts for oxidation of *o*-xylene and other hydrocarbons", **Appl. Catal. 157** (1997) : 263.

Guerrero-Ruiz, A., Rodriguez-Ramos, I., Ferrira-Aparicia, P. and Volta, J.C., "Study of surface and lattice oxygen atoms over magnesium vanadate phases by isotopic exchange with $C^{18}O_2$", **Catal. Lett. 45** (1997) : 113.

Kanokrattana, O., "Effect of alkali metals on V-Mg-O catalyst in the oxidative dehydrogenation of propane", **Master of Engineering thesis**, Chulalongkorn University, (1997).

Korili, S.A. and Delmon, P.R.B., "Oxidative dehydrogenation of n-pentane on magnesium vanadate catalysts", **Catal. Today. 32** (1996) : 229.

Leklertsunthorn, R., "Oxidation property of the V-Mg-O/TiO_2 catalyst", **Master of Engineering thesis**, Chulalongkorn University, (1997).

Lopez Nieto, J.M., Kremenic, G., and Fierro, J.L.G., "Selective oxidation of propene over supported vanadium oxide catalysts", **Appl. Catal. 61** (1990) : v235.

Mori, K., Inomata, M., Miyamoto, A. and Murakami, Y., "Activity and selectivity in the oxidation of benzene on supported vanadium oxide catalysts", **J. Chem. Soc. Faraday Trans. 1, 80** (1984) : 2655.

Nakamura, H., Matsuhashi, H. and Arata, K., "Heterogeneous Liquid phase oxidation of alcohols with zirconia-supported vanadium oxide as solid oxidizing reagent", **Chemistry Letters.** (1993) : 749.

Nieto, J.M.L., Kremenic, G. and Fierro, J.L.G., "Selective oxidation of propene over supported vanadium oxide catalysts. **Appl. Catal. 61** (1990) : 235.

Okuhara, T., Inimaru, K., Misono, M., Matsubayashi, N., Shimada, H. and Nishijma, A., "Structures and dehydrogenation activities of vanadium oxide overlayers on supports", **Catal. Lett. 20** (1993) : 73.

Peng, X.D. and Barteua, M.A., "Acid-base reactions on model MgO surfaces", **Catal. Lett. 12** (1992) : 245.

Ponzi, M., Duschatzky, C., Carrascull, A. and Ponzi, E., "Obtaining benzaldehyde via promoted V_2O_5 catalysts", **Appl. Catal. A. General. 169** (1998) : 397.

Reddy, B.M., Ganesh, I., Chowdhury, B., "Design of stable and reactive vanadium oxide catalysts supported on binary oxides", **Catal. Today. 49** (1999) : 115.

Reid, Robert, C., Pranusnitz, John, M., and Poling Bruce, E., **The Properties of Gases and Liquids**, McGraw-Hill International Book Company, 4th ed., 1988

Sokolovskii, V.D., "Principles of oxidative catalysts on solid oxides", **Catal. Rev.-Sci. Eng., 32 (1&2)**, (1990) : 1.

Sundaram, K., Baker, J.P. and Amiridis, M.D., "Catalytic oxidation of 1,2-dichlorobenzene over V_2O_5/TiO_2-based catalysts", **Catal.Today. 40** (1998) : 39.

Thammanonkul, H., "Oxidative dehydrogenation of propane over V-Mg-O catalysts", **Master of Engineering thesis**, Chulalongkorn University, (1996).

Wildberger, M.D., Mallat, T. and Gobel, U., "Oxidation of butane and butadiene to furan over vanadia-silica mixed oxides", **Appl. Catal. 168** (1998) : 69.

Wachs, I.E., Weckhuysen, B.M., "Structure and reactivity of surface vanadium oxide species on oxide supports", **Appl. Catal. 157** (1997) : 67.

APPENDICES

APPENDIX A

CALCULATION OF CATALYST PREPARATION

A.1 Calculation for the preparation of the 10V2MgTi catalyst

The aqueous solution used for catalyst preparation consists of 0.4 wt% NH_4VO_3. The volume of this solution is designed to be 50 ml., hence NH_4VO_3 and H_2O are weighted for 0.2 and 49.8 gram, respectively.

$$\text{The amount of V in 0.2 g of } NH_4VO_3 = \frac{0.2 \times 50.9414}{116.98}$$

$$\approx 0.0871 \text{ g}$$

$$\text{Therefore, mole of V} = \frac{0.0871}{50.9414}$$

$$\approx 0.0017 \text{ mole}$$

$$\text{The amount of V calculated as } V_2O_5 = \frac{0.0871 \times 181.8828}{101.8828}$$

$$\approx 0.1555 \text{ g}$$

If the weight of catalyst is 100 gram, 10VTi would compose of 10 g of V_2O_5 and 95 g of TiO_2. Thus, in this system,

$$\text{The amount of } TiO_2 = \frac{90 \times 0.1555}{10}$$

$$\approx 1.3995 \text{ g}$$

Then 2 wt% of Mg is added to the 10VTi catalyst (when the weight of V_2O_5 plus TiO_2 is calculated as 100%).

$$\text{The amount of Mg in 10V2MgTi} = 0.02 \times (0.1555 + 1.3995)$$

$$\approx 0.0311 \text{ g}$$

$$\text{The amount of } Mg(NO_3)_2 \text{ used} = \frac{0.0311 \times 256.41}{24.305}$$

$$\approx 0.3286 \text{ g}$$

APPENDIX B

CALCULATION OF DIFFUSIONAL LIMITATION EFFECT

In the present work there are doubt whether the external and internal diffusion limitations interfere with the 1-propanol reaction. Hence, the kinetic parameters were calculated based on the experimental data so as to prove the controlled system. The calculation is divided into two parts; one of which is the external diffusion limitation, and the other is the internal diffusion limitation.

B.1 External diffusion limitation

The 1-propanol oxidation reaction is considered to be an irreversible first order reaction occurred on the interior pore surface of catalyst particles in a fixed bed reactor. Assume isothermal operation for the reaction.

In the experiment, 4 vol% 1-propanol in air was used as the unique reactant in the system. Molecular weight of 1-propanol and air are 60 and 29, respectively. Thus, the average molecular weight of the gas mixture was calculated as follows:

$$M_{AB} = 0.04\times60 + 0.96\times29$$
$$= 30.24 \text{ g/mol}$$

Calculation of reactant gas density

Consider the 1-propanol oxidation operated at low pressure and high temperature. We assume that the gases are respect to ideal gas law. The density of such gas mixture reactant at various temperatures is calculated in the following.

$$\rho = \frac{PM}{RT} = \frac{1.0\times10^{5}\times30.24\times10^{-3}}{8.314T}$$

We obtained : $\rho = 0.769$ kg/m^3 at T = 200°C

$\rho = 0.695$ kg/m^3 at T = 250°C

$\rho = 0.635$ kg/m^3 at T = 300°C

$\rho = 0.584$ kg/m^3 at T = 350°C

Calculation of the gas mixture viscosity

The simplified methods for determining the viscosity of low pressure binary are described anywhere (Reid, 1988). The method of Wilke is chosen to estimate the gas mixture viscosity.

For a binary system of 1 and 2,

$$\mu_m = \frac{y_1\mu_1}{y_1 + y_2\Phi_{12}} + \frac{y_2\mu_2}{y_2 + y_1\Phi_{21}}$$

where μ_m = viscosity of the mixture

μ_1, μ_2 = pure component viscosity

y_1 , y_2 = mole fractions

$$\phi_{12} = \frac{\left[1 + \left(\frac{\mu_1}{\mu_2}\right)^{1/2}\left(\frac{M_1}{M_2}\right)^{1/4}\right]^2}{\left[8\left(1 + \frac{M_1}{M_2}\right)\right]^{1/2}}$$

$$\phi_{21} = \phi_{12}\left(\frac{\mu_2}{\mu_1}\right)\left(\frac{M_1}{M_2}\right)$$

M_1, M_2 = molecular weight

Let 1 refer to 1-propanol and 2 to air

$M_1 = 60$ and $M_2 = 29$

From Perry the viscosity of pure 1-propanol at 200°C , 250°C, 300°C and 350°C are 0.0124, 0.0135, 0.015 and 0.0162 cP, respectively. The viscosity of pure air at 200 ^{0}C, 250 ^{0}C, 300 ^{0}C and 350 ^{0}C are 0.0248, 0.0265, 0.0285 and 0.030 cP, respectively.

At 200^{0}C :

$$\phi_{12} = \frac{\left[1+\left(\frac{0.0124}{0.0248}\right)^{1/2}\left(\frac{29}{60}\right)^{1/4}\right]^2}{\left[8\left(1+\frac{60}{29}\right)\right]^{1/2}} = 0.510$$

$$\phi_{21} = 0.510\left(\frac{0.0248}{0.0124}\right)\left(\frac{60}{29}\right) = 2.110$$

$$\mu_m = \frac{0.04\times 0.0124}{0.04+0.96\times 0.510} + \frac{0.96\times 0.0248}{0.96+0.04\times 2.110} = 0.0237cP = 2.37\times 10^{-5}\, kg/m-\sec$$

At 250^{0}C :

$$\phi_{12} = \frac{\left[1+\left(\frac{0.0135}{0.0265}\right)^{1/2}\left(\frac{29}{60}\right)^{1/4}\right]^2}{\left[8\left(1+\frac{60}{29}\right)\right]^{1/2}} = 0.514$$

$$\phi_{21} = 0.514\left(\frac{0.0265}{0.0135}\right)\left(\frac{60}{29}\right) = 2.086$$

$$\mu_m = \frac{0.04\times 0.0135}{0.04+0.96\times 0.514} + \frac{0.96\times 0.0265}{0.96+0.04\times 2.086} = 0.0254cP = 2.54\times 10^{-5}\, kg/m-\sec$$

At 300^{0}C :

$$\phi_{12} = \frac{\left[1+\left(\frac{0.015}{0.0265}\right)^{1/2}\left(\frac{29}{60}\right)^{1/4}\right]^2}{\left[8\left(1+\frac{60}{29}\right)\right]^{1/2}} = 0.52$$

$$\phi_{21} = 0.52\left(\frac{0.0265}{0.015}\right)\left(\frac{60}{29}\right) = 2.043$$

$$\mu_m = \frac{0.04\times 0.015}{0.04+0.96\times 0.52} + \frac{0.96\times 0.0265}{0.96+0.04\times 2.043} = 0.0274cP = 2.74\times 10^{-5}\, kg/m-\sec$$

At 350^0C :

$$\phi_{12} = \frac{\left[1+\left(\frac{0.0162}{0.030}\right)^{1/2}\left(\frac{29}{60}\right)^{1/4}\right]^2}{\left[8\left(1+\frac{60}{29}\right)\right]^{1/2}} = 0.525$$

$$\phi_{21} = 0.525\left(\frac{0.030}{0.0162}\right)\left(\frac{60}{29}\right) = 2.011$$

$$\mu_m = \frac{0.04\times 0.0162}{0.04+0.96\times 0.525} + \frac{0.96\times 0.030}{0.96+0.04\times 2.011} = 0.0289cP = 2.89\times 10^{-5}\, kg/m-\text{sec}$$

Calculation of diffusion coefficients

Diffusion coefficients for binary gas system at low pressure calculated by empirical correlation are proposed by Reid (1988). Wilke and Lee method is chosen to estimate the value of D_{AB} due to the general and reliable method. The empirical correlation is

$$D_{AB} = \frac{\left(3.03-\frac{0.98}{M_{AB}^{1/2}}\right)(10^{-3})T^{3/2}}{PM_{AB}^{1/2}\sigma_{AB}^2\Omega_D}$$

where D_{AB} = binary diffusion coefficient,cm^2/s

T = temperature,K

M_A,M_B = molecular weights of A and B ,g/mol

$$M_{AB} = 2\left[\left(\frac{1}{M_A}\right)+\left(\frac{1}{M_B}\right)\right]^{-1}$$

P = pressure,bar

σ = characteristic length,Å

Ω_D = diffusion collision integral, dimensionless

The characteristic Lennard-Jones energy and Length, ε and σ, of 1-propanol and air are as follows: (Reid,1988)

For C_3H_7OH : σ (C_3H_7OH) = 4.549 Å, ε /k = 576.7
For air : σ (air) = 3.711 Å , ε /k = 78.6

The sample rules are usually employed.

$$\sigma_{AB} = \frac{\sigma_A + \sigma_B}{2} = \frac{4.549 + 3.711}{2} = 4.13$$

$$\varepsilon_{AB}/k = \left(\frac{\varepsilon_A \varepsilon_B}{k^2}\right)^{1/2} = (576.7 \times 78.6)^{1/2} = 212.9$$

Ω_D is tabulated as a function of kT/ε for the Lennard-Jones potential. The accurate relation is

$$\Omega_D = \frac{A}{(T^*)^B} + \frac{C}{\exp(DT^*)} + \frac{E}{\exp(FT^*)} + \frac{G}{\exp(HT^*)}$$

where $T^* = \frac{kT}{\varepsilon_{AB}}$, A = 1.06036 , B = 0.15610 , C = 0.19300 , D = 0.47635 , E = 1.03587 , F = 1.52996 , G = 1.76474 , H = 3.89411

Then $T^* = \frac{473}{212.9} = 2.222$ at 200°C

$T^* = \frac{523}{212.9} = 2.456$ at 250°C

$T^* = \frac{573}{212.9} = 2.691$ at 300°C

$T^* = \frac{623}{212.9} = 2.926$ at 350°C

$$\Omega_D = \frac{1.06036}{(T^*)^{0.15610}} + \frac{0.19300}{\exp(0.47635T^*)} + \frac{1.03587}{\exp(1.52996T^*)} + \frac{1.76474}{\exp(3.89411T^*)}$$

Ω_D = 1.038 ; 200°C

Ω_D = 1.006 ; 250°C

Ω_D = 0.979 ; 300°C

Ω_D = 0.956 ; 350°C

With Equation of D_{AB},

$$\text{At } 200^\circ\text{C} : D(C_3H_7OH\text{-air}) = \frac{\left(3.03 - \frac{0.98}{30.24^{0.5}}\right)(10^{-3})473^{3/2}}{1 \times 30.24^{0.5} \times 4.13^2 \times 1.038}$$

$$= 3.01 \times 10^{-5} \quad m^2/s$$

$$\text{At } 250^\circ\text{C} : D(C_3H_7OH\text{-air}) = \frac{\left(3.03 - \frac{0.98}{30.24^{0.5}}\right)(10^{-3})523^{3/2}}{1 \times 30.24^{0.5} \times 4.13^2 \times 1.006}$$

$$= 3.62 \times 10^{-5} \quad m^2/s$$

$$\text{At } 300^\circ\text{C} : D(C_3H_7OH\text{-air}) = \frac{\left(3.03 - \frac{0.98}{30.24^{0.5}}\right)(10^{-3})573^{3/2}}{1 \times 30.24^{0.5} \times 4.13^2 \times 0.979}$$

$$= 4.26 \times 10^{-5} \quad m^2/s$$

$$\text{At } 350^\circ\text{C} : D(C_3H_7OH\text{-air}) = \frac{\left(3.03 - \frac{0.98}{30.24^{0.5}}\right)(10^{-3})623^{3/2}}{1 \times 30.24^{0.5} \times 4.13^2 \times 0.956}$$

$$= 5.04 \times 10^{-5} \quad m^2/s$$

Reactant gas mixture was supplied at 100 ml/min. in tubular microreactor used in the 1-propanol oxidation system at 30°C

1-propanol flow rate through reactor = 100 ml/min. at 30°C

The density of 1-propanol , $\rho = \frac{1.0\times10^{5}\times30.24\times10^{-3}}{8.314(273+30)} = 1.216\ \text{kg/m}^3$

Mass flow rate = $1.216\left(\frac{100\times10^{-6}}{60}\right) = 2.03\times10^{-6}$ kg/s

Diameter of stainless steel tube reactor = 8 mm

Cross-sectional area of tube reactor = $\frac{\pi(8\times10^{-3})^2}{4} = 5.03\times10^{-5}$ m^2

Mass Velocity , $G = \frac{2.03\times10^{-6}}{5.03\times10^{-5}} = 0.04$ kg/m^2-s

Catalysis size = 100-150 mesh = 0.178-0.126 mm

Average catalysis = (0.126+0.178)/2 = 0.152 mm

Find Reynolds number, Re_p , which is well known as follows :

$$Re_p = \frac{d_p G}{\mu}$$

We obtained

At 200°C : $Re_p = \frac{(0.152\times10^{-3}\times0.04)}{2.37\times10^{-5}} = 0.257$

At 250°C : $Re_p = \frac{(0.152\times10^{-3}\times0.04)}{2.54\times10^{-5}} = 0.239$

At 300°C : $Re_p = \frac{(0.152\times10^{-3}\times0.04)}{2.74\times10^{-5}} = 0.222$

At 350°C : $Re_p = \frac{(0.152\times10^{-3}\times0.04)}{3.0\times10^{-5}} = 0.203$

Average transport coefficient between the bulk stream and particles surface could be correlated in terms of dimensionless groups, which characterize the flow conditions. For mass transfer the Sherwood number, $k_m\rho/G$, is an empirical function of the Reynolds number, d_pG/μ , and the Schmidt number , $\mu/\rho D$. The j-factors are defined as the following functions of the Schmidt number and Sherwood numbers:

$$j_D = \frac{k_m \rho}{G}\left(\frac{a_m}{a_t}\right)(\mu / \rho D)^{2/3}$$

The ratio (a_m/a_t) allows for the possibility that the effective mass-transfer area a_m, may be less than the total external area, a_t, of the particles. For Reynolds number greater than 10, the following relationship between j_D and the Reynolds number well represents available data.

$$j_D = \frac{0.458}{\varepsilon_B}\left(\frac{d_p G}{\mu}\right)^{-0.407}$$

where G = mass velocity(superficial) based upon cross-sectional area of empty reactor ($G = u\rho$)

d_p = diameter of catalyst particle for spheres

μ = viscosity of fluid

ρ = density of fluid

ε_B = void fraction of the interparticle space (void fraction of the bed)

D = molecular diffusivity of component being transferred

Assume $\varepsilon_B = 0.5$

At 200°C ; $j_D = \frac{0.458}{0.5}(0.257)^{-0.407} = 1.592$

At 250°C ; $j_D = \frac{0.458}{0.5}(0.239)^{-0.407} = 1.640$

At 300°C ; $j_D = \frac{0.458}{0.5}(0.222)^{-0.407} = 1.690$

At 350°C ; $j_D = \frac{0.458}{0.5}(0.203)^{-0.407} = 1.753$

A variation of the fixed bed reactor is an assembly of screens or gauze of catalytic solid over which the reacting fluid flows. Data on mass transfer from single screens has been reported by Gay and Maughan. Their correlation is of the form

$$j_D = \frac{\varepsilon k_m \rho}{G}(\mu / \rho D)^{2/3}$$

Where ε is the porosity of the single screen.

Hence, $k_m = \left(\frac{j_D G}{\mu}\right)(\mu / \rho D)^{2/3}$

$$k_m = \left(\frac{0.458G}{\varepsilon_B \rho}\right)\mathrm{Re}^{-0.407}\, Sc^{-2/3}$$

Find Schmidt number, Sc : $Sc = \frac{\mu}{\rho D}$

At 200°C : $Sc = \frac{2.37 \times 10^{-5}}{0.779 \times 3.01 \times 10^{-5}} = 0.541$

At 250°C : $Sc = \frac{2.54 \times 10^{-5}}{0.705 \times 3.62 \times 10^{-5}} = 0.601$

At 300°C : $Sc = \frac{2.74\times10^{-5}}{0.643\times4.26\times10^{-5}} = 0.663$

At 350°C : $Sc = \frac{2.89\times10^{-5}}{0.592\times5.04\times10^{-5}} = 0.723$

Find k_m : At 200°C, $k_m = \left(\frac{1.592\times0.04}{0.779}\right)(0.541)^{-2/3} = 0.123$ m/s

At 250°C, $k_m = \left(\frac{1.64\times0.04}{0.705}\right)(0.601)^{-2/3} = 0.131$ m/s

At 300°C, $k_m = \left(\frac{1.69\times0.04}{0.643}\right)(0.663)^{-2/3} = 0.138$ m/s

At 350°C, $k_m = \left(\frac{1.753\times0.04}{0.592}\right)(0.723)^{-2/3} = 0.147$ m/s

Properties of catalyst

Density = 1.125 g/ml catalyst

Diameter of 100-150 mesh catalyst particle = 0.152 mm

Weight per catalyst particle = $\frac{\pi(0.152\times0^{-1})^3\times1.125}{6} = 2.07*10^{-6}$ g/particle

External surface area per particle = $\pi(0.152\times10^{-3})^2 = 7.26\times10^{-7}$ m^2/particle

$a_m = \frac{7.26\times10^{-7}}{2.07\times10^{-6}} = 3.51\times10^{-2}$ m^2/gram catalyst

Volumetric flow rate of gaseous feed stream = 100 ml/min

Molar flow rate of gaseous feed stream = $\frac{(1\times10^5)\left(\frac{100\times10^{-6}}{60}\right)}{8.314(273+30)} = 6.62\times10^{-5}$ mol/s

1-propanol molar feed rate = $0.04\times6.62\times10^{-5} = 2.65\times10^{-6}$ mol/s

1-propanol conversion (experimental data): 3.3% at 200°C
4.8% at 250°C
31.2% at 300°C
79.4% at 350°C

The estimated rate of 1-propanol oxidation reaction is based on the ideal plug flow reactor which there is no mixing in the direction of flow and complete mixing perpendicular to the direction of flow (i.e., in the radial direction). The rate of reaction will vary with reaction length. Plug flow reactors are normally operated at steady state so that properties at any position are constant with respect to time. The mass balance around plug flow reactor becomes

{rate of i into volume element} - {rate of i out of volume element}
+ {rate of production of i within the volume element}
= {rate of accumulation of i within the volume elecment }

$$F_{Ao} = F_{Ao}(1-x) + (r_W W)$$
$$(r_W W) = F_{Ao} - F_{Ao}(1-x) = F_{Ao} = F_{Ao}x$$

$$r_W = \frac{F_{Ao}x}{W} = \frac{2.65\times10^{-6}\times0.033}{0.1} = 8.745\times10^{-7} \text{ mol/s-gram catalyst at 200°C}$$

$$r_W = \frac{F_{Ao}x}{W} = \frac{2.65\times10^{-6}\times0.048}{0.1} = 1.272\times10^{-6} \text{ mol/s-gram catalyst at 250°C}$$

$$r_W = \frac{F_{Ao}x}{W} = \frac{2.65\times10^{-6}\times0.312}{0.1} = 8.268\times10^{-6} \text{ mol/s-gram catalyst at 300°C}$$

$$r_W = \frac{F_{Ao}x}{W} = \frac{2.65\times10^{-6}\times0.790}{0.1} = 2.094\times10^{-5} \text{ mol/s-gram catalyst at 350°C}$$

At steady state the external transport rate may be written in terms of the diffusion rate from the bulk gas to the surface. The expression is:

$$R_{obs} = k_m a_m (C_b - C_s)$$

$$= \frac{\text{1-propanol converted (mole)}}{\text{(time)(gram of catalyst)}}$$

where C_b and C_s are the concentrations in the bulk gas and at the surface, respectively.

$$\text{At } 200^{\circ}\text{C}, \quad (C_b - C_s) = \frac{r_{obs}}{k_m a_m} = \frac{8.745\times10^{-7}}{0.123\times3.51\times10^{-2}} = 2.03\times10^{-4} \quad \text{mol/m}^3$$

$$\text{At } 250^{\circ}\text{C}, \quad (C_b - C_s) = \frac{r_{obs}}{k_m a_m} = \frac{1.272\times10^{-6}}{0.131\times3.51\times10^{-2}} = 2.77\times10^{-4} \quad \text{mol/m}^3$$

$$\text{At } 300^{\circ}\text{C}, \quad (C_b - C_s) = \frac{r_{obs}}{k_m a_m} = \frac{8.268\times10^{-6}}{0.138\times3.51\times10^{-2}} = 1.71\times10^{-3} \quad \text{mol/m}^3$$

$$\text{At } 350^{\circ}\text{C}, \quad (C_b - C_s) = \frac{r_{obs}}{k_m a_m} = \frac{2.094\times10^{-5}}{0.147\times3.51\times10^{-2}} = 4.06\times10^{-3} \quad \text{mol/m}^3$$

From C_b (1-propanol) = 1.59 mol/m^3

Consider the difference of the bulk and surface concentration is small. It means that the external mass transport has no effect on the 1-propanol oxidation reaction rate.

B.2 Internal diffusional limitation

Next, consider the internal diffusional limitation of the 1-propanol reaction. An effectiveness factor, η, was defined in order to express the rate of reaction for the whole catalyst pellet, r_p, in terms of the temperature and concentrations existing at the outer surface as follows:

$$\eta = \frac{\text{actual rate of whole pellet}}{\text{rate evaluated at outer surface conditions}} = \frac{r_p}{r_s}$$

The equation for the local rate (per unit mass of catalyst) may be expected functionally as $r = f(C,T)$.

Where C represents, symbolically, the concentrations of all the involved components

Then, $r_p = \eta r_s = \eta f(C_s, T_s)$

Suppose that the 1-propanol oxidation is an irreversible reaction A→B and first order reaction, so that for isothermal conditions $r = f(C_A) = k_1 C_A$. Then $r_p = \eta k_1 (C_A)_s$.

For a spherical pellet, a mass balance over the spherical-shell volume of thickness Δr. At steady state the rate of diffusion into the element less the rate of diffusion out will equal the rate of disappearance of reactant with in the element. This rate will be $\rho_p k_1 C_A$ per unit volume, where ρ_p is the density of the pellet. Hence, the balance may be written, omitting subscript A on C,

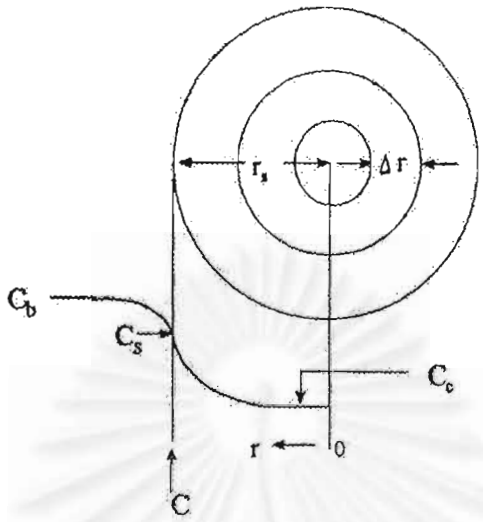

Figure B1. Reactant (A) concentration vs. position for first-order reaction on a spherical catalyst pellet.

$$\left(-4\pi r^2 D_e \frac{dC}{dr}\right)_r - \left(-4\pi r^2 D_e \frac{dC}{dr}\right)_{r+\Delta r} = -4\pi r^2 \Delta r_p k_1 C$$

Take the limit as $\Delta r \to 0$ and assume that the effective diffusivity is independent of the concentration of reactant, this difference equation becomes

$$\frac{d^2C}{dr^2} + 2\frac{dC}{dr} - \frac{k_1 \rho_p C}{D_e} = 0$$

At the center of the pellet symmetry requires

$$\frac{dC}{dr} = 0 \text{ at } r = 0$$

and at outer surface

$$C = C_s \text{ at } r = r_s$$

Solve linear differential equation by conventional methods to yield

$$\frac{C}{C_s} = \frac{r_s \sinh\left(3\phi_s \frac{r}{r_s}\right)}{r \sinh 3\phi_s}$$

where ϕ_s is Thiele modulus for a spherical pellet defined by $\phi_s = \frac{r_s}{3}\sqrt{\frac{k_1 \rho_p}{D_e}}$

Both D_e and k_1 are necessary to use $r_p = \eta k_1 (C_A)_s$. D_e could be obtained from the reduced pore volume equation in case of no tortuosity factor.

$$D_e = (\varepsilon_s^2 D_{AB})$$

At 200°C, $D_e = (0.5)^2 (3.01\times10^{-5}) = 7.53\times10^{-6}$

At 250°C, $D_e = (0.5)^2 (3.62\times10^{-5}) = 7.53\times10^{-6}$

At 300°C, $D_e = (0.5)^2 (4.26\times10^{-5}) = 7.53\times10^{-6}$

Substitute radius of catalyst pellet, $r_s = 0.0786\times10^{-3}$ m with ϕ_s equation

$$\phi_s = \frac{0.076\times10^{-3}\ \text{m}}{3}\sqrt{\frac{k(\text{m}^3/\text{s - kg cat.})\times1125(\text{kg/m}^3)}{7.53\times10^{-6}(\text{m}^2/\text{s})}}\text{, at 200°C}$$

$\phi_s = 0.310\sqrt{k}$ (dimensionless) at 200°C

$\phi_s = 0.283\sqrt{k}$ (dimensionless) at 250°C

$\phi_s = 0.261\sqrt{k}$ (dimensionless) at 300°C

Find k (at 200°C) from the mass balance equation around plug-flow reactor.

$$r_w = \frac{F_{Ao}\, dx}{dW}$$

where $r_w = kC_A$

Thus, $$kC_A = \frac{F_{Ao}\, dx}{dW}$$

$$kC_{Ao}(1-x) = \frac{F_{Ao}\, dx}{dW}$$

$$W = \frac{F_{Ao}}{kC_{Ao}} \int_0^{0.1} \frac{1}{1-x}\, dx$$

$$W = \frac{F_{Ao}}{kC_{Ao}} \left[-\ln(1-x)\right]_0^{0.1} = \frac{F_{Ao}}{kC_{Ao}}(-\ln(0.9))$$

$$k = \frac{F_{Ao}}{WC_{Ao}}(-\ln(0.9))$$

$$k = \frac{2.65 \times 10^{-6}\ (\text{mol/s})}{0.1 \times 10^{-3}\ (\text{kg}) \times 1.59\ (\text{mol/m}^3)}(-\ln(0.9))$$

$$= 1.76 \times 10^{-3}\ \text{m}^3\text{/s-kg catalyst}$$

Calculate ϕ_s : $\phi_s = 0.310\sqrt{1.76 \times 10^{-3}} = 0.013$ at 200°C

$$\phi_s = 0.268\sqrt{2.12 \times 10^{-2}} = 0.042 \text{ at } 250°C$$

$$\phi_s = 0.261\sqrt{6.52 \times 10^{-2}} = 0.067 \text{ at } 300°C$$

For such small values of ϕ_s it was concluded that the internal mass transport has no effect on the rate of 1-propanol oxidation reaction.

APPENDIX C

GAS CHROMATOGRAPH

C.1 Operating condition

Flame ionization detector gas chromatographs, model 14A and 14B, were used to analyze the concentration of oxygenated compounds and light hydrocarbons, respectively. Methanol, ethanol, 1-propanol, 2-propanol, formaldehyde, acetaldehyde and propionaldehyde were analyzed by GC model 14A while methane, ethene, propane and propene were analyzed by GC model 14B.

Gas chromatograph with the thermal conductivity detector, model 8A was used to analyze the concentrations of CO_2 and CO by using Porapak QS and Molecular Sieve 5A column, respectively.

The operation conditions for gas chromatograph are described below:

GC model	Shimadzu GC-14B	Shimadzu GC-14A	Shimadzu GC-8A
Detector	FID	FID	TCD
Column	VZ-10	Capillary	Porapak QS and Molecular sieve 5A
Nitrogen flow rate	60 ml/min	25 ml/min	
Helium flow rate	-	-	25 ml/min
Column temperature			-
- initial	55°C	40°C	80°C
- final	65°C	140°C	80°C
Injection temperature	100°C	150°C	130°C
Detector temperature	150°C	150°C	130°C

C.2 Calibration curve

The calibration curves of methane, ethene, propene, formaldehyde, acetaldehyde, propionaldehyde, methanol, ethanol, 1-propanol, 2-propanol, CO and CO_2 are presented in the following figures.

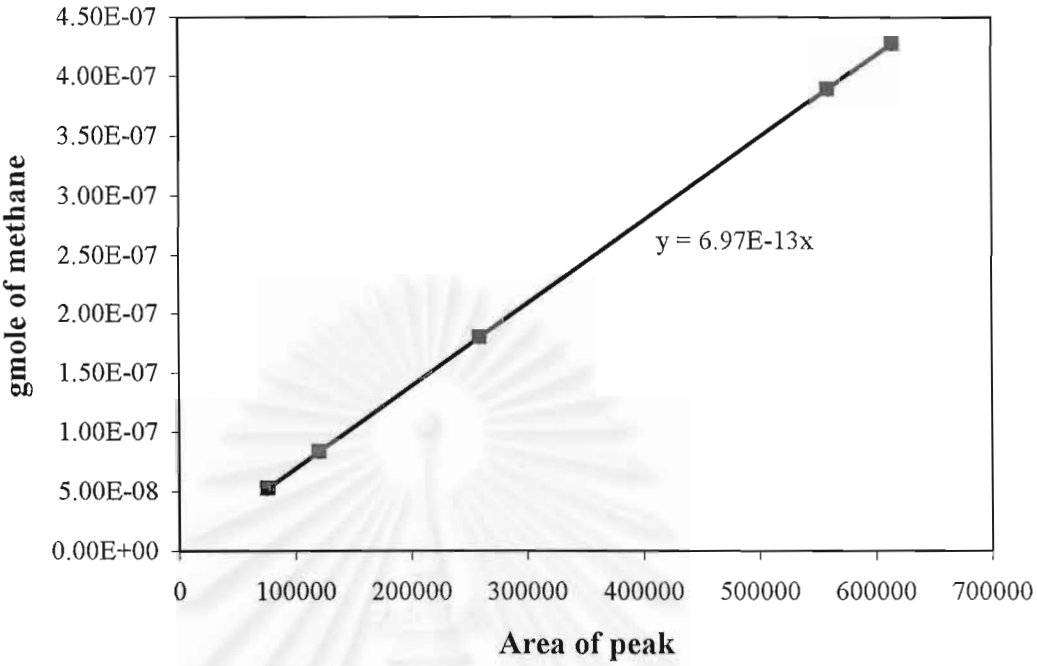

Figure C1 The calibration curve of methane

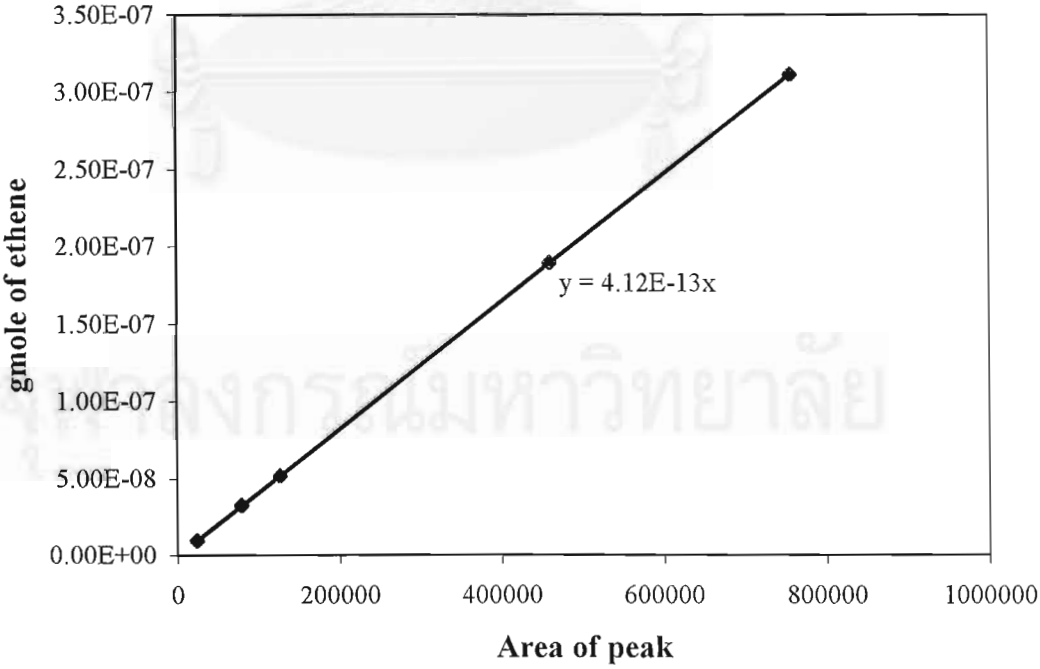

Figure C2 The calibration curve of ethene

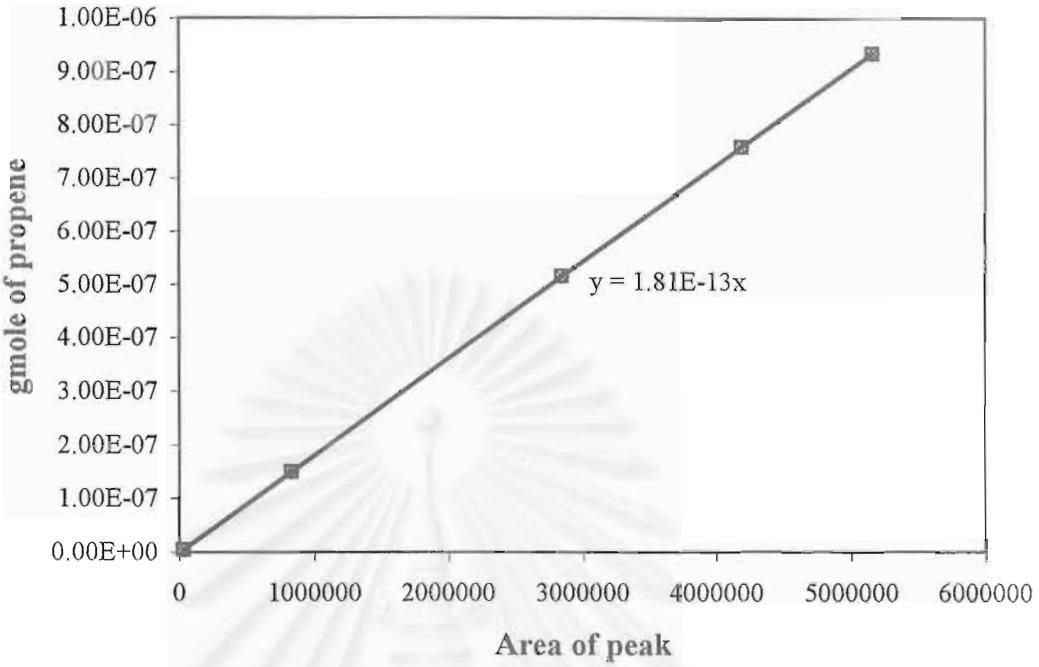

Figure C3 The calibration curve of propene

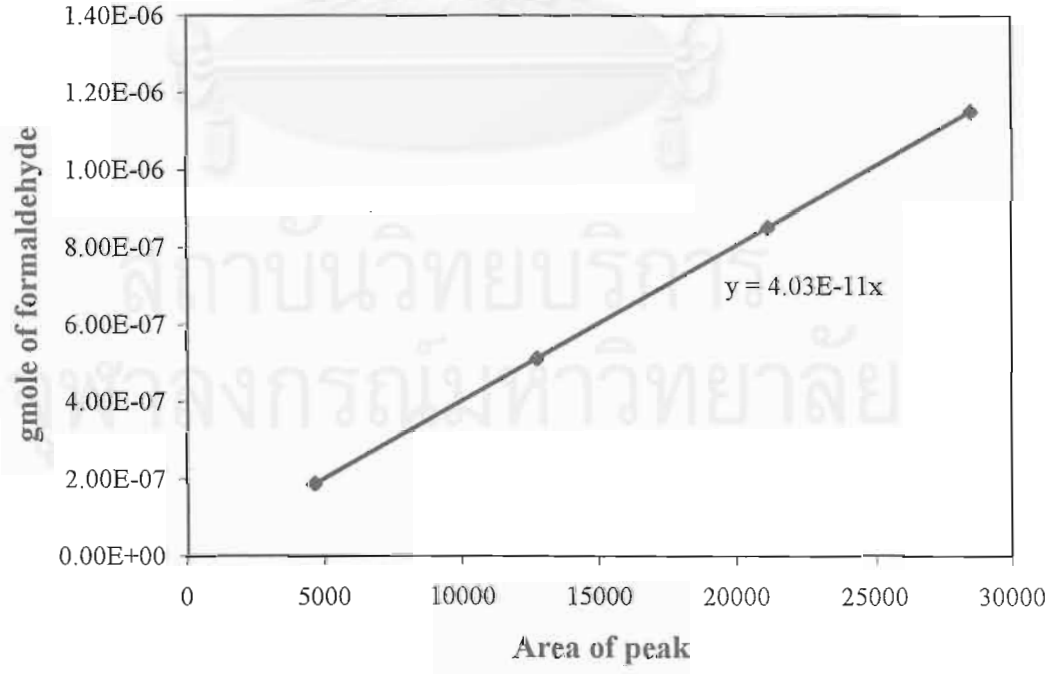

Figure C4 The calibration curve of formaldehyde

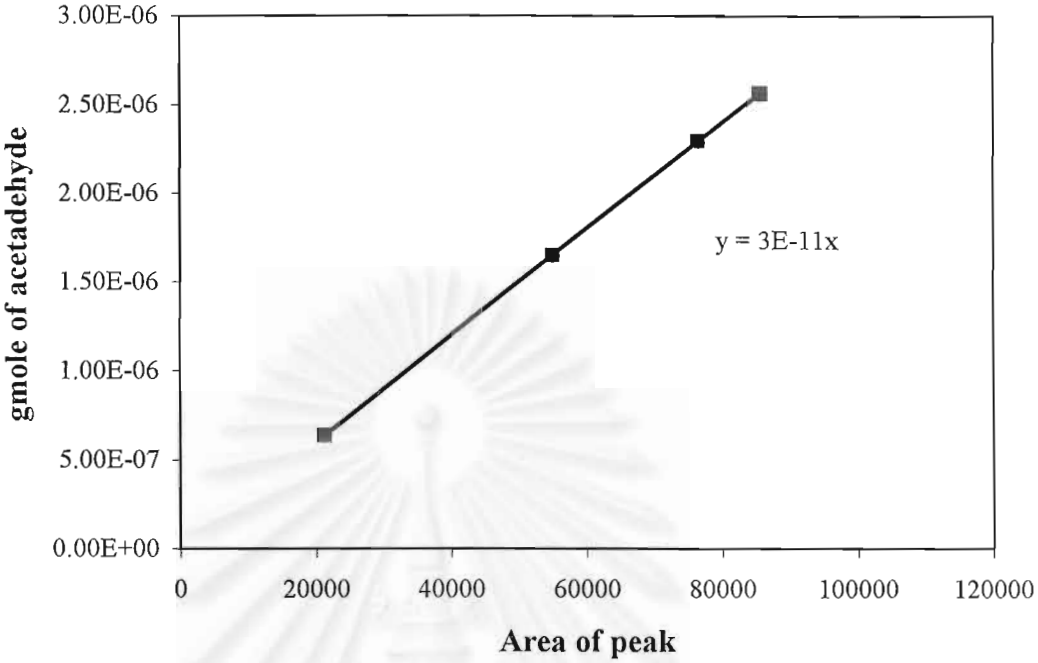

Figure C5 The calibration curve of acetaldehyde

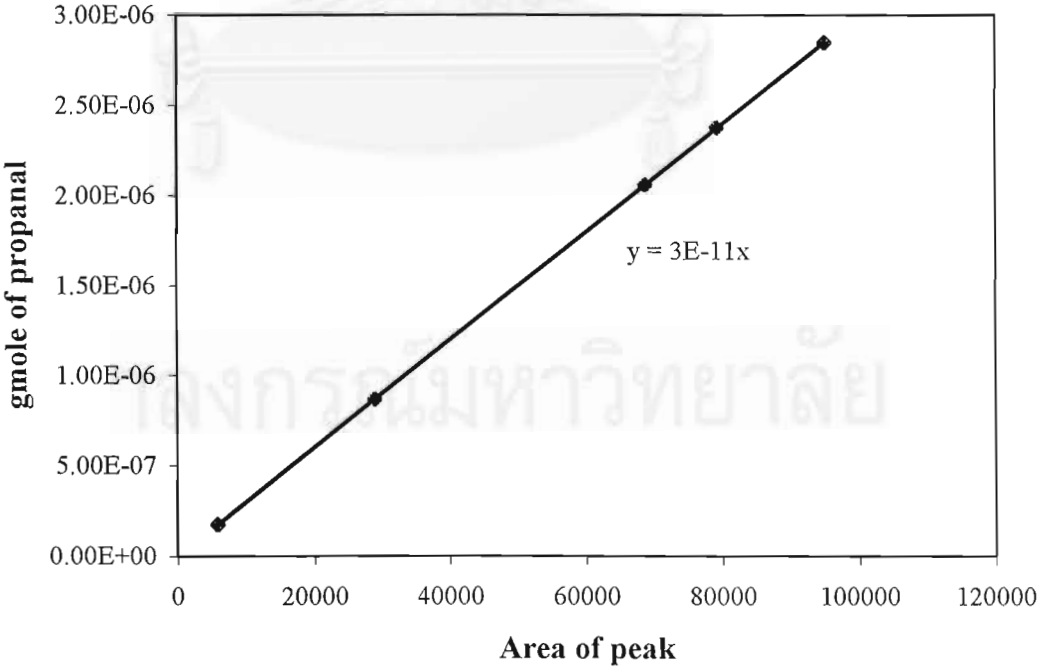

Figure C6 The calibration curve of propanal

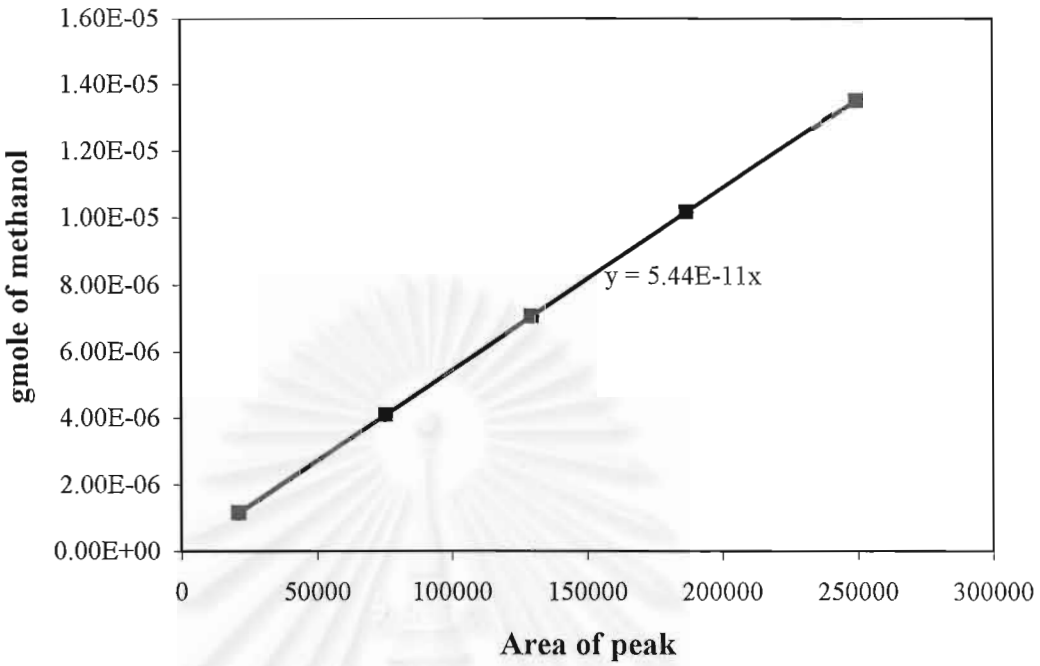

Figure C7 The calibration curve of methanol

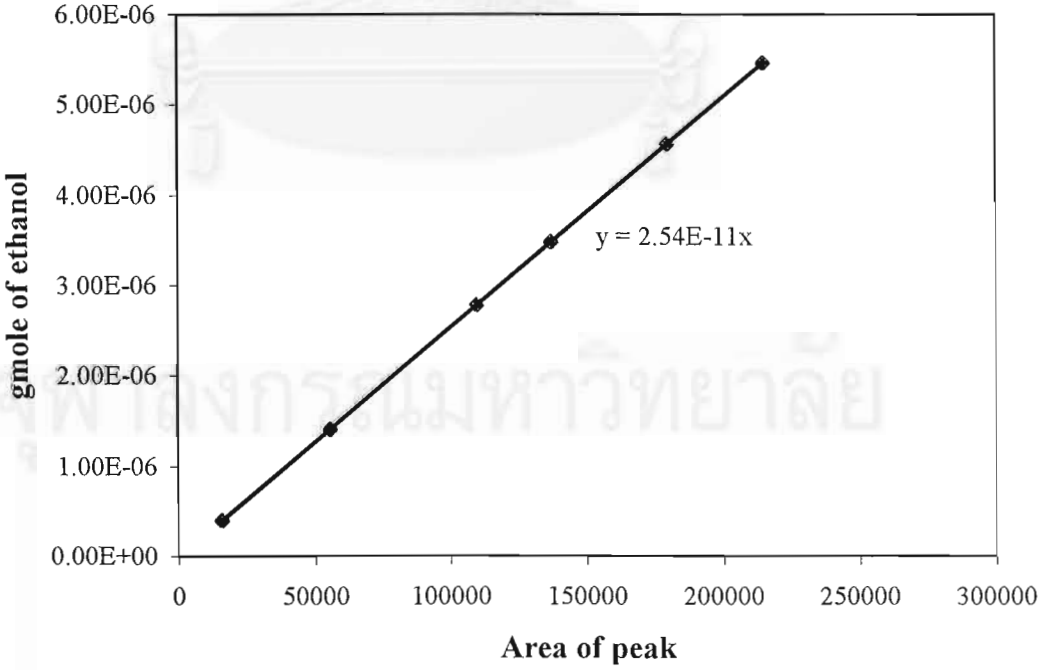

Figure C8 The calibration curve of ethanol

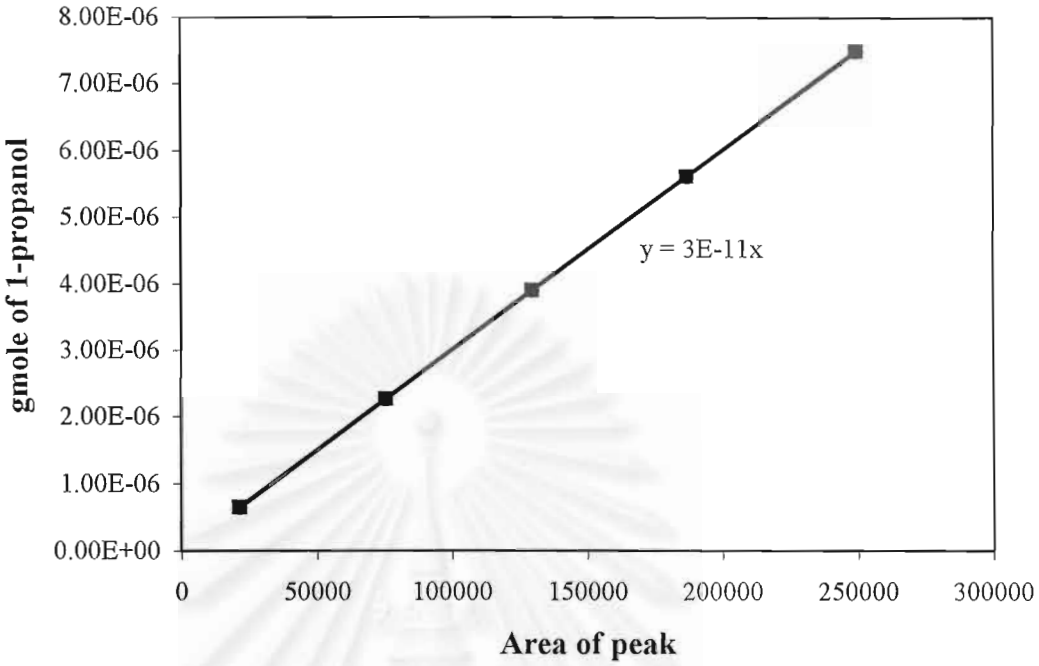

Figure C9 The calibration curve of 1-propanol

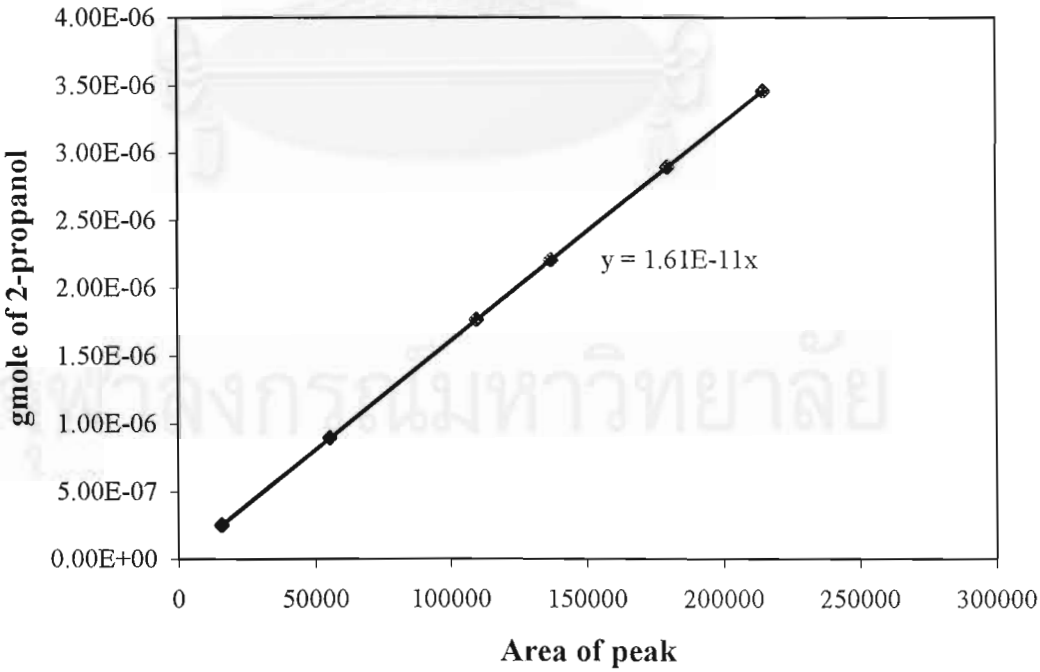

Figure C10 The calibration curve of 2-propanol

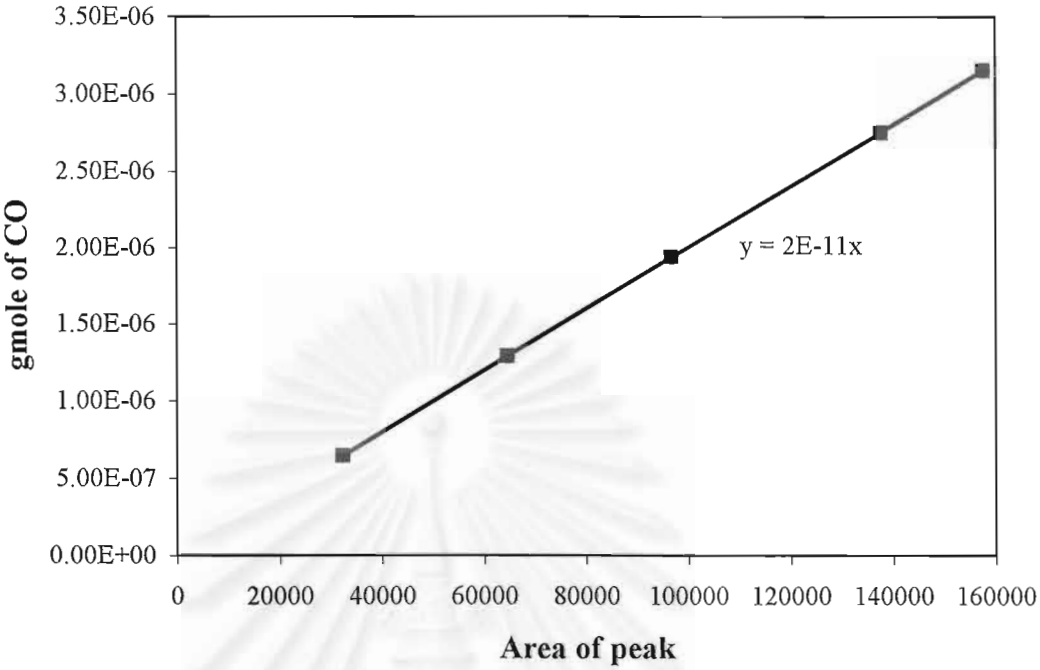

Figure C11 The calibration curve of CO

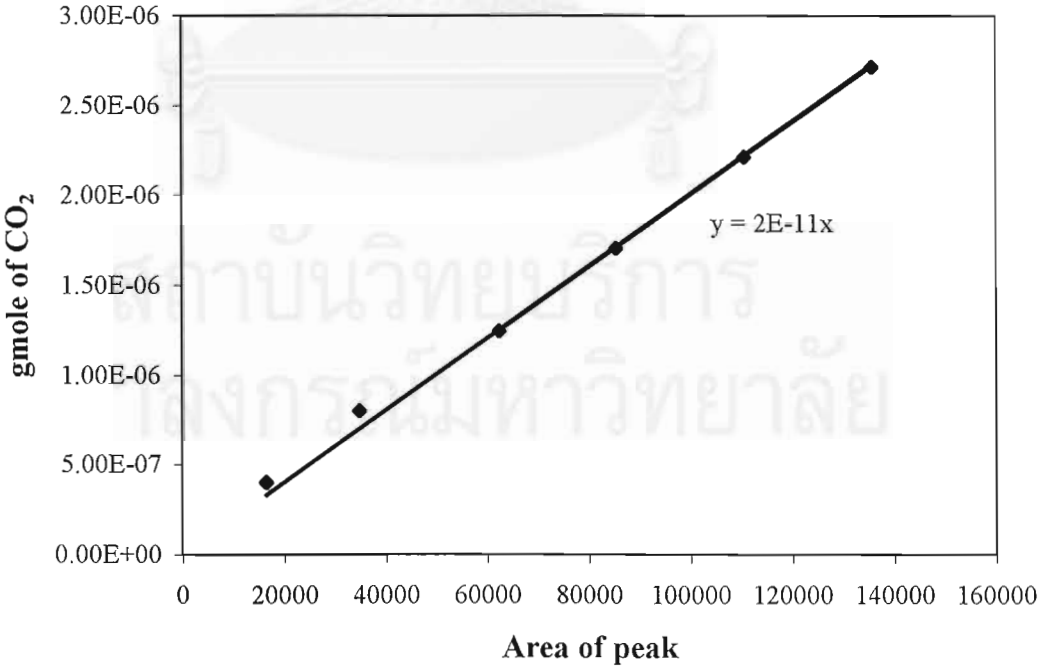

Figure C12 The calibration curve of CO_2

APPENDIX D

DATA OF EXPERIMENT

Table D1 Data of figure 5.6

Temperature (°C)	%C_3H_7OH conversion	%CH_4 selectivity	%C_2H_4 selectivity	%C_3H_6 selectivity	%CH_2O selectivity	%C_3H_6O selectivity	%CO_2 selectivity
200	3.31	0.22	0.23	0	0	96.79	0.57
250	4.84	0.16	0.81	1.553	5.91	79.06	10.24
300	31.17	0.03	0.84	3.64	9.08	67.34	18.1
350	79.37	0.04	0.87	2.02	7.29	34.1	52.68
400	99.77	0.03	0.94	0.06	0	12.58	83.88
450	100	0.04	1.17	0.04	0	0	96.57
500	100	0.05	1.98	0.02	0	0	95.57

Table D2 Data of figure 5.7

Temperature (°C)	%C_3H_7OH conversion	%CH_4 selectivity	%C_2H_4 selectivity	%C_3H_6 selectivity	%CH_2O selectivity	%C_3H_6O selectivity	%CO_2 selectivity
200	2.54	0.13	0.08	0	0	96.4	0.02
250	11.84	0.05	0.13	1.43	5.97	83.56	4.88
300	34.07	0.03	0.13	2.14	5.63	70.85	18.74
350	58.99	0.05	0.5	4.9	8.13	51.09	35.77
400	72.8	0.1	1.57	3.2	4.43	37.43	50.06
450	94.85	0.56	2.19	1.83	3.02	27.12	61.64
500	98.92	0.48	2.95	1.54	2.75	25.58	63.1

Table D3 Data of figure 5.8

Temperature (°C)	%C_3H_7OH conversion	%CH_4 selectivity	%C_2H_4 selectivity	%C_3H_6 selectivity	%CH_2O selectivity	%C_3H_6O selectivity	%CO_2 selectivity
200	6.76	0.03	0.05	0.38	0	95.20	0.81
250	31.86	0.01	0.06	1.33	2.8	91.76	2.9
300	68.95	0.02	0.11	2.38	5.72	72.86	16.65
350	72.41	0.05	0.42	2.60	6.01	62.23	25.64
400	81.15	0.18	1.22	2.07	6.31	59.41	28.17
450	81.86	0.41	1.69	1.56	4.41	55.05	33.61
500	84.72	0.82	3.76	1.08	4.77	52.23	34.16

Table D4 Data of figure 5.9

Temperature (°C)	%C_3H_7OH conversion	%CH_4 selectivity	%C_2H_4 selectivity	%C_3H_6 selectivity	%CH_2O selectivity	%C_3H_6O selectivity	%CO_2 selectivity
200	13.93	0.02	0.02	0.37	1.59	94.19	0.41
250	34.75	0.02	0.32	1.61	3.73	92.76	3.76
300	65.293	0.04	0.21	3.00	6.61	73.98	13.86
350	76.99	0.05	0.61	2.27	4.49	69.61	20.12
400	84.04	0.17	0.85	1.73	4.41	61.15	29.14
450	83.78	0.34	1.15	1.53	3.64	57.54	33.48
500	83.71	1.16	3.86	1.96	4.66	52.47	33.2

Table D5 Data of figure 5.10

Temperature (°C)	%C_3H_7OH conversion	%CH_4 selectivity	%C_2H_4 selectivity	%C_3H_6 selectivity	%CH_2O selectivity	%C_3H_6O selectivity	%CO_2 selectivity
200	8.83	0.05	0.15	0.18	0	96.42	0.58
250	17.09	0.03	0.22	1.84	4.19	90.99	2.14
300	48.87	0.06	0.22	2.96	5.67	73.78	16.69
350	60.98	0.08	0.96	3.11	6.02	68.72	20.92
400	61.35	0.19	1.01	2.24	5.28	58.13	32.86
450	60.26	0.40	1.6	1.79	5.31	58.33	32.26
500	61.11	1.23	4.54	1.92	5.84	54.1	31.35

Table D6 Data of figure 5.11

Temperature (°C)	%C_3H_7OH conversion	%CH_4 selectivity	%C_2H_4 selectivity	%C_3H_6 selectivity	%CH_2O selectivity	%C_3H_6O selectivity	%CO_2 selectivity
200	18.94	0.01	0.05	0.06	1.79	94.78	0.87
250	57.43	0.02	0.08	0.55	4.53	81.28	11.38
300	85.01	0.04	0.1	0.92	5.14	77.37	12.9
350	85.39	0.05	0.31	1.23	4.86	72.07	19.21
400	85.23	0.24	1.19	1.73	4.94	63.68	25.56
450	82.77	0.48	1.61	1.68	4.86	62.76	25.89
500	84.74	0.85	2.9	1.53	4.02	62.3	25.84

Table D7 Data of figure 5.12

Temperature	1-Propanol/O_2 ratio, The amount of catalyst (g)						
(°C)	4/20, 0 g	4/20, 0.1 g	4/10, 0.1 g	4/5, 0.1 g	8/5, 0.1 g	12/5, 0.1 g	8/5, 0.3 g
200	0.0027	0.0056	0.0040	0.0095	0.0279	0.0192	0.0126
250	0.0063	0.0067	0.0164	0.0043	0.0685	0.0350	0.0326
300	0.0203	0.0366	0.0399	0.0768	0.1026	0.0812	0.0496
350	0	0.0471	0.0498	0.0662	0.1138	0.0944	0.0430
400	0	0.0184	0.0450	0.0708	0.1092	0.0803	0.0380
450	0	0	0.0425	0.0662	0.1024	0.0792	0.0363
500	0	0	0.0418	0.0650	0.0933	0.0745	0.0369

Table D8 Data of figure 5.13

Temperature	%C_2H_5OH	%CH_4	%C_2H_4	%C_3H_6	%C_2H_4O	%CO_2
(°C)	conversion	selectivity	selectivity	selectivity	selectivity	selectivity
200	4.8	0.31	0.12	0	96.71	1.28
250	22.04	0.14	0.56	0	92.14	5.23
300	59.99	0.36	1.55	0	71.24	24.27
350	89.55	0.39	2.80	0.01	50.01	44.67
400	99.62	1.10	3.39	0.01	20.86	72.52
450	100	0.66	3.28	0	15.40	78.62
500	100	1.38	3.53	0	11.46	81.54

Table D9 Data of figure 5.14

Temperature	%C_2H_5OH	%CH_4	%C_2H_4	%C_3H_6	%C_2H_4O	%CO_2
(°C)	conversion	selectivity	selectivity	selectivity	selectivity	selectivity
200	4.51	0.61	0.12	0	94.81	2.15
250	20.57	0.42	0.56	0	93.08	4.63
300	58.93	0.84	1.60	0	87.63	7.06
350	92.22	1.27	3.47	0.03	59.13	33.36
400	96.74	4.35	4.49	0.06	41.15	47.86
450	96.89	2.45	4.80	0.11	20.91	68.88
500	98.65	3.58	3.63	0.06	19.51	70.59

Table D10 Data of figure 5.15

Temperature (°C)	%C_2H_5OH conversion	%CH_4 selectivity	%C_2H_4 selectivity	%C_3H_6 selectivity	%C_2H_4O selectivity	%CO_2 selectivity
200	3.17	0.14	0.14	0	97.03	0
250	16.89	0.09	0.56	0	95.99	1.47
300	57.21	0.27	1.27	0	88.98	6.78
350	84.3	1.29	2.43	0.04	71.22	22.71
400	90.75	1.83	3.13	0.05	57.61	34.66
450	88.55	1.99	3.94	0.08	55.44	35.93
500	90	2.97	3.7	0.08	55.9	34.81

Table D11 Data of figure 5.16

Temperature (°C)	%C_2H_5OH conversion	%CH_4 selectivity	%C_2H_4 selectivity	%C_3H_6 selectivity	%C_2H_4O selectivity	%CO_2 selectivity
200	3.36	1.42	0.26	0	96.33	0.6
250	18.15	0.44	1.13	0	94.92	1.1
300	56.20	0.64	1.33	0.01	91.22	3.55
350	76.36	1.33	2.22	0.04	80.76	13.38
400	87.79	4.83	2.93	0.07	69.77	20.01
450	86.03	3.64	3.11	0.1	68.75	22.24
500	86.67	4.07	2.78	0.09	65.88	25.15

Table D12 Data of figure 5.17

Temperature (°C)	%C_2H_5OH conversion	%CH_4 selectivity	%C_2H_4 selectivity	%C_3H_6 selectivity	%C_2H_4O selectivity	%CO_2 selectivity
200	2.16	1.36	0.11	0	95.88	0.20
250	11.16	1.51	0.26	0.29	92.04	3.51
300	45.54	1.87	1.29	1.01	83.74	9.03
350	68.27	2.08	2.71	0.81	75.88	16.54
400	75.42	2.11	1.17	0.30	70.37	23.25
450	73.87	3.28	3.31	0.72	65.50	24.31
500	70.75	3.45	3.53	0.47	63.34	25.84

Table D13 Data of figure 5.18

Temperature (°C)	%C_2H_5OH conversion	%CH_4 selectivity	%C_2H_4 selectivity	%C_3H_6 selectivity	%C_2H_4O selectivity	%CO_2 selectivity
200	9.86	0.03	0.14	0	96.23	0.97
250	34.32	0.06	0.36	0	95.24	1.08
300	76.34	0.3	0.97	0	91.21	4.33
350	87.54	1.79	1.86	0.02	83.79	9.88
400	85.16	2.47	2.74	0.11	76.84	15.07
450	79.08	3.33	3.88	0.2	72.71	18.63
500	78.22	5.51	3.22	0.11	70.18	19.88

Table D14 Data of figure 5.19

Temperature (°C)	Ethanol/O_2 ratio, The amount of catalyst (g)						
	4/20, 0 g	4/20, 0.1 g	4/10, 0.1 g	4/5, 0.1 g	8/5, 0.1 g	12/5, 0.1 g	8/5, 0.3 g
200	0.0026	0.0048	0.0044	0.0032	0.0052	0.0039	0.0046
250	0.0191	0.0209	0.0197	0.0167	0.0276	0.0193	0.0159
300	0.0254	0.0439	0.0531	0.0523	0.0822	0.0718	0.0338
350	0.0276	0.0460	0.0560	0.0617	0.0989	0.0975	0.0356
400	0.0125	0.0214	0.0409	0.0537	0.0983	0.0999	0.0318
450	0.0073	0.0158	0.0208	0.0504	0.0949	0.0911	0.0279
500	0.0046	0.0118	0.0198	0.0517	0.0916	0.0843	0.0267

Table D15 Data of figure 5.20

Temperature (°C)	%CH_3OH conversion	%CH_4 Selectivity	%C_2H_4 selectivity	%C_3H_6 selectivity	%CO_2 selectivity	%CO selectivity
200	0.05	3.16	0	0	95.65	0
250	7.16	3.93	0	0	95.49	0
300	18.25	4.67	0	0	92.85	0.85
350	70.39	5.3	0	0.01	91.36	3.02
400	86.05	6.18	0.01	0.01	82.94	10.21
450	95.21	6.12	0.02	0.01	77.57	14.49
500	99.21	5.3	0.04	0.01	74.64	18.45

Table D16 Data of figure 5.21

Temperature (°C)	%CH_3OH conversion	%CH_4 Selectivity	%CO_2 selectivity
200	4.83	0.14	98.59
250	28.99	0.06	97.04
300	77.71	0.03	97.71
350	99.63	0.01	97.48
400	100	0.01	98.75
450	100	0.01	98.73
500	100	0.01	98.39

Table D17 Data of figure 5.22

Temperature (°C)	%2-C_3H_7OH conversion	%CH_4 selectivity	%C_2H_4 selectivity	%C_3H_6 selectivity	%C_3H_8 selectivity	%CH_2O selectivity	%CO_2 selectivity
200	1.05	0.15	0	95.23	0	0	2.75
250	3.70	0.08	0	90.06	0	3.53	4.22
300	25.95	0.10	0	78.89	0	0.66	17.63
350	43.86	0.08	0.07	65.54	0	0.51	31.65
400	45.31	0.33	0.19	56.36	1.65	3.01	36.16
450	48.91	0.79	0.27	44.73	1.58	3.81	46.95
500	48.88	2.44	0.58	35.80	0.79	4.3	55.83

Table D18 Data of figure 5.25

Time (hour)	%2-C_3H_7OH conversion	%CH_4 selectivity	%C_2H_4 selectivity	%C_3H_6 selectivity	%C_3H_8 selectivity	%CH_2O selectivity	%CO_2 selectivity
1	96.93	2.68	0.60	24.37	6.53	4.89	1.94
2	96.40	2.67	0.60	26.86	7.41	4.70	0.00
3	96.45	2.10	0.49	24.96	6.44	4.10	0.00
4	95.65	2.10	0.43	23.91	5.88	3.98	0.00
5	96.01	2.09	0.42	24.09	5.64	3.25	0.00

VITA

Miss Purida Pimanmas was born in Bangkok on December 14, 1976. She graduated high school from Strivithaya II School, Bangkok on 1993 and received her Bachelor degree of Chemical Engineering from the faculty of Engineering, Chalalongkorn University in 1997.